

University of Windsor

## Scholarship at UWindor

---

Electronic Theses and Dissertations

Theses, Dissertations, and Major Papers

---

9-12-2019

## Failure Prognosis of Wind Turbine Components

Milad Rezamand

*University of Windsor*

Follow this and additional works at: <https://scholar.uwindsor.ca/etd>

---

### Recommended Citation

Rezamand, Milad, "Failure Prognosis of Wind Turbine Components" (2019). *Electronic Theses and Dissertations*. 7836.

<https://scholar.uwindsor.ca/etd/7836>

This online database contains the full-text of PhD dissertations and Masters' theses of University of Windsor students from 1954 forward. These documents are made available for personal study and research purposes only, in accordance with the Canadian Copyright Act and the Creative Commons license—CC BY-NC-ND (Attribution, Non-Commercial, No Derivative Works). Under this license, works must always be attributed to the copyright holder (original author), cannot be used for any commercial purposes, and may not be altered. Any other use would require the permission of the copyright holder. Students may inquire about withdrawing their dissertation and/or thesis from this database. For additional inquiries, please contact the repository administrator via email ([scholarship@uwindsor.ca](mailto:scholarship@uwindsor.ca)) or by telephone at 519-253-3000ext. 3208.

# **Failure Prognosis of Wind Turbine Components**

By

**Milad Rezamand**

A Dissertation

Submitted to the Faculty of Graduate Studies through the  
Department of Mechanical, Automotive and Materials Engineering  
in Partial Fulfillment of the Requirements for  
the Degree of Doctor of Philosophy at the  
University of Windsor

Windsor, Ontario, Canada

2019

©2019 Milad Rezamand

# Failure Prognosis of Wind Turbine Components

by

Milad Rezamand

APPROVED BY:

---

P.A.Sandborn, External Examiner  
University of Maryland

---

A.Edrisy  
Department of Mechanical, Automotive and Materials Engineering

---

J.Johrendt  
Department of Mechanical, Automotive and Materials Engineering

---

B.Minaker  
Department of Mechanical, Automotive and Materials Engineering

---

R.Carriveau, Co-Advisor  
Department of Civil and Environmental Engineering

---

D.S-K.Ting, Co-Advisor  
Department of Mechanical, Automotive and Materials Engineering

September 12, 2019

## DECLARATION OF CO-AUTHORSHIP/PREVIOUS PUBLICATIONS

### I. Co-Authorship

I hereby declare that this dissertation incorporates material that is result of joint research, as follows:

<b>Dissertation Chapters</b>	<b>Details</b>
Chapters 2, 3, 4, 5 and 6	This research is part of the YR21 Investment Decision Support Program generously sponsored by Kruger Energy, Enbridge Inc., and the Wind Energy Institute of Canada. Significant funding has also been provided the Natural Sciences and Engineering Research Council of Canada and the Ontario Centres of Excellence with grant number 860002. Furthermore, this dissertation incorporates the outcome of a joint research project undertaken in collaboration with Dr. Matt Davison from Western University, Canada, Mr. Justin Jeffrey Davis from Kruger Energy, Canada, Dr. Mojtaba Kordestani from University of Windsor, Canada, Dr. Mehrdad Saif, from University of Windsor, Canada, Dr. Marcos E. Orchard from University of Chile, Chile under the supervision of Dr. Rupp Carriveau and Dr. David S-K. Ting. In all cases, the author performed the key ideas, primary contributions and data analysis and interpretation, and the contribution of co-authors was primarily through the provision of monitoring and manuscript structure checking.

I am aware of the University of Windsor Senate Policy on Authorship and I certify that I have properly acknowledged the contribution of other researchers to my dissertation, and have obtained written permission from each of the co-author(s) to include the above material(s) in my dissertation.

I certify that, with the above qualification, this dissertation, and the research to which it refers, is the product of my own work.

## II. Previous Publications

This dissertation includes five original papers that have been previously published/submitted for publication in peer reviewed journals, as follows:

<b>Chapters</b>	<b>Publication title</b>	<b>Publication status</b>
2	M. Rezamand, R. Carriveau, D. S-K. Ting, M. Davison, J. J. Davis, Aggregate Reliability Analysis of Wind Turbine Generators, IET Renewable Power Generation. 2019	accepted and published
3	M. Rezamand, M. Kordestani, R. Carriveau, D. S-K. Ting, M. Saif, A New Hybrid Fault Detection Method for Wind Turbine Blades Using Recursive PCA and Wavelet-based PDF, IEEE Sensors Journal	under revision
4	M. Rezamand, M. Kordestani, R. Carriveau, D. S-K. Ting, M. Saif, A Review of Health Monitoring and Failure Prognosis of Wind Turbine Bearings	to be submitted
5	M. Rezamand, M. Kordestani, R. Carriveau, D. S-K. Ting, M. Saif, An Integrated Feature-based Failure Prognosis Method for Wind Turbine Bearings, IEEE/ASME Transactions on Mechatronics	under revision
6	M. Rezamand, M. Kordestani, R. Carriveau, D. S-K. Ting, M. Orchard, M. Saif, Remaining Useful Life Estimation of Wind Turbine Bearings Under Varying Operating Conditions	to be submitted

I certify that I have obtained a written permission from the copyright owner(s) to include the above published material(s) in my dissertation. I certify that the above material describes work completed during my registration as graduate student at the University of

Windsor.

I declare that, to the best of my knowledge, my dissertation does not infringe upon any ones copyright nor violate any proprietary rights and that any ideas, techniques, quotations, or any other material from the work of other people included in my dissertation, published or otherwise, are fully acknowledged in accordance with the standard referencing practices. Furthermore, to the extent that I have included copyrighted material that surpasses the bounds of fair dealing within the meaning of the Canada Copyright Act, I certify that I have obtained a written permission from the copyright owner(s) to include such material(s) in my dissertation.

I declare that this is a true copy of my dissertation, including any final revisions, as approved by my dissertation committee and the Graduate Studies office, and that this dissertation has not been submitted for a higher degree to any other University or Institution.

## ABSTRACT

Wind energy is playing an increasingly significant role in the World's energy supply mix. In North America, many utility-scale wind turbines are approaching, or are beyond the half-way point of their originally anticipated lifespan. Accurate estimation of the times to failure of major turbine components can provide wind farm owners insight into how to optimize the life and value of their farm assets. This dissertation deals with fault detection and failure prognosis of critical wind turbine sub-assemblies, including generators, blades, and bearings based on data-driven approaches. The main aim of the data-driven methods is to utilize measurement data from the system and forecast the Remaining Useful Life (RUL) of faulty components accurately and efficiently. The main contributions of this dissertation are in the application of ALTA lifetime analysis to help illustrate a possible relationship between varying loads and generators reliability, a wavelet-based Probability Density Function (PDF) to effectively detecting incipient wind turbine blade failure, an adaptive Bayesian algorithm for modeling the uncertainty inherent in the bearings RUL prediction horizon, and a Hidden Markov Model (HMM) for characterizing the bearing damage progression based on varying operating states to mimic a real condition in which wind turbines operate and to recognize that the damage progression is a function of the stress applied to each component using data from historical failures across three different Canadian wind farms.

Keywords: Failure Prognosis, Wind Turbine, Generator, Blades, Bearings

## DEDICATION

To my lovely wife, Maryam,  
who has been a perpetual source of support, encouragement, and inspiration.  
To my beloved parents, Shahnaz and Mohammadreza,  
who have blessed me with their unconditionally love.  
To my kind-hearted mother-in-law, Mojgan,  
who has given me positive vibes.  
To my forever favorite brother on planet, Mohammadmahdi,  
who has always inspired me to pursue my dreams.  
To my caring and loving family, Mahnaz and Randy,  
who have been my strength and greatest support all these years.  
And to my precious unborn baby girl,  
who is a greatest gift and a blessing to us.



## ACKNOWLEDGEMENTS

Praise and thanks to the beneficent God who with his boundless mercies has bestowed his favors upon me in each moment of my life. This dissertation appears in its current form due to the assistance and guidance of several people. I would, therefore, like to express my sincere thanks to all of them.

I wish to express my deepest sense of gratitude to Dr. Rupp Carriveau, and Dr. David S-K. Ting, for having dedicated to me their perpetual support, profound knowledge, and experience throughout my Ph.D. studies. I surely recognize that without their help and kind consideration, this work would never have come into existence. I cannot express my appreciation for their enthusiasm throughout my academic career at University of Windsor. I would also like to express my gratitude to the members of my supervisory and examination committee, Dr. Afsaneh Edrisy, Dr. Jennifer Johrendt and Dr. Bruce Minaker for agreeing to serve in the committee and sharing their comments to improve this work.

This research would not be possible without the generous support from our industrial partners, and I wish to thank Mr. J.J. Davis, Dr. Marianne Rodgers, and Mr. John Bridges for their great help. The efforts and insights provided by Mr. J.J. Davis are particularly noted.

My sincere thanks also go to Dr. Mojtaba Kordestani from University of Windsor, Dr. Mehrdad Saif from University of Windsor, Dr. Matt Davison from Western University and Dr. Marcos E. Orchard from University of Chile for their continuous support during my research, for their motivation and open arms to share their knowledge. I would like to thank all my teachers and friends at University of Windsor for their invaluable support during my graduate study. I am genuinely thankful to my parents and my brother for all their love and encouragement.

I saved the last spot for the person who deserves this degree as much as I do. I do not know how I could manage this without her. Maryam, I thank you so much for everything.

Milad Rezamand

September 2019

## TABLE OF CONTENTS

<b>DECLARATION OF CO-AUTHORSHIP/PREVIOUS PUBLICATIONS</b>	<b>III</b>
<b>ABSTRACT</b>	<b>VI</b>
<b>DEDICATION</b>	<b>VII</b>
<b>ACKNOWLEDGEMENTS</b>	<b>VIII</b>
<b>LIST OF TABLES</b>	<b>XII</b>
<b>LIST OF FIGURES</b>	<b>XIII</b>
<b>1 Introduction</b>	<b>1</b>
1.1 Dissertation Motivation and Objectives . . . . .	1
1.2 Dissertation Organization . . . . .	3
REFERENCES . . . . .	4
<b>2 Aggregate reliability analysis of wind turbine generators</b>	<b>6</b>
2.1 Introduction . . . . .	6
2.2 A Preliminary theory of the reliability analysis . . . . .	11
2.2.1 Nonparametric life data analysis . . . . .	11
2.2.2 Parametric life data analysis . . . . .	12
2.3 Simulation studies and experimental results . . . . .	15
2.3.1 Failure scenario . . . . .	15
2.3.2 The proposed nonparametric life data analysis . . . . .	18
2.3.3 The proposed parametric life data analysis . . . . .	19
2.4 Conclusion and areas for future research . . . . .	28
2.5 List of Abbreviations . . . . .	30
REFERENCES . . . . .	31
<b>3 A Fault Detection Method for WT Blades Using Recursive PCA and Wavelet-based PDF</b>	<b>35</b>
3.1 Introduction . . . . .	35
3.2 Wind farm description . . . . .	39
3.3 Primary theory of the proposed hybrid fault detection method . . . . .	40
3.3.1 Preprocessing of the data using the GRNN-ESI . . . . .	40
3.3.2 PCA algorithm . . . . .	43
3.3.3 Wavelet-based PDF method . . . . .	44
3.4 Simulation and test results . . . . .	47
3.4.1 Experimental data collection and fault scenarios . . . . .	47
3.4.2 Design implementations and experimental test results . . . . .	48
3.4.3 Methodology evaluation . . . . .	50
3.5 Conclusions and future work . . . . .	53

3.6	List of Abbreviations . . . . .	55
	REFERENCES . . . . .	56
<b>4</b>	<b>A Review of Health Monitoring and Failure Prognosis of Wind Turbine Bearings</b>	<b>62</b>
4.1	Introduction . . . . .	62
4.2	Prognosis definition . . . . .	64
4.3	Bearings . . . . .	64
4.4	Review of bearing prognosis . . . . .	65
4.4.1	Intelligent method-based prognostics . . . . .	66
4.4.2	Bayesian network-based techniques . . . . .	70
4.4.3	Hybrid prognostic techniques . . . . .	73
4.5	Conclusions and Future Guidelines . . . . .	81
4.6	List of Abbreviations . . . . .	84
	REFERENCES . . . . .	87
<b>5</b>	<b>An Integrated Feature-based Failure Prognosis Method for Wind Turbine Bearings</b>	<b>98</b>
5.1	Introduction . . . . .	98
5.2	Wind Turbine Drivetrain . . . . .	103
5.3	A preliminary theory of the proposed fault prognosis method . . . . .	104
5.3.1	The bearing failures . . . . .	105
5.3.2	Feature extraction . . . . .	105
5.3.3	Feature selection . . . . .	106
5.3.4	The discrete wavelet transform method (DWT) . . . . .	106
5.3.5	The remaining useful life (RUL) . . . . .	107
5.3.6	Fusion method . . . . .	110
5.4	Simulation studies and experimental results . . . . .	110
5.4.1	Failure Scenarios . . . . .	112
5.4.2	The proposed feature extraction and selection . . . . .	113
5.4.3	The proposed de-noising method . . . . .	115
5.4.4	The proposed RUL . . . . .	116
5.4.5	The proposed Fusion . . . . .	116
5.4.6	Test results . . . . .	117
5.5	Conclusion . . . . .	120
5.6	List of Abbreviations . . . . .	122
	REFERENCES . . . . .	123
<b>6</b>	<b>RUL Estimation of Wind Turbine Bearings Under Varying Operating Conditions</b>	<b>127</b>
6.1	Introduction . . . . .	127
6.2	Wind Turbine Bearings . . . . .	130
6.2.1	The bearing failures . . . . .	132
6.3	A preliminary theory of the proposed fault prognosis method . . . . .	132
6.3.1	KFCM-based clustering . . . . .	134

6.3.2	Hidden Markov Models and the Viterbi Algorithm . . . . .	135
6.3.3	Signal de-noising based on DWT method . . . . .	136
6.3.4	Feature extraction . . . . .	138
6.3.5	Feature selection . . . . .	138
6.3.6	Bayesian RUL Prediction Algorithm . . . . .	139
6.4	Simulation studies and experimental results . . . . .	141
6.4.1	Failure Scenarios . . . . .	141
6.4.2	Off-line phase design implementation . . . . .	144
6.4.3	Online phase design implementation . . . . .	146
6.4.4	Test results . . . . .	147
6.5	Conclusion . . . . .	151
6.6	List of Abbreviations . . . . .	152
	REFERENCES . . . . .	153
<b>7</b>	<b>Conclusion</b>	<b>157</b>
7.1	Contributions . . . . .	158
7.2	Future Work . . . . .	159
<b>8</b>	<b>Bayesian RUL Prediction Algorithm</b>	<b>161</b>
	REFERENCES . . . . .	164
	<b>Vita Auctoris</b>	<b>165</b>

## LIST OF TABLES

2.2.1 Weibull distribution models . . . . .	13
2.2.2 ALTA distribution models . . . . .	15
2.3.1 Population reliability estimates at data points in which individual failures occurred, nonparametric results . . . . .	18
2.3.2 RMSE estimates for Weibull distribution models . . . . .	20
2.3.3 RMSE estimates for parameter estimation methods . . . . .	21
2.3.4 Reliability estimates for the failures times, nonparametric results . . . . .	23
2.3.5 RMSE estimates for ALTA distribution models . . . . .	24
2.3.6 The probability of failure of individual generators with varying average power generated at 10 years of operation . . . . .	27
3.4.1 Various types of data studied in this work . . . . .	48
3.4.2 Method evaluation . . . . .	52
4.4.1 Summary of intelligent method-based prognostics literature review . . . . .	69
4.4.2 Summary of Bayesian network-based techniques literature review . . . . .	73
4.4.3 Summary of hybrid prognostic techniques literature review . . . . .	82
5.4.1 Complete failure criteria coefficient $\lambda_k$ for each feature . . . . .	115
5.4.2 The estimated values of the $\eta_q$ . . . . .	117
5.4.3 Fusion weights estimated by the OWA operator for each feature . . . . .	117
6.3.1 Time domain features for signal $x$ . . . . .	139
6.4.1 Complete failure criteria coefficient $\lambda_k$ for each feature . . . . .	145
6.4.2 Comparison of the RULs estimated by different approach for outer raceway failure . . . . .	148
6.4.3 Comparison of the RULs estimated by different approach for inner raceway failure . . . . .	150

## LIST OF FIGURES

2.3.1 Ambient temperature during 4 years of wind turbine operation . . . . .	16
2.3.2 Cumulative power generated (kWh) by the failed generator at the time of failure . . . . .	17
2.3.3 Power curve of wind Turbine T04 in January 2015 . . . . .	17
2.3.4 Population reliability estimates at data points in which individual failures occurred, nonparametric results . . . . .	19
2.3.5 Probability plot, Weibull Standard Folio life data analysis based on 3P- Weibull distribution) . . . . .	20
2.3.6 Probability plot, Weibull Standard Folio life data analysis based on 1P- Exponential distribution . . . . .	21
2.3.7 Unreliability vs. Time, Weibull Standard Folio life data analysis based on 3P-Weibull distribution . . . . .	22
2.3.8 Predictions for the remaining life of 15 generators by the Naive method . .	23
2.3.9 Use Level Probability plot for the generator with 952.66 kW, ALTA Stan- dard Folio life data analysis (IPL-Lognormal) . . . . .	24
2.3.10 Use Level Probability plot for the generator with 952.66 kW, ALTA Stan- dard Folio life data analysis (IPL-Weibull) . . . . .	25
2.3.11 Unreliability vs. Time for the generator with 952.66 kW, ALTA Standard Folio life data analysis . . . . .	26
2.3.12 The probability of failure for the generator with 1015.33 kW, failed at the age of 5.8 years . . . . .	26
2.3.13 The Naive Predictions for the remaining life of the generators with the average power of 952.7 kW . . . . .	27
2.3.14 The probability of failure for generators with two different generated power	28
3.2.1 Various components of a typical wind turbine . . . . .	39
3.2.2 The layout of the wind farm . . . . .	40
3.3.1 The proposed hybrid fault detection method . . . . .	41

3.3.2 A typical wavelet-based PDF, $h(x)$ , for variable $x$ . . . . .	46
3.4.1 Blade erosion (a) and crack (b) . . . . .	48
3.4.2 The cumulative variance of the PCs. . . . .	49
3.4.3 The PDF $h(x)$ of the first selected PC ( $x$ ), and PDF $h(y)$ of the second selected PC ( $y$ ). . . . .	51
3.4.4 Power curve of wind Turbine T72 in October and November 2017 . . . . .	53
3.4.5 Blade fault detection in the WT T72 . . . . .	54
4.3.1 Rolling bearings components . . . . .	65
4.4.1 A combination of VM, LR and ARMA GARCH for bearings RUL estima- tion [61] . . . . .	74
4.4.2 A combination of PCA and LSSVM for bearings RUL estimation [64] . . .	75
4.4.3 A combination of WPD, EMD and SOM neural network techniques for bearings RUL estimation [66] . . . . .	76
4.4.4 A combination of HMM and NAP bearing performance descending evalu- ation [77] . . . . .	78
4.4.5 Flowchart for prognosis approach based on a NARX neural network model in association with a wavelet-filter technique for bearing RUL estimation [87]	81
5.2.1 Wind turbine drivetrain Schematic including gearbox and Sensor Configu- ration . . . . .	103
5.3.1 The block diagram of the proposed failure prognosis method. . . . .	104
5.3.2 The decomposition of a signal based on MRA method . . . . .	109
5.4.1 Outer raceway failure . . . . .	112
5.4.2 Inner raceway failure . . . . .	112
5.4.3 Vibration signal samples of the main-shaft bearing with outer raceway fail- ure recorded in healthy and faulty states . . . . .	113
5.4.4 Vibration signal samples of the generator DE bearing with the inner race- way failure recorded in healthy and faulty states . . . . .	114
5.4.5 Selected features for outer raceway failure . . . . .	115
5.4.6 Selected features for inner raceway failure . . . . .	116

5.4.7 Comparison of the RUL estimated by each feature and OWA for outer raceway failure . . . . .	118
5.4.8 Predicted PDFs of the RULs of outer raceway failure at the chosen sampling points for OWA . . . . .	119
5.4.9 Comparison of the RUL estimated by each feature and OWA for inner raceway failure . . . . .	120
5.4.10 Predicted PDFs of the RULs of inner raceway failure at the chosen sampling points for OWA . . . . .	121
6.2.1 Rolling bearings components . . . . .	131
6.2.2 Bearing Sensors Configuration . . . . .	132
6.3.1 The block diagram of the proposed failure prognosis method. . . . .	133
6.3.2 The decomposition of a signal based on MRA method . . . . .	138
6.4.1 Outer raceway failure . . . . .	142
6.4.2 Inner raceway failure . . . . .	142
6.4.3 Vibration signal samples of the main-shaft bearing with outer raceway failure recorded in healthy and faulty states . . . . .	143
6.4.4 Vibration signal samples of the generator DE bearing with the inner raceway failure recorded in healthy and faulty states . . . . .	144
6.4.5 Selected features for the bearing #1 RUL estimation prediction . . . . .	145
6.4.6 Selected features for the bearing #2 RUL estimation prediction . . . . .	146
6.4.7 Varying states sequences for outer raceway failure . . . . .	147
6.4.8 Comparison of the RULs estimated by averaging 15 selected realizations of VOC and COC . . . . .	148
6.4.9 Varying states sequences for inner raceway failure . . . . .	149
6.4.10 Comparison of the RULs estimated by averaging 12 selected realizations of VOC and COC . . . . .	150
8.0.1 The adaptive Bayesian RUL method . . . . .	162



---

# CHAPTER 1

## *Introduction*

---

### **1.1 Dissertation Motivation and Objectives**

Wind energy is playing an increasingly pivotal role in Canada's energy demands. Canada finished 2018 with 12,816 MW of wind energy capacity, enough to power over 3 million homes, or six percent of electricity demand [1]. Wind is also assuming a nascent and growing role in the expanding ancillary services market associated with evolving grids.

Wind Turbines (WTs) are complex machines, assembled combinations of numerous technologies, operating in challenging environments [2]. As for any integrated system, some of the components are more critical than others, so for a WT, it is necessary to rank components based on failure rate and downtime. There have been some seminal efforts in recent decades on the reliability of wind farm components that indicate that the most frequent failures are related to generators and gearboxes in the component level, and bearings in sub-assembly level. Furthermore, generators, gearboxes, and blades have the most downtime [3, 4, 5, 6, 7, 8]. The unexpected failure of WT components can cause substantial economic losses, so, it may be prudent to consider wind turbine components safety and reliability as a more distinct category.

Safety and reliability are vital concerns for critical systems. Fault diagnosis and prognosis (FDP), i.e., estimation of remaining useful life (RUL) can provide wind farm owners insight into how to optimize the life and value of their farm assets by isolating incipient faults and anticipating the future status of the faulty systems [9, 10]. An improved understanding of the RUL of turbine components is particularly important as many owners consider retiring, life-extending, or re-powering their farms [11]. Proper performance mon-

itoring based on Supervisory Control and Data Acquisition (SCADA) data and condition monitoring (CM) are essential components of this pursuit [12].

This performance monitoring technique correlates different groups of SCADA data (e.g., the power generated, wind speed and ambient temperature), develops models for normal operational states, and uses these models to identify abnormalities. However, this technique may not be straightforward in pinpointing specific damaged components. On the other hand, CM is capable of pinpointing damage locations/components precisely [13]. The outcomes of the CM enable condition-based maintenance (CBM) that reduce maintenance cost [14]. FDP as an essential step of the CBM procedure is crucial and fundamental in successful CBM [15]. FDP information is employed to isolate an incipient fault, predict future behavior of faulty components, and then, schedule the maintenance.

Although fault diagnosis is a well-known task, and it has been widely considered, failure prognosis is a relatively new area of research, which is often more challenging owing to the uncertainty inherent in the potential for multiple failure degradation paths. The main objective of this dissertation is to deepen the insight into the shortcomings and existing methods and also introduce new modern methods for health monitoring of wind turbine elements.

The primary research objective of this dissertation is to introduce new failure prognosis methods for critical WT components. For this aim, various monitoring and failure prognosis methods for health monitoring of systems are investigated to enhance current estimation and increase the prediction accuracy of failure prognosis approaches. Note that due to the availability of historical data across three different Canadian wind farms, data-driven methods are employed. Data-driven methods transform historical data into relevant models of the degradation behavior rather than a direct physical account of the failure processes. For this aim, a complete set of failure data based on all operating conditions is required to develop thorough and accurate data-driven prognosis methods.

## 1.2 Dissertation Organization

The remainder of this dissertation is organized as follows. Chapter 2 focuses on a limited data set for reliability prediction of a wind turbine generator population. Furthermore, a Naive procedure is proposed for the prediction of individual generator lifetime intervals. A real-time hybrid fault detection method is developed in Chapter 3 for wind turbine blades. Chapter 4 reviews the most recent literature on RUL anticipation of wind turbine bearings and highlights some directions that merit further study, which mainly are addressed in the next two chapters. A combination of signal processing, adaptive Bayesian, and fusion techniques is employed in Chapter 5 for RUL prediction of faulty bearings. In Chapter 6, a hybrid data-driven prognostics method for RUL forecast of wind turbine bearings under varying operating conditions is presented. The proposed method leverages signal processing, data clustering, Viterbi-based Hidden Markov Model, and an adaptive Bayesian algorithm. Chapter 7 draws the conclusion of the dissertation, and it also examines open problems and possible developments and highlights a number of challenges that merit further study.

## REFERENCES

- [1] C. Ridge. (2018) Installed capacity. [Online]. Available: <https://canwea.ca/wind-energy/installed-capacity/>
- [2] Q. Gao, C. Liu, B. Xie, and X. Cai, "Evaluation of the mainstream wind turbine concepts considering their reliabilities," *IET Renewable Power Generation*, vol. 6, no. 5, pp. 348–357, 2012.
- [3] M. Shafiee and F. Dinmohammadi, "An fmea-based risk assessment approach for wind turbine systems: a comparative study of onshore and offshore," *Energies*, vol. 7, no. 2, pp. 619–642, 2014.
- [4] N. Chen, R. Yu, Y. Chen, and H. Xie, "Hierarchical method for wind turbine prognosis using scada data," *IET Renewable Power Generation*, vol. 11, no. 4, pp. 403–410, 2016.
- [5] B. Hahn, M. Durstewitz, and K. Rohrig, "Reliability of wind turbines, experiences of 15 years with 1,500 wts, in 'wind energy,'" in *Proceedings of the Euromech Colloquium*. Springer-Verlag Berlin Heidelberg, 2007, pp. 329–332.
- [6] A. Stenberg and H. Holttinen, "Analysing failure statistics of wind turbines in finland," in *European Wind Energy Conference, April*, 2010, pp. 20–23.
- [7] Y. Sun, P. Wang, L. Cheng, and H. Liu, "Operational reliability assessment of power systems considering condition-dependent failure rate," *IET generation, transmission & distribution*, vol. 4, no. 1, pp. 60–72, 2010.
- [8] B. Nivedh, "Major failures in the wind turbine components and the importance of periodic inspections," *Wind Insid*, vol. 2014, p. 5, 2014.
- [9] M. Pecht, "Prognostics and health management of electronics," *Encyclopedia of Structural Health Monitoring*, 2009.

- [10] W. Ahmad, S. A. Khan, and J.-M. Kim, “A hybrid prognostics technique for rolling element bearings using adaptive predictive models,” *IEEE Transactions on Industrial Electronics*, vol. 65, no. 2, pp. 1577–1584, 2017.
- [11] L. R. Rodrigues, “Remaining useful life prediction for multiple-component systems based on a system-level performance indicator,” *IEEE/ASME Transactions on Mechatronics*, vol. 23, no. 1, pp. 141–150, 2018.
- [12] A. P. Ompusunggu, J.-M. Papy, and S. Vandenplas, “Kalman-filtering-based prognostics for automatic transmission clutches,” *IEEE/ASME Transactions on Mechatronics*, vol. 21, no. 1, pp. 419–430, 2016.
- [13] S. Sheng, “Improving component reliability through performance and condition monitoring data analysis; nrel (national renewable energy laboratory),” National Renewable Energy Lab.(NREL), Golden, CO (United States), Tech. Rep., 2015.
- [14] L. Feng, H. Wang, X. Si, and H. Zou, “A state-space-based prognostic model for hidden and age-dependent nonlinear degradation process,” *IEEE Transactions on Automation Science and Engineering*, vol. 10, no. 4, pp. 1072–1086, 2013.
- [15] A. Heng, S. Zhang, A. C. Tan, and J. Mathew, “Rotating machinery prognostics: State of the art, challenges and opportunities,” *Mechanical systems and signal processing*, vol. 23, no. 3, pp. 724–739, 2009.

---

## CHAPTER 2

# *Aggregate reliability analysis of wind turbine generators*

---

### 2.1 Introduction

Energy is a primary key to economic growth and industrialization. Fossil fuels presently play a vital role meeting world energy demand. Finite supply and significant environmental footprints limit the appeal of these fuels. Among renewables, wind energy is recognized as one of the lowest-cost and fastest growing clean power options [1]. Wind now plays an important and expanding role in many energy systems worldwide. According to the Global Wind Energy Council (GWEC)'s report [2], wind energy capacity could reach almost 2.1 TW, supplying up to 20% of global electricity by 2030.

A wind turbine (WT) is a complex machine functioning in a complex environment. Wind turbines are an assembled combination of technologies from aeronautics, mechanical engineering, hydraulics, electrical engineering, automation, information technologies, as well as civil engineering infrastructure. The unexpected failure of wind turbine components can cause substantial economic losses. As for any integrated system, some of the components are more critical than others, so, for a wind turbine, it is necessary to rank components based on failure rate and downtime [3]. There have been some seminal efforts in recent decades on the reliability of wind farm components as reviewed below.

Shafiee and Dinmohammadi [4] indicated that, for onshore machines, the most frequent failures are related to the tower, gearbox, rotor blades, rotor hub, and the transformer in that order whereas in offshore settings, the gearbox, rotor blades, generator, tower and the trans-

former have the highest failure rates. In Chen et al. [5], it was shown that the generator and gearbox have the highest failure rate. Hahn et al. [6] showed that generator, gearbox, drive train, and rotor blade have the most downtime based on 1467 WTGs (below 1 MW) data in the period from 1989 until the end of 2004. In Stenberg and Holttinen [7] 1996-2008 data from 72 operating wind turbines in Finland revealed that the gearbox, hydraulic system, brake, and generator had the most downtime. The reliability of more than 6000 WTs in Denmark and Germany over 11 years was investigated in Spinato et al. [8]. This work illustrated that the sub-assemblies with the highest failure rates included, in descending order of significance, the electrical system, rotor, converter, generator, hydraulics, and gearbox. This paper mainly studied the changes in the reliability of generators and gearboxes in a subset of 650 of these WTs in Schleswig-Holstein, Germany. This analysis showed that wind turbine gearboxes seemed to be achieving reliabilities similar to gearboxes outside the wind industry. However, wind turbine generator reliability is significantly below that of other industries.

A review of such reliability summary studies reveals the generator as a critical wind turbine sub-assembly. They are prone to faults caused by the corrosive, high temperature, and high-speed environments in which they usually operate. Major generator failure in wind turbines can lead to significant downtime if maintenance activities are reactive. One of the principal causes of generator failure is the continuous insulation degradation in the stator windings and subsequent melting of the copper coils of the windings, or the iron cores [8]. Further, since it has been indicated in Spinato et al. [9] that wind turbine generators are achieving reliabilities considerably below that of other industries, it may be prudent to consider wind turbine generator reliability as a more distinct category.

Reliability speaks to the the ability of a system or a component to fulfill a required role under given operational and environmental conditions for a stated period of time. Reliability may be determined by various means depending on the situation. Particularly useful reliability measures include: mean time to failure (MTTF), number of failures per time unit (failure rate), the probability that the item does not fail in a time interval (survival probability), and the probability that the item is able to function at any time [10]. Any model engaged for reliability estimation is constrained by factors such as the accuracy of

the initial prediction, the deficiencies of historical data, sensitivity to variations, human errors in management, production, and application, the discrepancy between the domain and the conditions of applicability, and unclear understanding of the logical and physical relationship between the model and its prototype [11]. In the following, studies on reliability analysis are reviewed. This review focuses principally on the reliability analysis of generators.

A method for determining the impact of energy generation on generator reliability was developed in Giorestto and Utsurogi [12] which helped with the determination of the useful load carrying capability of a wind farm. Fitzgibbon et al. [13] presented a method that combines Weibull analysis and statistical algorithms to forecast failures applied to electronic systems. Batzel and Swanson [14] developed prognostic tools to detect the onset of electrical failures in an aircraft power generator and to predict the generator's time to failure (TTF) which helps to avoid unexpected failures. Yang et al. [15] investigated the application of wavelet transforms to condition monitoring and fault diagnosis of a synchronous wind turbine generator. The developed technique was confirmed as robust for detecting electrical faults in a direct drive generator. Guo et al. [16] presented a three-parameter Weibull failure rate function to obtain an accurate reliability projection of wind turbines based on incomplete wind farm failure data. Hong et al. [17] used a parametric lifetime model to define the lifetime distribution of high-voltage power transformers based on left truncated and right censored data. A statistical procedure was developed, based on age-adjusted life distributions, for computing a prediction interval for remaining life for individual transformers in service. A simple prediction interval procedure, the Naive method, was used to provide an approximate interval, and was used as a start towards obtaining a more refined interval. This work showed how to produce calibrated prediction intervals through the use of a random weighted bootstrap technique and an approximation based on a sophisticated central limit theorem. These ideas were extended to provide predictions and prediction intervals for the cumulative number of failures, over a range of time for the entire fleet of transformers. In He et al. [18], reliability evaluation indicators for a hybrid power supply system were proposed. The indicators include the average failure rate, the average duration of power outage for each failure, and the average duration of power outages per



year, which were simple and very useful in their reliability analysis. Sikorska et al. [19] presented classification tables and process flow diagrams to select appropriate prognostic models for predicting the remaining useful life of engineering assets within their specific industrial environment. The paper then investigated the strengths and weaknesses of the significant prognostics model classes. Infield and Wang [20] proposed a non-linear state estimation technique to model a healthy wind turbine gearbox using stored historical data. These data take the correlation between the model input and output parameters. This study employed TWelch's t-test in the fault detection algorithm, together with suitable time series filtering, to identify incipient anomalies in the turbine gearbox before they develop into catastrophic faults. Okoh et al. [21] expressed the classification of techniques used in TTF prediction for optimization of products' future use. This was based on the predictability, availability, and reliability of current in-service products. This study presented a mapping of degradation mechanisms against techniques for knowledge acquisition with the objective of presenting designers and manufacturers ways to improve the life-span of components. Sankararaman et al. [22] described three first-order reliability-based methods for TTF uncertainty quantification, the first-order second moment method, the first order reliability method, and the inverse first-order reliability method, to quantify the uncertainty in the TTF estimate of a lithium-ion battery. A method called power density (PD) was developed by Akdağ and Dinler [23] to determine Weibull distribution parameters for wind energy applications. Results of this study indicated that the PD method outperformed maximum likelihood and moment methods in estimating Weibull parameters. This resulted in higher accuracy in reliability analysis for wind energy applications. Although PD does not require binning and the solution of a linear least square problem, or iterative procedures for Weibull parameters estimation, its accessibility might be considered challenging. The combination of Simplified Fuzzy Adaptive Resonance Theory Map neural network and Weibull distribution (WD) was explored in Ali et al. [24] to predict the TTF of rolling element bearings (REBs) based on vibration signals. The proposed prediction approach can be applied to prognostic other various mechanical assets. An intelligent prognostic system was developed for gear performance degradation assessment and TTF estimation in Wang et al. [25]. For gear TTF estimation, a general sequential Monte Carlo algorithm was applied to infer

gear failure probability density function iteratively. The results illustrated the ability of the prognostic system to detect early gear faults, to track gear performance degradation, and to predict gear TTF. Chen and co-authors [26] proposed an approach for automated detection of wind turbine pitch faults by employing a priori knowledge-based adaptive neuro-fuzzy inference system on SCADA data. The proposed method was applied to two datasets, illustrating the strong potential of the approach to providing automated online WT pitch fault detection and prognosis and its adaptability to a variety of techniques. A hierarchical method based on Gaussian Processes (GP) and Principal Component Analysis (PCA) was proposed in Chen et al. [5] for turbine prognosis using SCADA data. This study provided the detection of the abnormality behaviour of a wind turbine and the determination of the defective components in the abnormal turbine.

Although several approaches have been proposed for reliability prediction, generator reliability analysis on limited historical data and varying load conditions remains challenging. To overcome this difficulty, this chapter examines aggregate reliability analysis. Here the truncated generator data records of a wind farm operating through variable conditions and associated loads, were used to offer estimation of generator lifetime. To pursue this objective, the chapter engages a variety of lifetime data analyses. We examine those that are most relevant to this application based on the amount and the type of data available. We emphasize here that wind farm owners are often faced with major investment decisions with very little notice. Historical failure data is often not ideal or sufficiently complete to offer ultimately conclusive direction. Subsequently, decision makers are looking for tools to at least improve the level of information available to them when making major financial investments critical to the farm bottom line. This chapter explores such tools. The main contributions of this study are as follows:

- The unprecedented application of the ALTA lifetime analysis method for reliability estimation of wind turbine generators to help illustrate a possible relationship between varying loads and generator reliability.
- The novel employment of aggregate reliability methods in the analysis of times to failure for a generator population to provide a means to generate a probability den-

sity function and a related hazard function. This probability density function is not representative of a single fault progression from incipience to final failure. Rather, it explores the likelihood of the next failure event. Theoretically, this approach can be performed at all equipment hierarchy levels, particularly when a small number of failure modes dominate.

- The proposed methods described herein can significantly improve the accuracy of generator failure rate estimation when limited data records are available compared to the classical approaches.

This chapter is organized as follows: A brief theory background of the proposed reliability approach is provided in Section 2.2. Design implementations and experimental test results are presented in 2.3. Section 2.4 concludes with some discussion and describes areas for future research.

## 2.2 A Preliminary theory of the reliability analysis

This section introduces the preliminary theory of the proposed reliability analysis. The proposed method includes nonparametric and parametric life data analyses.

### 2.2.1 Nonparametric life data analysis

Here we begin by engaging graphical data illustration techniques without considering strong model assumptions. Such methods allow the data to be interpreted without distortion that could ensue by assuming an inappropriate model. There are, however, many problems in reliability data analysis where it is either useful or essential to use a parametric distribution form. Indeed, a nonparametric analysis provides an intermediate step forward towards a more structured model that may deliver more accurate results, provided that the additional assumptions of such a model are valid [27]. A nonparametric analysis allows the user to analyze data without considering an underlying distribution. It is advantageous since it avoids potentially significant errors brought about by assuming an inappropriate distribution. On the other hand, the analysis is limited to reliability measures only for the failure times in the

data set, therefore making it impossible to make reliability predictions outside the range of data values. Thus, nonparametric life data analysis has been used in this study to provide an initial high-level view of how the components are behaving over time. There are several techniques for conducting a nonparametric analysis including the Kaplan-Meier, simple actuarial, and standard actuarial methods.

The Kaplan-Meier technique provides very useful measures of survival probabilities and graphical illustration of survival distributions. It has been broadly used in survival data analysis [28, 29]. The actuarial models are alternative nonparametric analyses that display information for groupings of failure times.

The Kaplan-Meier estimates reliability for a population with multiple failures and suspensions at data points in which individual failures occurred by the use of Equation 2.2.1.

$$R(t_i) = \prod_{j=1}^i \frac{(n_j - r_j)}{n_j}, i = 1, \dots, m \quad (2.2.1)$$

where  $m$  is the total number of data points,  $n$  is the total number of units,  $r_j$  is the number of failures in the  $j^{th}$  data group and the variable  $n_i$  is defined by Equation 2.2.2.

$$n_i = n - \sum_{j=0}^{i-1} s_j - \sum_{j=0}^{i-1} r_j, i = 1, \dots, m \quad (2.2.2)$$

where  $s_j$  is the number of suspensions in the  $j^{th}$  data group.

### 2.2.2 Parametric life data analysis

Parametric statistics is a category of statistics that assumes that sample data comes from a population that follows a probability distribution based on a fixed set of parameters. Using parametric distributions can be viewed as a way of extending nonparametric techniques, they also provide the following advantages [27]:

- Parametric models can be compactly defined while including all critical information, with just a few parameters, instead of having to report an entire curve.
- It is possible to use a parametric model to extrapolate (in time) to the lower or upper tail of a distribution.

- Parametric models provide smooth estimates of failure time distribution.

Some major parametric models are Weibull Standard Folio life data analysis, Naive Prediction Interval Procedure and ALTA Standard Folio life data analysis.

### Weibull Standard Folio life data analysis

The Weibull analysis makes projections about the future behaviour of a population by fitting a statistical distribution to the life data. From this analysis, several life characteristics can be estimated, such as the probability of failure, reliability, mean life or failure rate.

There are several distribution models to choose from, depending on which one best fits the data based on the selected analysis method. Some principal distribution models with their cumulative distribution function (CDF) and probability density function (PDF) are illustrated in Table 2.2.1.

TABLE 2.2.1: Weibull distribution models

Distribution model	CDF	PDF
1P-Exponential	$F(t) = 1 - \exp(-\frac{t}{\eta})$	$f(t) = \frac{1}{\eta} \exp(-\frac{t}{\eta})$
2P-Weibull	$F(t) = 1 - \exp(-(\frac{t}{\eta})^\beta)$	$f(t) = \frac{\beta}{\eta} (\frac{t}{\eta})^{\beta-1} \exp(-(\frac{t}{\eta})^\beta)$
3P-Weibull	$F(t) = 1 - \exp(-(\frac{t-\gamma}{\eta})^\beta)$	$f(t) = \frac{\beta}{\eta} (\frac{t-\gamma}{\eta})^{\beta-1} \exp(-(\frac{t-\gamma}{\eta})^\beta)$
Gamma	$F(t) = \frac{\Gamma_t(\beta)}{\Gamma(\beta)}$	$f(t) = \frac{(\frac{t-\gamma}{\eta})^{\beta-1} \exp(-\frac{t-\gamma}{\eta})}{\eta \Gamma(\beta)}$
Gaussian	$F(t) = 0.5 + 0.5 \operatorname{erf}(\frac{t-\mu}{\sigma\sqrt{2}})$	$f(t) = \frac{1}{\sigma\sqrt{2\pi}} \exp(-\frac{(t-\mu)^2}{2\sigma^2})$
Gumbel	$F(t) = \exp(-\exp(\frac{\gamma-t}{\eta}))$	$f(t) = \frac{1}{\eta} \exp(\frac{\gamma-t}{\eta} - \exp(\frac{\gamma-t}{\eta}))$
Log-normal	$F(t) = 0.5 + 0.5 \operatorname{erf}(\frac{\ln t - \mu}{\sigma\sqrt{2}})$	$f(t) = \frac{1}{t\sigma\sqrt{2\pi}} \exp(-\frac{(\ln t - \mu)^2}{2\sigma^2})$
Logistic	$F(t) = \frac{1}{1 + \exp(-\frac{t-\gamma}{\eta})}$	$f(t) = \frac{\exp(-\frac{t-\gamma}{\eta})}{\eta(1 + \exp(-\frac{t-\gamma}{\eta}))^2}$

where  $\eta$  is the scale parameter,  $\beta$  is the shape parameter,  $\gamma$  is the location parameter,  $\mu$  is the mean or expectation of the distribution and  $\sigma$  is the standard deviation.

Typical analysis methods that help determine the best technique for estimating the parameters of chosen distribution include: rank regression (rank regression on X, Y (RRX and RRY) and nonlinear rank regression (NLRR)) and maximum likelihood estimation (MLE) [30]. These techniques are investigated in this chapter to figure out which one is the most suitable for reliability projection of truncated data.

### Naive Prediction Interval Procedure

The Naive Prediction provides an approximate interval that can be used as a start toward obtaining a more refined interval. The procedure takes the regression estimates of the parameters and substitutes them into the estimated conditional probability distributions in expression 2.2.3 (one distribution for each generator) [15].

$$F(t|t_i; \theta) = \frac{F(t; \theta) - F(t_i; \theta)}{1 - F(t_i; \theta)} \quad (2.2.3)$$

where  $\theta$  is a vector that gives the location parameter and scale parameters for each generator and  $t_i$  denotes the lifetime or survival time of generator  $i$ . The required parameters for this analysis includes the shape parameter, the scale parameter and the location parameter.

### ALTA Standard Folio life data analysis

In ALTA analysis, a product's failure behaviour is extrapolated at standard conditions from life data acquired at accelerated stress levels. As products fail much faster at accelerated stress levels, this sort of analysis enables the engineer to gain reliability information about a product (e.g., the probability of failure at a specific time) in a shorter time [27]. This technique aims to perform quantitative accelerated life testing data analysis. There are several life-stress relationships including the Arrhenius, the Eyring, the Inverse power law (IPL), the Temperature-humidity (TH), etc. and three life distributions including Weibull, Lognormal and Exponential for ALTA analysis. The Reliability and PDF of some of them are indicated in Table 2.2.2. The choice of the life stress relationship depends on various factors, including the types and number of stresses used in the test.

where  $T' = \ln T$ ,  $T$  is time-to-failure,  $\sigma_{T'}$  is the standard deviation of the natural logarithms of the time-to-failure,  $V$  represents the stress level,  $K$  and  $n$  are IPL parameters,  $A$  and  $B$  are Eyring parameters, and  $\beta$  is the Weibull shape parameter.

TABLE 2.2.2: ALTA distribution models

Distribution model	Reliability
IPL Exponential	$R(T, V) = \exp(-KV^nT)$
IPL Weibull	$R(T, V) = \exp(-(KV^nT)^\beta)$
IPL Log-normal	$R(T, V) = \int_{T'}^{\infty} \frac{1}{\sigma_{T'}\sqrt{2\pi}} \exp(-0.5(\frac{t+\ln(K)+\ln(V)}{\sigma_{T'}})^2) dt$
Eyring Exponential	$R(T, V) = \exp(-TV \exp(A - \frac{B}{V}))$
Eyring Weibull	$R(T, V) = \exp(-(TV \exp(A - \frac{B}{V}))^\beta)$
Eyring Log-normal	$R(T, V) = \int_{T'}^{\infty} \frac{1}{\sigma_{T'}\sqrt{2\pi}} \exp(-0.5(\frac{t+\ln(V)+A-\frac{B}{V}}{\sigma_{T'}})^2) dt$
Distribution model	PDF
IPL Exponential	$f(T, V) = KV^n \exp(-KV^nT)$
IPL Weibull	$f(T, V) = \beta KV^n (KV^nT)^{\beta-1} \exp(-(KV^nT)^\beta)$
IPL Log-normal	$f(T, V) = \frac{1}{\sigma_{T'}\sqrt{2\pi}T} \exp(-0.5(\frac{t+\ln(K)+\ln(V)}{\sigma_{T'}})^2)$
Eyring Exponential	$f(T, V) = V \exp(A - \frac{B}{V}) \exp(-TV \exp(A - \frac{B}{V}))$
Eyring Weibull	$f(T, V) = \frac{(TV \exp(A - \frac{B}{V}))^{\beta-1} \exp(-(TV \exp(A - \frac{B}{V}))^\beta)}{\frac{1}{BV \exp(A - \frac{B}{V})}}$
Eyring Log-normal	$f(T, V) = \frac{1}{\sigma_{T'}\sqrt{2\pi}T} \exp(-0.5(\frac{t+\ln(V)+A-\frac{B}{V}}{\sigma_{T'}})^2)$

## 2.3 Simulation studies and experimental results

This section introduces the structure of the reliability analysis and considers the experimental test study to investigate the performance of life data methods. In the sections that follow, the failure scenario is illustrated. Afterwards, the proposed structure of reliability analysis is developed and the results of the proposed techniques are evaluated using historical field data from wind turbine generators.

### 2.3.1 Failure scenario

Data records of a wind farm including generators operating hours, power generated and environmental conditions such as ambient temperature, shown in Figure 2.3.1 as a box plot, have been used for this study.

The dataset contains 88 units, all asynchronous type, half of which were installed in 2008, and the other half were installed in 2011. The cumulative power generated by the failed generators with a total number of 12, is shown in Figure 2.3.2. Here we also confirm that the failures occurred mainly due to several poor design issues surrounding the stator



FIGURE 2.3.1: Ambient temperature during 4 years of wind turbine operation

resin/wedge which resulted in the generator insulation failure. It is worth mentioning that the failed generators were replaced by new ones which are included in the analysis.

One generator (T74), which was a substitute for failed generator (T73), failed within the first two years of installation. The cumulative power generated by this generator was not significant (0.84 GWh) compared to other units with the average power generated of 41.64 GWh. This early failure is believed to have been due to a defect that differed from common causes of generator failure. Therefore, if this unexpected failure were considered in the analysis (with its relatively modest population size), it could potentially lead to an implication of an approximately constant hazard function in generator life, which is incompatible with the known dominant ageing failure mode. Thus, we considered this early failure to be still in service at the time of failure.

For additional qualitative insights into the characteristics of the turbines under study, a January 2015 power curve of a failed generator (T04) is shown in Figure 2.3.3. Here, 10-minute averaged, data points from T04 in January 2015 are used. This was a few months before complete failure occurred. It is worth noting that the data points far from the normal distribution might be due to turbine operational fault conditions.



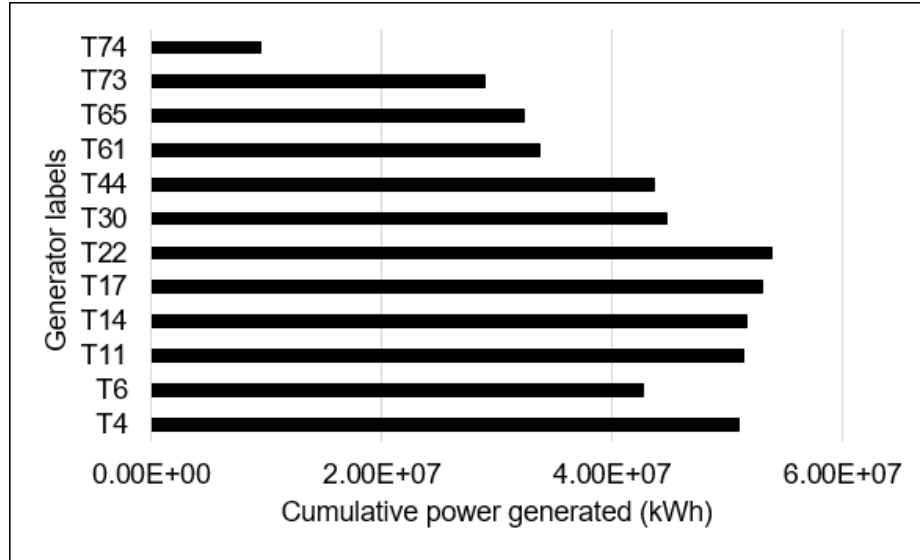


FIGURE 2.3.2: Cumulative power generated (kWh) by the failed generator at the time of failure

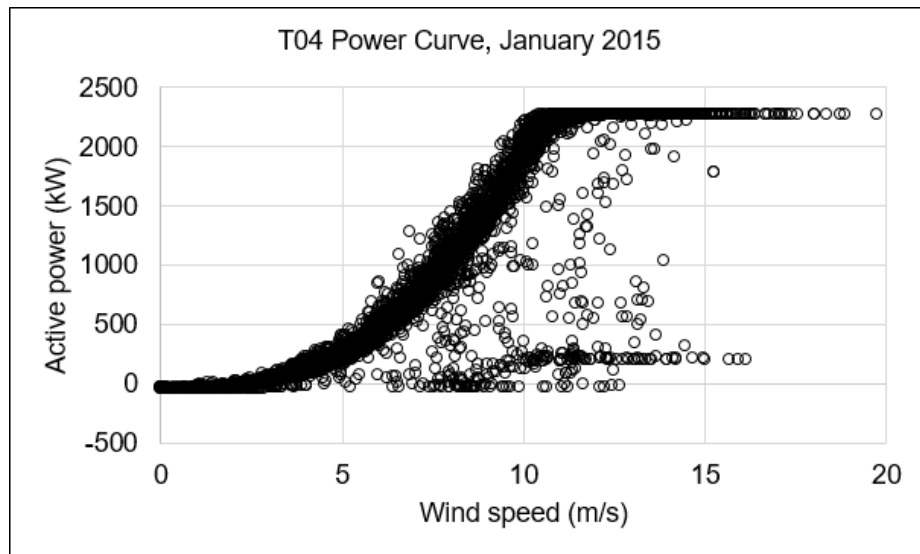


FIGURE 2.3.3: Power curve of wind Turbine T04 in January 2015

### 2.3.2 The proposed nonparametric life data analysis

In this section, based on the type of available data, the Kaplan-Meier method, Equation 2.2.1, is employed to estimate reliability for the population of generators. Figure 2.3.4 indicates the population reliability estimates at data points where individual failures occurred. It shows that the population of generators exhibits a slow decline in reliability over the course of years. It is worth mentioning that the dots on the plot show the reliability estimates and the triangles show the lower 1-sided confidence bounds of the estimates and the upper 1-sided confidence bounds. The calculated reliability values are illustrated in Table 2.3.1. The results show that the reliability of the generators at around three and a half years of operation is estimated to be 98.9 %; however, by seven years of operation, the reliability estimate is around 79.0 % and may be as low as 67.9 %. It is concluded that the reliability estimate for the wind turbine generators under study decreased totally by about 20 percent when time of operation increased from about 3.5 years to 7 years, at its limit this estimate was as high as 26 percent.

Since nonparametric analysis is not able to provide reliability predictions outside of the points of observation, it is feasible to utilize parametric analysis, and fit a distribution to the free-form data set in order to interpolate (and to some extent, extrapolate) the life characteristics of the component.

TABLE 2.3.1: Population reliability estimates at data points in which individual failures occurred, nonparametric results

<b>Time(yr.)</b>	<b>Lower Bound</b>	<b>Reliability</b>	<b>Upper Bound</b>
3.56	0.943	0.989	0.998
3.85	0.930	0.977	0.993
3.97	0.915	0.966	0.987
5.28	0.889	0.950	0.978
5.77	0.852	0.927	0.966
5.81	0.820	0.905	0.953
5.82	0.791	0.883	0.938
6.42	0.763	0.861	0.923
6.52	0.736	0.839	0.907
6.63	0.710	0.817	0.891
7.00	0.679	0.792	0.872

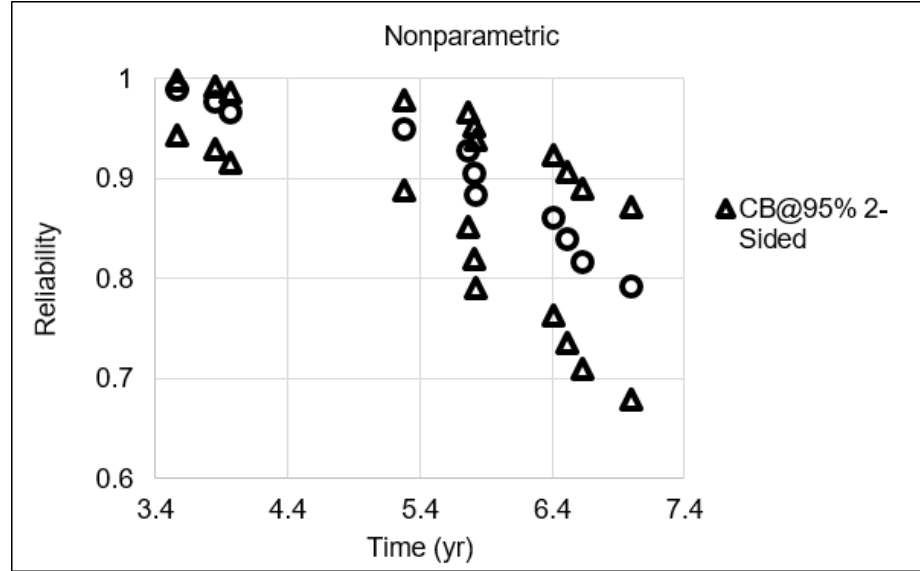


FIGURE 2.3.4: Population reliability estimates at data points in which individual failures occurred, nonparametric results

### 2.3.3 The proposed parametric life data analysis

In this section, first, parametric analysis methods are employed for the reliability estimation of generators using experimental data. Then, root mean square error (RMSE) is estimated that indicates which distribution model best fits the generator truncated data records and which parameter estimation method best approximates the distribution function parameters. Finally, a sensitivity analysis is proposed to relate the generator failure rate to varying loads.

Here, Weibull Standard Folio life data analysis is employed to project the future behaviour of the generator population. For this purpose, first, distribution models, presented in Table 2.2.1, are compared by calculating RMSE to find the one most suitable. As a result, Table 2.3.2 indicates RMSE estimates for each model. It is clear from Table 2.3.2 that 3P-Weibull has the lowest RMSE and, therefore, is the most suitable model for fitting generator truncated data sets. As an example, the probability line with respect to the values obtained from 3P-Weibull and 1P-Exponential are plotted in Figures 2.3.5 and 2.3.6, respectively. It is obvious that the 3P-Weibull provides a better fit to the values compared to the 1P-Exponential.

Here, parameter estimation methods are investigated to find the most appropriate one. As a result, Table 2.3.3 indicates RMSE estimates for each method. It is clear from Table

TABLE 2.3.2: RMSE estimates for Weibull distribution models

Distribution model	RMSE
1P-Exponential	4.5556
2P-Weibull	2.4256
3P-Weibull	1.1517
Gamma	1.6218
Gaussian	3.4215
Gumbel	4.2570
Log-normal	2.8865
Logistic	3.8562

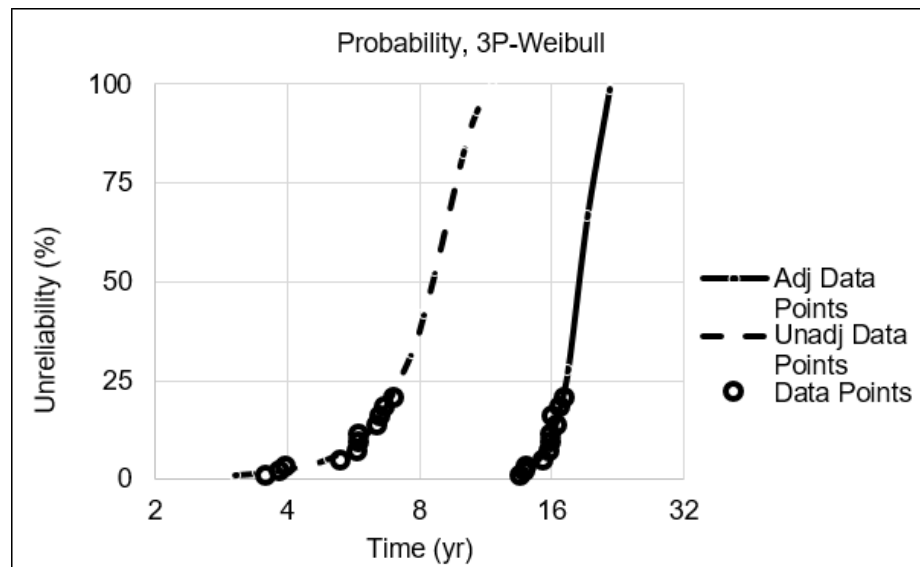


FIGURE 2.3.5: Probability plot, Weibull Standard Folio life data analysis based on 3P-Weibull distribution)

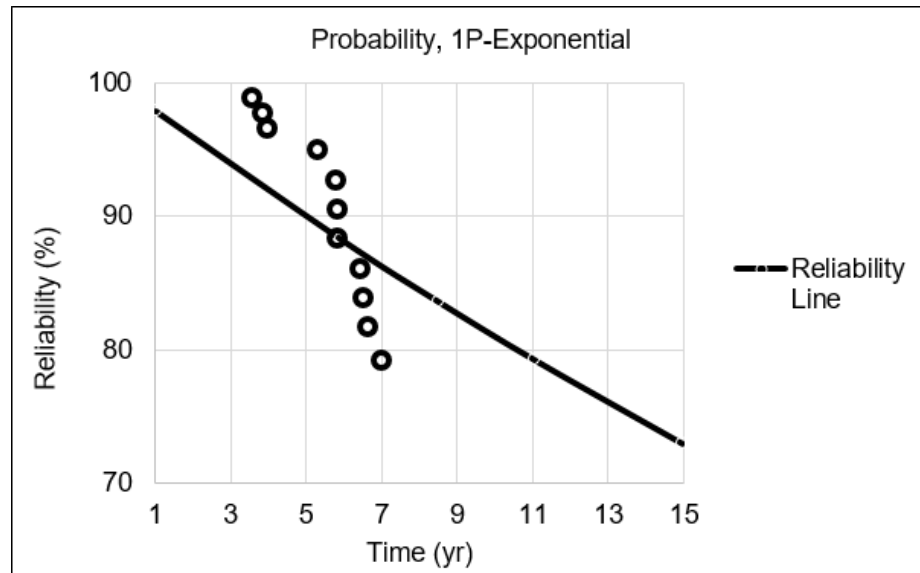


FIGURE 2.3.6: Probability plot, Weibull Standard Folio life data analysis based on 1P-Exponential distribution

2.3.3 that NLRR has more potential than the more classical, MLE, proposed by Gourdin et al. [31]. Where the objective was also the estimation of 3P-Weibull distribution function parameters based on a limited dataset. It may be concluded that small data sets are best analysed with regression, while MLE may be more appropriate for data sets with a large number of suspensions, interval data or several observed failures. The MLE solution tends to be severely biased when implemented on small sample sizes. As the sample size increases, the difference between the two techniques become less important. Factors such as the variability in the data set and the acceptable level of uncertainty or margin of error in the estimates need to be considered when assessing whether the sample dimension is large enough for MLE.

TABLE 2.3.3: RMSE estimates for parameter estimation methods

Parameter estimation method	RMSE
Non-linear rank regression (NLRR)	1.1517
Maximum likelihood estimation (MLE)	4.8628

The probability of failure of the product over time, using a Weibull failure rate, is indicated in Figure 2.3.7. It is clear from the plot that the failure probability rises sharply after around six years of operation, and by ten years of operation, the failure probability estimate

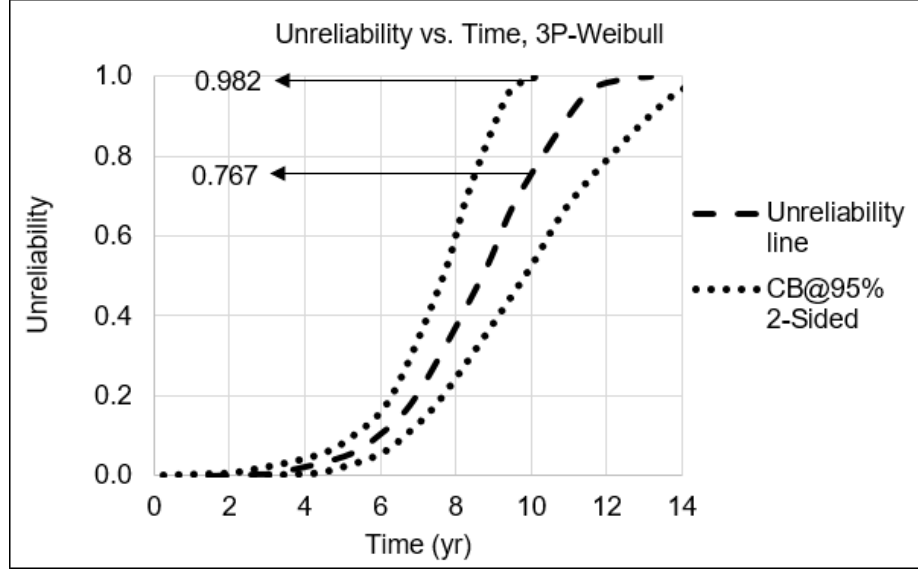


FIGURE 2.3.7: Unreliability vs. Time, Weibull Standard Folio life data analysis based on 3P-Weibull distribution

is around 76.7% and may be as high as 98.2% which is indicated from the top confidence bound. The proposed probability density function and related hazard function for the population of wind farm generators are defined by Equations 2.3.1 and 2.3.2, respectively.

$$f(t) = 0.57 \left( \frac{t + 3.75}{13.1} \right)^{6.5} e^{-\left( \frac{t + 3.75}{13.1} \right)^{7.5}} \quad (2.3.1)$$

$$\lambda(t) = 0.57 \left( \frac{t + 3.75}{13.1} \right)^{6.5} \quad (2.3.2)$$

The required parameters for Naive analysis including the shape parameter, the scale parameter and the location parameter which have been calculated in Weibull Standard Folio life data analysis, since the 3P-Weibull provides a good fit to the values (see Figure 2.3.5), can be found in Table 2.3.4.

Predictions for the remaining life of individual generators achieved by the Naive method are illustrated in Figure 2.3.8. The solid line shows the survival time of generators which are still under operation and the failure time for those which failed, and the dotted line indicates the remaining useful life predicted for those which are still under operation. Such graphs can offer valuable utility where if an imminent failure can be detected early enough,

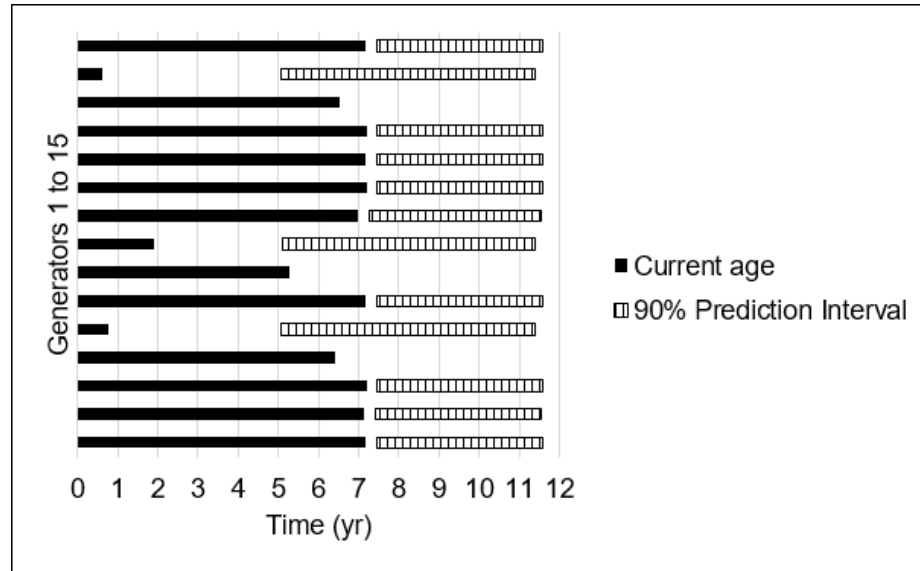


FIGURE 2.3.8: Predictions for the remaining life of 15 generators by the Naive method

the generator can be operated under reduced loading until replaced, to avoid costly catastrophic failures.

TABLE 2.3.4: Reliability estimates for the failures times, nonparametric results

Analysis	NLRR
$\beta$	7.499258
$\eta$ (yr.)	13.092321
$\gamma$	-3.753434
$LK$ Value	-43.898648
$Var. - \beta$	2.683202
$Var. - \eta$	0.612978
$CV.\eta\beta$	-0.999152

In this study, the rate of energy (kWh) generated by each generator over hours of its operation (the average power (kW)) is considered as a stress level. Since the stress level for each generator is available, ALTA can be used to predict the probability of failure for each generator which is still under operation with respect to its average power. According to the type and the number of stresses available, i.e. the average power (kW), the inverse power law, a single-stress model typically used with a non-thermal tension, is chosen for this analysis.

For this purpose, first, IPL distribution models, presented in Table 2.2.2, are compared

by calculating RMSE to find the best fit. As a result, Table 2.3.5 indicates RMSE estimates for each model. It is clear from Table 2.3.5 that the IPL-Lognormal best fits values. We look at the generator with an average power production of 952.66 kW as an example, the probability line with respect to the values obtained from the IPL-Lognormal and IPL-Weibull are plotted in Figures 2.3.9 and 2.3.10, respectively. Inspection of these plots reveals that the IPL-Lognormal reliability provides a better fit to the values compared to the IPL-Weibull.

TABLE 2.3.5: RMSE estimates for ALTA distribution models

Distribution model	RMSE
IPL Lognormal	2.1233
ILP Weibull	3.03367
IPL Exponential	4.3504

The probability of failure of the generator with the average lifetime power production of 952.66 kW is illustrated in Figure 2.3.11. It is evident from the plot that the failure probability increases dramatically after around six years of operation, and by ten years of operation, the failure probability estimate is around 91.4 %. The probability of failure for a generator which failed at the age of 5.8 years is shown in Figure 2.3.12. The probability of failure estimate for this unit with the average generated power of 1015.32 kW is notable

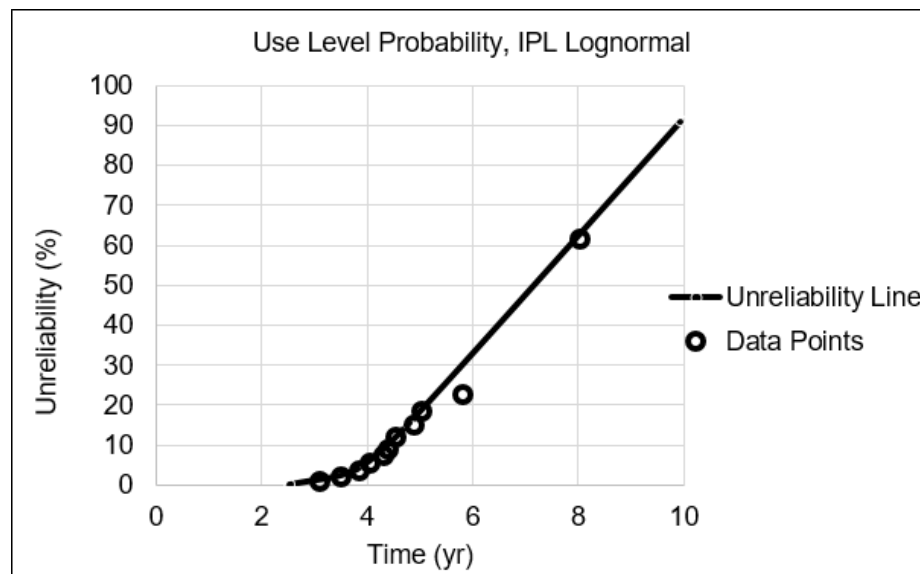


FIGURE 2.3.9: Use Level Probability plot for the generator with 952.66 kW, ALTA Standard Folio life data analysis (IPL-Lognormal)



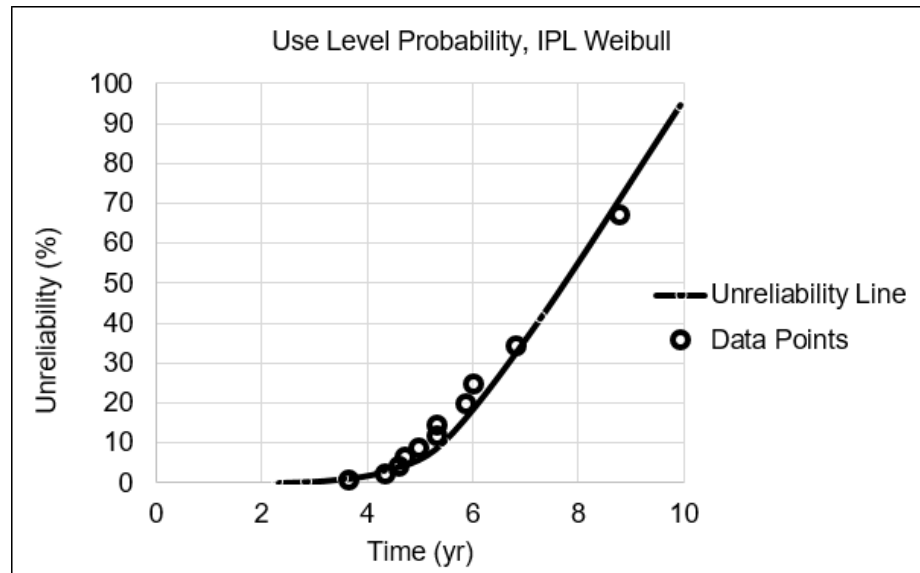


FIGURE 2.3.10: Use Level Probability plot for the generator with 952.66 kW, ALTA Standard Folio life data analysis (IPL-Weibull)

at 73.9 % at the age of failure.

The results of this technique have been compared to the Naive results. For instance, for the generator with the average power of 952.7 kW, the Naive predicts 11 years of operation with 91.4 % probability of failure (as shown in Figure 2.3.13 with dotted line) which is more than ALTA prediction with ten years of operation (as illustrated in Figure 2.3.11 with dash line). This could be due to the consideration of power as stress in ALTA technique.

### Sensitivity Analysis

Here we suggest that typically higher average generated power (electrical load), would imply larger mechanical load and thus the more likely failure is. To indicate that the probability of failure of individual generators with varying average power generated at 10 years of operation are estimated and compared in Table 2.3.6.

The probability plots, for instance, for two of the generators with stress levels of 952.7 kW (dash line) and 853.73 kW (dotted line) are shown in Figure 2.3.14. This plot reveals that by ten years of operation the probability of failure estimate for the generator with the average generated power of 952.7 kW is 91.4 %, and with the average generated power of 853.73 kW would be around 33 %. As shown in Figure 2.3.14, the higher the average

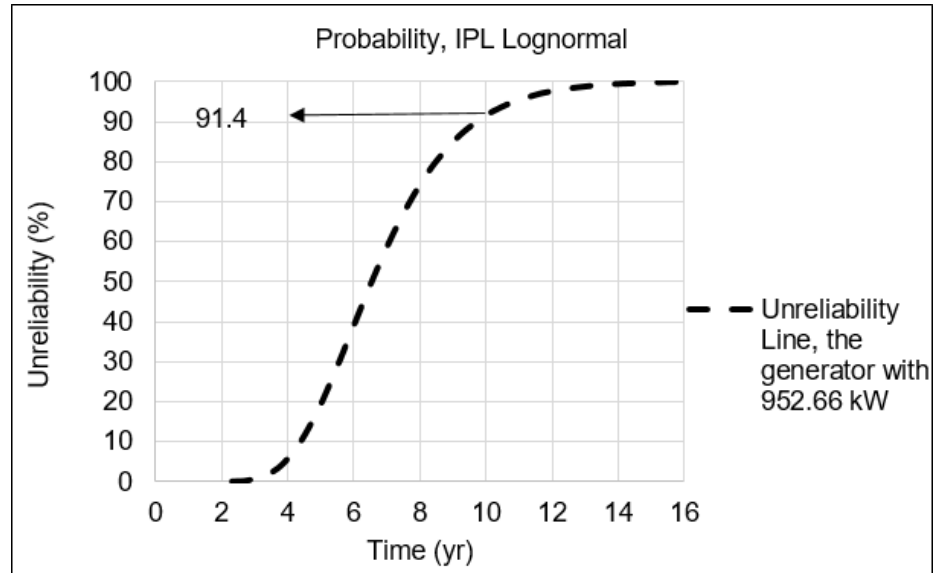


FIGURE 2.3.11: Unreliability vs. Time for the generator with 952.66 kW, ALTA Standard Folio life data analysis

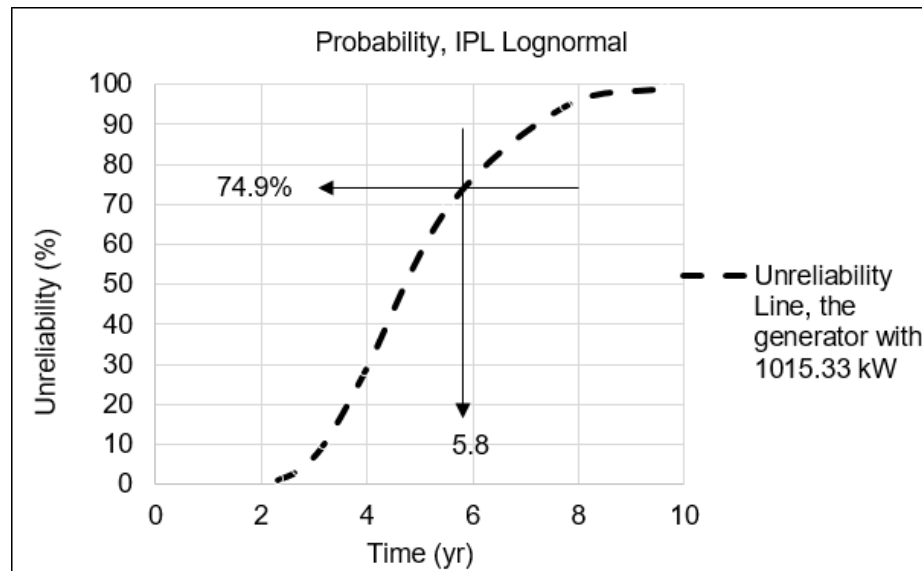


FIGURE 2.3.12: The probability of failure for the generator with 1015.33 kW, failed at the age of 5.8 years

## 2. AGGREGATE RELIABILITY ANALYSIS OF WIND TURBINE GENERATORS

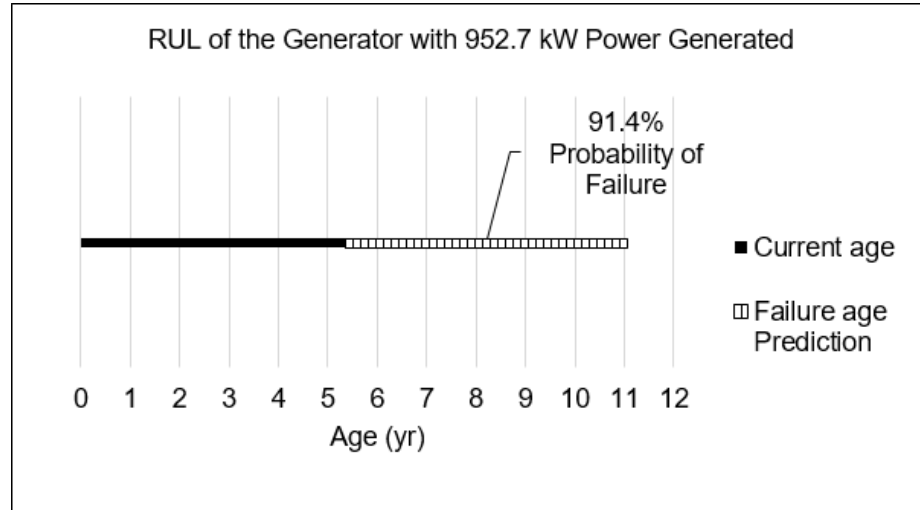


FIGURE 2.3.13: The Naive Predictions for the remaining life of the generators with the average power of 952.7 kW

TABLE 2.3.6: The probability of failure of individual generators with varying average power generated at 10 years of operation

Average power generated (kW)	The probability of failure at 10 years of operation
801.28	18.4 %
853.73	33 %
922.4	80.61 %
952.66	91.4 %
1015.33	100 %

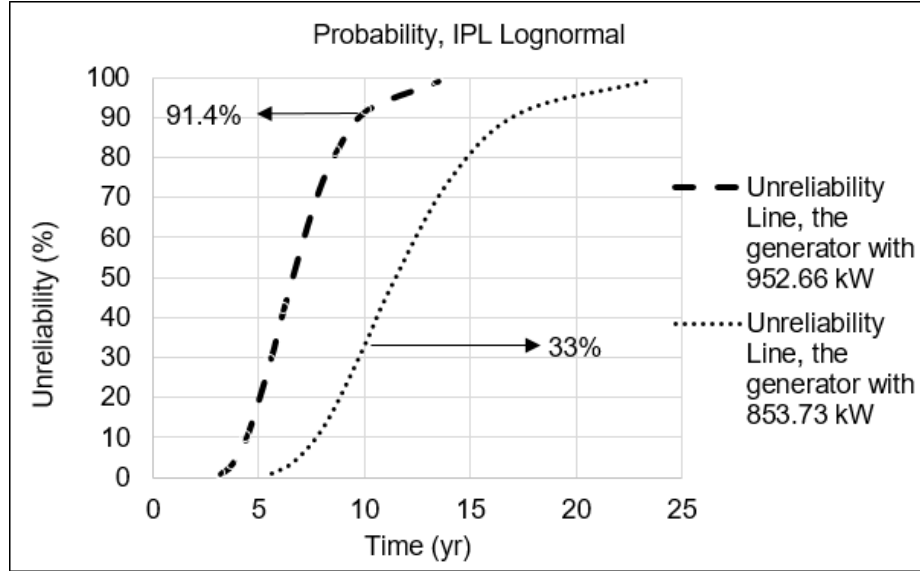


FIGURE 2.3.14: The probability of failure for generators with two different generated power

generated power, the more likely failure is. This implies that the probability of failure for a wind turbine generator increased by about 58 percent with a 12 percent increase in the 10-year average power production for that machine. This suggested in our study that the higher the average generated power over a generator lifetime, the more likely failure is.

## 2.4 Conclusion and areas for future research

This study investigated reliability metrics for a set of truncated wind turbine generator data records. The generators were from a 100 MW wind farm that is less than half way through its originally projected 20-year service life. The proposed approach employed different life data analysis methods including Weibull and ALTA. It was shown that 3P-Weibull and IPL-Lognormal were the best fitted distribution models of the Weibull and ALTA analyses, respectively. Their fit to the limited data sets was better than other distribution models proposed in other studies. It was indicated that small data sets are best analysed with regression methods over MLE. A sensitivity analysis was developed which showed that higher average generated power (electricity load) would increase the likelihood of failure for this population. As a result, a probability density function and related hazard function was pro-

posed for the generator group studied. The experimental results illustrate the capability of the proposed method in the estimation of failure rate when truncated data records are what is available.

Prediction of remaining life, achieved by the Naive method in this study has value when utilized to achieve early detection. In these cases, generators can be operated under reduced loading until replaced, to avoid costly catastrophic failures. Furthermore, predictions for the remaining life of individual generators achieved by this method can provide a basis for obtaining a more refined life range estimate.

This study provides valuable high level insights into utility scale wind turbine generator reliability for a limited data set. Outcomes built from this work may help the research community with the development of investment decision support mechanisms designed to optimize the value of wind farming. The work also highlights useful tools for potential wind farm prognostic maintenance. This study also contributed to identifying how electrical loads may affect wind turbine generator reliability and how it accelerated their failure rate for our data. The process presented in this study shows how to move forward estimating turbine component remaining useful life based on truncated/limited data records. It is worth noting that proactive maintenance actions can change the population under study and will subsequently impact the results of an analysis like this.

In future works, the Naive prediction interval procedure will be calibrated to account for statistical uncertainty by using Monte Carlo simulation/bootstrap re-sampling methods. Based on available data, lifetime distributions and remaining life of other critical components will be estimated.

## 2.5 List of Abbreviations

CDF	Cumulative Distribution Function
GP	Gaussian Processes
GWEC	Global Wind Energy Council
IPL	Inverse Power Law
MLE	Maximum Likelihood Estimation
MTTF	Mean Time To Failure
NLRR	Nonlinear Rank Regression
PCA	Principal Component Analysis
PD	Power Density
PDF	Probability Density Function
REB	Rolling Element Bearing
RMSE	Root Mean Square Error
RRX	Rank Regression on X
RRY	Rank Regression on Y
SCADA	Supervisory Control and Data Acquisition
TH	Temperature-Humidity
TTF	Time To Failure
WD	Weibull Distribution
WT	Wind Turbine

## REFERENCES

- [1] R. Moeini, P. Tricoli, H. Hemida, and C. Baniotopoulos, “Increasing the reliability of wind turbines using condition monitoring of semiconductor devices: a review,” *IET Renewable Power Generation*, vol. 12, no. 2, pp. 182–189, 2017.
- [2] G. W. E. Council, “Global wind energy outlook 2016: Wind power to dominate power sector growth,” *Global Wind Energy Council, Tech. Rep.*, 2016.
- [3] Q. Gao, C. Liu, B. Xie, and X. Cai, “Evaluation of the mainstream wind turbine concepts considering their reliabilities,” *IET Renewable Power Generation*, vol. 6, no. 5, pp. 348–357, 2012.
- [4] M. Shafiee and F. Dinmohammadi, “An fmea-based risk assessment approach for wind turbine systems: a comparative study of onshore and offshore,” *Energies*, vol. 7, no. 2, pp. 619–642, 2014.
- [5] N. Chen, R. Yu, Y. Chen, and H. Xie, “Hierarchical method for wind turbine prognosis using scada data,” *IET Renewable Power Generation*, vol. 11, no. 4, pp. 403–410, 2016.
- [6] B. Hahn, M. Durstewitz, and K. Rohrig, “Reliability of wind turbines, experiences of 15 years with 1,500 wts, in ‘wind energy,” in *Proceedings of the Euromech Colloquium*. Springer-Verlag Berlin Heidelberg, 2007, pp. 329–332.
- [7] A. Stenberg and H. Holttinen, “Analysing failure statistics of wind turbines in finland,” in *European Wind Energy Conference, April*, 2010, pp. 20–23.
- [8] Y. Sun, P. Wang, L. Cheng, and H. Liu, “Operational reliability assessment of power systems considering condition-dependent failure rate,” *IET generation, transmission & distribution*, vol. 4, no. 1, pp. 60–72, 2010.
- [9] F. Spinato, P. J. Tavner, G. Van Bussel, and E. Koutoulakos, “Reliability of wind turbine subassemblies,” *IET Renewable Power Generation*, vol. 3, no. 4, pp. 387–401, 2009.

- [10] V. Kumar, L. Singh, and A. K. Tripathi, "Reliability analysis of safety-critical and control systems: a state-of-the-art review," *IET Software*, vol. 12, no. 1, pp. 1–18, 2017.
- [11] P. O'Connor and L. Harris, "Reliability prediction: a state-of-the-art review," *IEE Proceedings A (Physical Science, Measurement and Instrumentation, Management and Education, Reviews)*, vol. 133, no. 4, pp. 202–216, 1986.
- [12] P. Giorsetto and K. F. Utsurogi, "Development of a new procedure for reliability modeling of wind turbine generators," *IEEE transactions on power apparatus and systems*, no. 1, pp. 134–143, 1983.
- [13] K. Fitzgibbon, R. Barker, T. Clayton, and N. Wilson, "A failure-forecast method based on weibull and statistical-pattern analysis," in *Annual Reliability and Maintainability Symposium. 2002 Proceedings (Cat. No. 02CH37318)*. IEEE, 2002, pp. 516–521.
- [14] T. D. Batzel and D. C. Swanson, "Prognostic health management of aircraft power generators," *IEEE Transactions on Aerospace and Electronic Systems*, vol. 45, no. 2, pp. 473–482, 2009.
- [15] W. Yang, P. Tavner, and M. Wilkinson, "Condition monitoring and fault diagnosis of a wind turbine synchronous generator drive train," *IET Renewable Power Generation*, vol. 3, no. 1, pp. 1–11, 2009.
- [16] H. Guo, S. Watson, P. Tavner, and J. Xiang, "Reliability analysis for wind turbines with incomplete failure data collected from after the date of initial installation," *Reliability Engineering & System Safety*, vol. 94, no. 6, pp. 1057–1063, 2009.
- [17] Y. Hong, W. Q. Meeker, J. D. McCalley *et al.*, "Prediction of remaining life of power transformers based on left truncated and right censored lifetime data," *The Annals of Applied Statistics*, vol. 3, no. 2, pp. 857–879, 2009.
- [18] J. He, X. Xiao, R. Zhong, W. Huang, D. Li, and Q. Chen, "New ac & dc hybrid power supply system and its reliability analysis in data centre," *The Journal of Engineering*, vol. 2019, no. 16, pp. 2800–2803, 2019.



- [19] J. Sikorska, M. Hodkiewicz, and L. Ma, “Prognostic modelling options for remaining useful life estimation by industry,” *Mechanical systems and signal processing*, vol. 25, no. 5, pp. 1803–1836, 2011.
- [20] Y. Wang and D. Infield, “Supervisory control and data acquisition data-based non-linear state estimation technique for wind turbine gearbox condition monitoring,” *IET Renewable Power Generation*, vol. 7, no. 4, pp. 350–358, 2013.
- [21] C. Okoh, R. Roy, J. Mehnen, and L. Redding, “Overview of remaining useful life prediction techniques in through-life engineering services,” *Procedia CIRP*, vol. 16, pp. 158–163, 2014.
- [22] S. Sankararaman, M. J. Daigle, and K. Goebel, “Uncertainty quantification in remaining useful life prediction using first-order reliability methods,” *IEEE Transactions on Reliability*, vol. 63, no. 2, pp. 603–619, 2014.
- [23] S. A. Akdağ and A. Dinler, “A new method to estimate weibull parameters for wind energy applications,” *Energy conversion and management*, vol. 50, no. 7, pp. 1761–1766, 2009.
- [24] J. B. Ali, B. Chebel-Morello, L. Saidi, S. Malinowski, and F. Fnaiech, “Accurate bearing remaining useful life prediction based on weibull distribution and artificial neural network,” *Mechanical Systems and Signal Processing*, vol. 56, pp. 150–172, 2015.
- [25] D. Wang, Q. Miao, Q. Zhou, and G. Zhou, “An intelligent prognostic system for gear performance degradation assessment and remaining useful life estimation,” *Journal of Vibration and Acoustics*, vol. 137, no. 2, p. 021004, 2015.
- [26] B. Chen, P. C. Matthews, and P. J. Tavner, “Automated on-line fault prognosis for wind turbine pitch systems using supervisory control and data acquisition,” *IET Renewable Power Generation*, vol. 9, no. 5, pp. 503–513, 2015.
- [27] W. Q. Meeker and L. A. Escobar, “Statistical methods for reliability data using sas software,” *Technometrics*, vol. 20, no. 3, pp. 245–247, 1978.

- [28] E. T. Lee and J. Wang, *Statistical methods for survival data analysis*. John Wiley & Sons, 2003, vol. 476.
- [29] E. L. Kaplan and P. Meier, “Nonparametric estimation from incomplete observations,” *Journal of the American statistical association*, vol. 53, no. 282, pp. 457–481, 1958.
- [30] V. Coria, S. Maximov, F. Rivas-Dávalos, and C. Melchor-Hernández, “Perturbative method for maximum likelihood estimation of the weibull distribution parameters,” *SpringerPlus*, vol. 5, no. 1, p. 1802, 2016.
- [31] E. Gourdin, P. Hansen, and B. Jaumard, “Finding maximum likelihood estimators for the three-parameter weibull distribution,” *Journal of Global Optimization*, vol. 5, no. 4, pp. 373–397, 1994.

---

## CHAPTER 3

# *A Fault Detection Method for WT Blades Using Recursive PCA and Wavelet-based PDF*

---

### 3.1 Introduction

Wind energy is considered as one of the lowest-cost and fastest growing renewable clean power options. However, downtime and maintenance costs of Wind Turbines (WTs) are critical challenges that need to be addressed if wind energy is to take a more significant share of the renewable energy market [1, 2]. At present, at an estimated 10 – 15% of power generation cost, the maintenance cost of the WTs comprises a relatively high proportion of the total operating costs. Furthermore, a notable percentage of the maintenance cost is often associated with unanticipated faults. These faults also cause extended downtime as heavy components must be carried to a maintenance site which may be far from the wind farm [3].

Condition monitoring is an essential means for reducing the maintenance cost and downtime of the WTs. Condition monitoring can be accomplished by observing the WT measurements such as vibration, electrical quantities (power, voltage, current), temperature, and blade direction to assess the health of the system based on those observations [4].

Fault Detection and Diagnosis (FDD) are indispensable tasks often performed within a condition monitoring system. Generally, FDD methods are categorized into three classes

of model-based, data-driven, and knowledge-based approaches. Model-based FDD techniques including Kalman Filter (KF) [5], Extended Kalman Filter (EKF) [6], Unscented Kalman Filter (UKF) [7], and Particle Filter (PF) [8] often assume that an accurate mathematical representation of the system is available for fault diagnosis. However, obtaining an accurate model of a complex engineering system is challenging in practice. Data-driven FDD methods such as Neural Networks (NN) [9], Adaptive Neuro-Fuzzy Inference System (ANFIS) [10], Aggregate Reliability Analysis [11], Support Vector Machine (SVM) [12] require a large volume of historical data from the system under various operating conditions. The performance of data-driven methods depends on the quality of the data that is available. Knowledge-based FDD methods such as Fuzzy Logic (FL) [13] rely on the knowledge of experts about the system under consideration. The weakness of this class of techniques stems from the fact that the knowledge from an expert is either expensive to capture or may not be accessible in many instances.

Amongst the data based approaches, those based on Principal Component Analysis (PCA) have proven to be capable of developing wind turbine fault detection to differentiate between healthy and unhealthy component conditions [14, 15, 16, 17]. In Fang and Guo [18], PCA is utilized to model the wind turbine tower vibration, hence, providing a good insight into the tower vibration dynamic properties. The proposed method monitors the operation of the wind turbine by determining the monitoring statistic Hotelling's two-sample ( $T^2$ ) and Squared Prediction Error (SPE) to detect abnormalities and the origin of the fault. Experimental results show the effectiveness of the suggested fault detection approach. Wang et al. [19] proposes an algorithm using PCA to select an optimal set of variables while still capturing the variation of data in the original dataset. The paper employs selected variables to detect wind turbine faults, to determine the corresponding time and location where the fault occurs, and to estimate the severity of the faults. Results confirm that the proposed technique can choose a reduced set of variables with minimum information loss while detecting faults efficiently and effectively.

Blade fault detection has recently become an essential topic of research. An NN based fault detection system is developed in Bangalore et. al. [20] to detect any anomaly in the SCADA data. Their work applies preprocessing and post-processing to achieve high

accuracy of the fault detection. Schlechtingen and Santos [21] introduced an ANFIS to determine whether or not a specific wind turbine is operating in a healthy mode. A fuzzy approach is proposed by Li et. al. [22] for fault diagnosis of wind turbine blades. The results show that the suggested FL method accurately detects the fault. A wavelet transform-based method is employed by Tsai et. al. [23] to improve the fault detection ability of wind turbine blades using time-frequency localization features embedded in the wavelets. Test results indicate the practicality of the proposed method for blades fault diagnosis application. An Acoustic Emission (AE) monitoring technique is developed by Joosse et. al. [24] for the test of fiber composite blades to identify damaged states and evaluate blade conditions. The test results prove the effectiveness of the proposed detection method.

In Jorgensen et. al. [25], an AE is employed to investigate the blade for irregularities. The results indicate that the AE method is promising and helpful in blade damage detection. In Park et. al. [26], a new laser ultrasonic imaging approach is introduced for rotating blades fault diagnosis. The effectiveness of the imaging procedure is verified by visualizing ultrasonic wave distribution on a rotating steel blade. The results show that the damage is successfully identified and its visibility is improved by applying the standing wave filter. Kirikera et. al. [27] develop a Structural Neural System (SNS) based on AE monitoring for low-cost Structural Health Monitoring (SHM) of wind turbine blades. The results show the capability of SNS in identifying where the damage is initiated or how the damage is propagated. In Dutton [28], a thermoelastic stress analysis approach is developed for blade damage detection. The results show the ability of the proposed method to verify the overall stress propagation at the blade surface as well as growing damage detection. Rumsey and Paquette [29] introduce several SHM techniques for detecting blade fault. The SHM techniques are evaluated using blade AE data, and the test results show the effectiveness of the proposed method. A hybrid method including wavelet transform and Ensemble Empirical Mode Decomposition (EEMD) technique is presented by Bouhali et. al. [30] for early identification of blade state. Experimental results confirm that the proposed method efficiently detects blade faults. In Munoz et. al. [31], a combination of ultrasonic techniques and wavelet transform is presented for detecting ice on the blades. A real case study reveals the system's detection capability regardless of whether the blade is covered with ice or not.

This research work falls into the data-driven category and is based on real data from a wind farm located in southwestern Ontario, in Canada. The following is known about the particular wind farm in Ontario:

1. Real-time SCADA measurement data from various sensors is recorded. Measurements are sent to the Turbine Condition Monitoring (TCM) site server in the wind farm station and are accessed through the TCM site server.
2. Raw data contains noisy and missing values. Therefore, a proper preprocessing method is required before the fault detection procedure is initiated.

The primary goal of this work is to detect the blade faults in an early stage. The blades operate in a harsh environment with wind gusts, water inclusions, sand particle erosion, icing, and atmospheric oxidation [32]. These conditions can initiate minor faults such as cracks, fatigue, increased surface roughness, and reduced stiffness which may grow slowly at first, but then, over time leading to the deformation and breakage of the blades; hence, significantly affecting the wind turbine performance. Therefore, early fault detection for wind turbine blades is essential, yet a challenging task.

In this research work, we introduce a new hybrid fault detection system based on Generalized Regression Neural Network Ensemble for Single Imputation (GRNN-ESI) algorithm, recursive PCA and wavelet-based PDF to detect incipient blade faults in the WTs. Towards this, a preprocessing is performed to exclude noise and impute the missing measurements' values. Then, the recursive PCA method is employed to reduce the data dimension and obtain enriched features. Finally, the wavelet-based PDF allows the FDD system to detect blade faults. The original contributions of this study are:

1. Early fault detection is possible thanks to the utilization of the wavelet-based PDF method, which can accurately estimate the probability density functions of Principal Components (PCs) and consequently detect the incipient faults.
2. Using the GRNN-ESI algorithm to efficiently impute the missing data, noise, and disturbances, and therefore intensify the hybrid method accuracy.

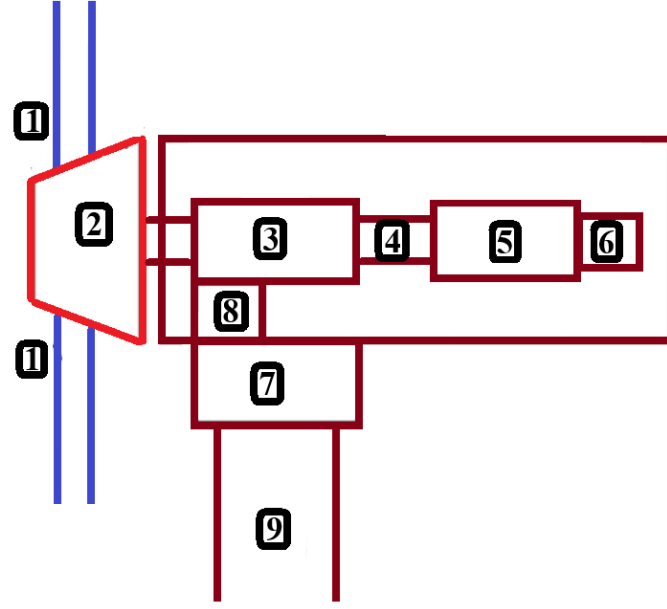


FIGURE 3.2.1: Various components of a typical wind turbine

3. Implementation of a recursive PCA technique that extracts low dimensional features from the SCADA data is novel as well. It recursively captures the failure dynamics and improves the failure detection accuracy.

This chapter is organized as follows: Section 3.2 demonstrates the description of the wind turbine system. The primary theory of the proposed hybrid method is provided in Section 3.3. Section 3.4 explains the design implementation of the hybrid method and illustrates the experimental test results. A summary of the outcomes is presented in Section 3.5.

## 3.2 Wind farm description

Wind turbines are electromechanical machines that convert the kinetic energy of wind into electrical power. They often have a complex structure including several components: 1) blades, 2) rotor, 3) gearbox, 4) shaft 5) generator, 6) controller, 7) yaw drive and motor, 8) brake and 9) tower. Figure 3.2.1 depicts various components of a typical wind turbine.

In this research work, the SCADA data from a wind farm in southwestern Ontario is

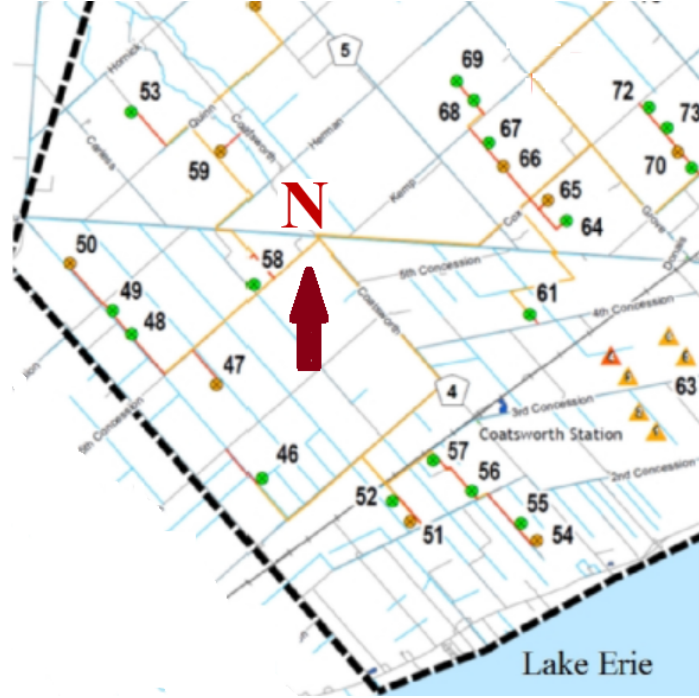


FIGURE 3.2.2: The layout of the wind farm

used. Figure 3.2.2 shows the layout of the particular wind farm.

### 3.3 Primary theory of the proposed hybrid fault detection method

This section introduces a primary theory of the proposed hybrid system for detecting WT blade fault. Figure 3.3.1 demonstrates the hybrid fault detection method.

The proposed hybrid fault detection consists of data collection, preprocessing of the data, recursive PCA, and wavelet-based PDF methods. In the following, first, the preprocessing phase using the GRNN-ESI method is illustrated. Then, the recursive PCA is developed. Finally, the wavelet-based PDF method is introduced.

#### 3.3.1 Preprocessing of the data using the GRNN-ESI

The SCADA system gathers data from various sensors in the wind farm. However, the data acquisition system is not ideal due to instruments errors and disturbance in the sys-



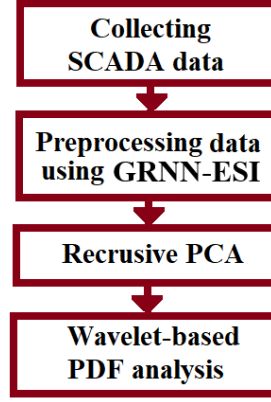


FIGURE 3.3.1: The proposed hybrid fault detection method

tem. Moreover, wind farm operators often turn off the WTs during low demand periods or harsh conditions. As a result, the recorded data often contains noisy values, incorrect measurements, and missing values that it may lead to less accurate estimation [33, 34]. The GRNN-ESI algorithm is a robust preprocessing technique for dealing with incomplete or noisy data [35]. The GRNN-ESI algorithm, explained in Algorithm 1, constructs an ensemble model of Generalized Regression Neural Networks (GRNN) [36], presented in Algorithm 2, and employs a Simulated Annealing Genetic Algorithm (SAGA) to optimize the ensemble makeup.

---

**Algorithm 1** GRNN-ESI method
 

---

- 1) Setting a training dataset with  $m$  variables:  $x^{(1)}, x^{(2)}, \dots, x^{(m)}$  each has  $n$  measurements:  $f = (f_1, f_2, \dots, f_n)$
- 2) Normalizing each variable to the range  $[0, 1]$  using min-max normalization method.
- 3) Constructing of prototype Model-P with a set of models  $P_1, P_2, \dots, P_q$  in which each element is a single ensemble model that estimates the conditional mean of a missing value in an iterative EM-style algorithm including two steps:

- M-step: fitting one model for each of the  $n$  missing values using GRNN.
- E-step: Computing missing values using the models fitted in the first M-step

Note that  $q$  is the number of missing values.

---

In Algorithm 1, the following points are to be taken into consideration:

1. In the first iteration, the algorithm divides the data into the complete part and incomplete part and then, it fits multiple models on variables with no missing values. Next,

missing values are estimated in the E-step of the first iteration of GRNN-ESI by applying the models fitted in the first M-step. Thus, the first E-step generates a new complete dataset. In the next iterations, the M-step of each iteration fits imputation models for missing values of the original dataset to the data imputed at the E-step of the last iteration. Then, the new imputation models are utilized to re-estimate the missing values of the original matrix in the next E-step; thereby, setting a new matrix which serves as the training sample for the next M-step. The SAGA method is used in each iteration to choose an optimal features subset. The iterations proceed until the conditional means of missing values become stable. Note that the new incoming data goes through the same process.

2. The proposed algorithm GRNN-ESI applies an improved algorithm SAGA [37] for choosing an optimal subset of features for estimating the missing values. Here, SAGA employs a combination of the Simulated Annealing (SA) algorithm and the Genetic Algorithm (GA) to achieve this.

---

**Algorithm 2** GRNN

---

- 1) Considering  $f = (f_1, f_2, \dots, f_n)$  as new input measurements
- 2) Setting a membership value  $g_i$  to  $f$  based on the Euclidean distance  $D$  using  $i^{th}$  prototype pattern  $P_i = (P_{i1}, P_{i2}, \dots, P_{in})$  as follows:

$$D = D(f, P_i) = \sqrt{\sum_{j=1}^n (f_j - P_{ij})^2} \quad (3.3.1)$$

$$g_i = \exp \frac{D^2}{2\sigma^2} \quad (3.3.2)$$

Note that  $n$  is the total number of measurements,  $f_j$  is the value of the  $j^{th}$  feature of the presented pattern,  $P_{ij}$  is the value of the  $j^{th}$  feature of the  $i^{th}$  prototype pattern, and  $\sigma$  is the smoothing function parameter.

- 3) Estimating the missing value  $z$  of the pattern  $f$  using the weighted average of the outputs of all prototype patterns as follows:

$$z = \frac{\sum_i (g_i \times P_i output)}{\sum_i g_i} \quad (3.3.3)$$


---

### 3.3.2 PCA algorithm

The PCA technique is a well-known statistical algorithm for data dimensionality reduction [38, 39]. The PCA performs an orthogonal transformation on the raw data to convert it to a set of linearly uncorrelated values known as Principal Components (PCs). The PCs are arranged in a way that the first component has the highest variance, the second component includes the second high variance and is orthogonal to the first one, and so on. Therefore, the PCA algorithm creates a new data set where all data columns are orthogonal and uncorrelated.

#### Off-line PCA

The PCA technique is an off-line algorithm, which can be computed as explained in Algorithm 3.

---

#### Algorithm 3 Off-line PCA

---

- 1) Setting a training dataset with  $m$  variables:  $x^{(1)}, x^{(2)}, \dots, x^{(m)}$ .
- 2) Calculating mean of the dataset:

$$\mu = \frac{1}{m} \sum_{i=1}^m x^{(i)} \quad (3.3.4)$$

- 3) Constructing a zero-mean dataset by deducting the mean from the dataset  $(x^{(i)} - \mu)$
- 4) Computing the covariance of the dataset:

$$S = \frac{1}{m} \sum_{i=1}^m (x^{(i)} - \mu)(x^{(i)} - \mu)^T \quad (3.3.5)$$

- 5) Computing eigenvectors and eigenvalues of the covariance matrix by using Singular Value Decomposition (SVD) algorithm [40].
  - 6) Sorting eigenvectors using eigenvalues from the highest to the lowest. It allows arranging the components in decreasing order of significance
  - 7) Discarding those components with lower eigenvalues
- 

Therefore, a new compressed dataset will be created by orthogonal transformation using sorted eigenvectors and eigenvalues, then, ignoring those eigenvalues which are smaller than the others. This dataset still holds the main properties of the original dataset and can be used in data mining algorithms when high-quality dataset of lower size is required.

The off-line PCA algorithm is simple, yet prevalent in stationary applications. However, it is not suitable for online applications where the process is non-stationary. To address this issue, the recursive PCA can be employed to track the dynamic behavior of the system.

### Recursive PCA

Here, a recursive PCA is utilized to capture failure dynamics in real-time [41]. To formulate a recursive version for the PCA, consider that there exists a current training set without pre-treatment ( $X_k^p$ ) and its PCs. We need to update the PCA whenever a new block of data becomes available. Algorithm 4 was introduced by Li et. al. [41] for recursive PCA.

It is noted that Eqs. (3.3.9) and (3.3.10) are utilized to compute the augmenting new data block to the previous one and formulate the new correlation matrix. Finally, the new eigenvalues and eigenvectors are computed from steps 4, 5 and 6 in the off-line PCA.

### 3.3.3 Wavelet-based PDF method

PDF can be considered for fault detection purposes. For this aim, PDF is applied to determine the probability of the random variable falling within a particular range of values. PDF can be formulated using Gaussian distribution. In the Gaussian distribution, the mean and the variance of the distribution are calculated to determine its PDF. However, in real industrial applications, it is possible for the variables not to be Gaussian. Thus, it is not realistic to model them with the Gaussian probability formula [42].

In this research work, the a wavelet-based PDF method is utilized to compute the PDF of the variables. This method neither assumes that the variable is Gaussian nor compute the means and variance of the distribution. The PDF of each variable is calculated by wavelet basis function [42].

Wavelet method is implemented using Multi-Resolution Analysis (MRA) to provide a unique framework to analyze a signal and capture its characteristics. Particularly, Wavelet method can estimate a signal using a scaling function  $\phi(t)$  and a wavelet function  $\psi(t)$ . This estimation is formulated, as shown in Algorithm 5.

Figure 3.3.2 presents a typical wavelet-based PDF,  $h(x)$ , for variable  $x$ . It is noted

---

**Algorithm 4** Recursive PCA
 

---

 1) Let  $X_k^p \in \mathbb{R}^{n_k \times m}$  be the last updated training set with the dimension of  $n_k$ .

2) Implementing the data pre-treatment:

- Calculating the means:  $b_k = \frac{1}{n_k} (X_k^p)^T I_{n_k}$ ,  $I_{n_k} = [11\dots 1]^T \in \mathbb{R}^{n_k}$
- Calculating the current standard deviation:  $\Sigma_k = \text{diag}(\sigma_1^{(k)}, \sigma_2^{(k)}, \dots, \sigma_m^{(k)})$
- Calculating the current training set after pre-treatment:  $X_k = (X_k^p - I_{n_k} b_k^T) \Sigma_k^{-1}$

 3) Computing the covariance matrix ( $S_k$ ) of  $X_k$ :

$$S_k = \frac{1}{n_k - 1} (X_k)^T (X_k) \in \mathbb{R}^{m \times m} \quad (3.3.6)$$

 4) Let  $X_{k+1}^p = \begin{pmatrix} X_k^p \\ X_{k+1}^{p*} \end{pmatrix} \in \mathbb{R}^{n_{k+1} \times m}$  be defined as the new training set without a pre-treatment.

5) Implementing the data pre-treatment:

- Calculating the means of this new training set

$$b_{k+1} = \frac{n_k}{n_{k+1}} b_k + \frac{n_{k+1} - n_k}{n_{k+1}} b_{*k} \quad (3.3.7)$$

- Calculating the standard deviations of this new training set

$$\begin{aligned} \Sigma_{k+1} &= \frac{n_k - 1}{n_{k+1} - 1} \Sigma_k + \frac{n_{k+1} - n_k - 1}{n_{k+1} - 1} \Sigma_{*k} \\ &\quad + \frac{n_k}{n_{k+1} - 1} \text{diag}(\Delta b_{k+1} \Delta b_{k+1}^T(i, i)) \end{aligned} \quad (3.3.8)$$

- Calculating the new training set after pre-treatment

$$X_{k+1} = \begin{pmatrix} (X_k \Sigma_k + I_{n_k} \Delta b_{k+1}) \Sigma_k^{-1} \\ X_{*k+1} \end{pmatrix} \quad (3.3.9)$$

 6) Computing the covariance matrix of  $X_{k+1}$ :

$$\begin{aligned} S_{k+1} &= \frac{n_k - 1}{n_{k+1} - 1} \Sigma_{k+1}^{-1} \Sigma_k S_k \Sigma_k \Sigma_{k+1}^{-1} + \frac{n_{k+1} - n_k - 1}{n_{k+1} - 1} S_{*k} \\ &\quad + \frac{n_k}{n_{k+1} - 1} \Sigma_{k+1}^{-1} \Delta b_{k+1} \Delta b_{k+1}^T \Sigma_{k+1}^{-1} \end{aligned} \quad (3.3.10)$$


---

**Algorithm 5** Wavelet-based PDF

1) Formulating PDF function using a scaling function  $\phi(t)$  and a wavelet function  $\psi(t)$ :

$$h(t) = \sum_k a_k \phi_k(t - k) + \sum_k \sum_j d_{j,k} \psi_{j,k}(2^j t - k) \quad (3.3.11)$$

where  $a_k$  and  $d_{j,k}$  represent approximation coefficients and detailed coefficients, respectively. Indices  $k$  and  $j$  denote the translation and dilation factors, respectively.

2) Determination of the approximation coefficients,  $a_k$ , and detailed coefficients,  $d_{j,k}$ , using a filtering procedure [43]:

$$a_k = \langle h(x), \phi_k(x) \rangle = \int \phi_k(x) h(x) dx \quad (3.3.12)$$

$$d_{j,k} = \langle h(x), \psi_{j,k}(x) \rangle = \int \psi_{j,k}(x) h(x) dx \quad (3.3.13)$$

Note that  $h(x)$  denotes a density function, and since  $\int \phi_k(x) h(x) dx$  is the expectation of  $\phi_k(x)$  and  $\int \psi_{j,k}(x) h(x) dx$  is the expectation of  $\psi_{j,k}(x)$ , thus,  $a_k$  and  $d_{j,k}$  are achieved as follows.

$$a_k = \int \phi_k(x) h(x) dx = \frac{1}{n} \sum_{t=1}^n \phi_k(x(t)) \quad (3.3.14)$$

$$d_{j,k} = \int \psi_{j,k}(x) h(x) dx = \frac{1}{n} \sum_{t=1}^n \psi_{j,k}(x(t)) \quad (3.3.15)$$

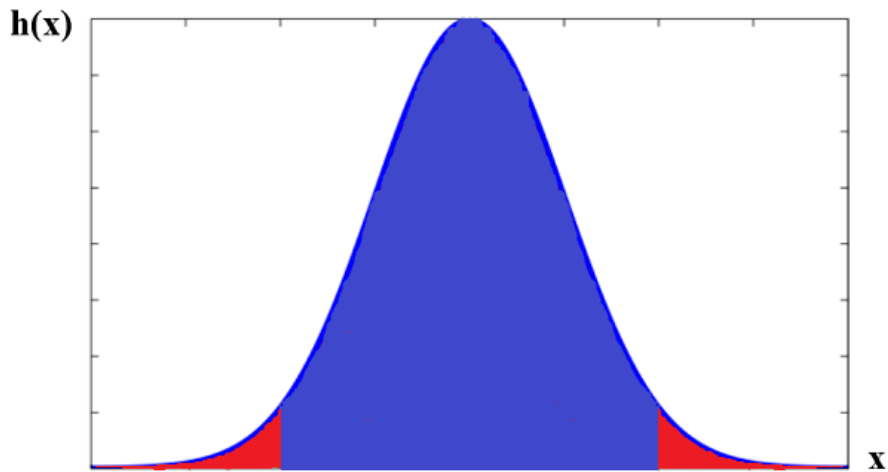


FIGURE 3.3.2: A typical wavelet-based PDF,  $h(x)$ , for variable  $x$ .

from Figure 3.3.2 that when a variable works at its normal operating points and the system is healthy, the PDF ( $h(x)$ ) takes a maximum value in the blue region. However, under an abnormal condition or when a fault occurs, the variable diverges from the normal range and takes a lower value in the red region. Therefore, the probability of staying healthy (the PDF value) at the time of fault begin to decline sharply. We utilize this fact to detect incipient faults in the system.

### 3.4 Simulation and test results

In this section, experimental test studies using SCADA data are considered to evaluate the accuracy of the proposed hybrid fault detection scheme. For this purpose, first, the experimental data collection and fault scenarios are illustrated. After this, the design implementations of the proposed hybrid method and test results are explained.

#### 3.4.1 Experimental data collection and fault scenarios

Blade faults are the most common malfunctions in wind farms [44]. Many WTs face blade faults sooner than original manufacturer specifications due to harsh weather conditions [45].

The major blade faults are outlined below.

1. **Fatigue** initiated by varying wind loading endured by the blades. Long-term fatigue can cause cracks on the surface or in the internal structure of a blade that will lessen the stiffness of the blade [46].
2. **Blade surface roughness** usually triggered by pollution, icing, blowholes, exfoliation, etc. [47].
3. **Deformation** usually caused by consecutive unbalanced loading and lessened stiffness of the blade [48].

Figure 3.4.1 illustrates blade erosion and crack. The defective blades can lead to severe lift reductions and drag increases [49].



FIGURE 3.4.1: Blade erosion (a) and crack (b)

Here, 10-minute single rate SCADA data of a wind farm, including 88 WTs, located in southwestern Ontario is studied. The dataset contains 70 blade faults during 3 years of operation. Various variables from SCADA data are investigated. Table 3.4.1 presents the measurements studied in this research work.

TABLE 3.4.1: Various types of data studied in this work

Number	Data type	Units
1	Active power	kW
2	Wind speed	m/s
3	Rotor speed	RPM
4	Ambient temperature	°C
5	Yaw	deg
6	Blade A pitch angle	deg
7	Blade B pitch angle	deg
8	Blade C pitch angle	deg

### 3.4.2 Design implementations and experimental test results

Design implementation consists of two phases of offline and online. In the offline phase, the first step is data preprocessing. For this aim, missing measurements, noise, and disturbances are estimated and imputed using an iterative EM-style GRNN-ESI technique, presented in Algorithm 1.

Here, the PCA technique is implemented to compress SCADA data. To choose the number of PCs, a cumulative variance of the PCs are computed. Figure 3.4.2 shows the cu-



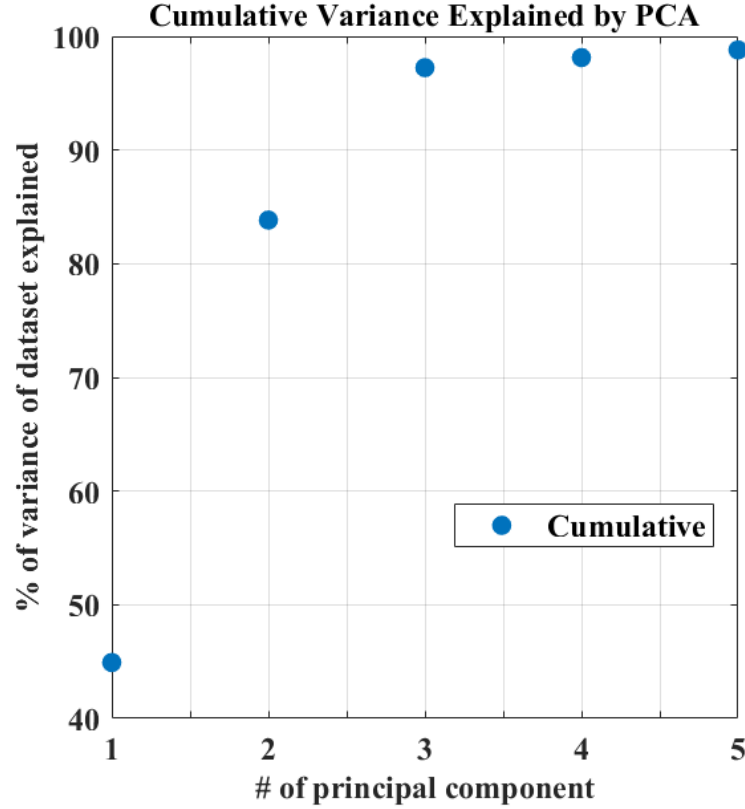


FIGURE 3.4.2: The cumulative variance of the PCs.

cumulative variance of the PCs. It is seen from Figure 3.4.2 that one PC cannot best describe the initial data properties because it captures as low as 45%. It is also clear from Figure 3.4.2 that with two principal components, approximately 84% of the initial input data characteristics is captured. Note that, adding additional components beyond two PCs, increases the complexity of analyzing the result using wavelet-based PDF method. Therefore, two PCs are kept to approximate the data. Then, the eigenvalues and eigenvectors are calculated, using PCA. Afterward, the approximation, and detailed coefficients are computed using Equations (3.3.14) and (3.3.15). Then, PDF is estimated by wavelet-based PDF in Equation (3.3.11) via the two PCs. Here, Daubechies wavelets with a length of five are employed in approximation and detailed coefficients which is due to their proper functionality and performance in estimation and fault diagnosis.

It is worth noting that the variables operate in normal condition most of the time until a failure occurs in the system. Therefore, the PDF of a variable mainly takes a maximum,

which shows a normal operating condition. When a failure occurs, the probability of staying healthy begins to decline, falling below a threshold. This threshold is chosen by trial and error procedure to make a compromise between early detection and false alarm rate.

In the online phase, at each sampling instant, whenever a new data is available, Eqs. (3.3.9) and (3.3.10) are recursively applied to augment new data block to the previous one and obtain the new correlation matrix. Then, the new eigenvalues and eigenvectors are calculated, and the selected PCs are updated at each iteration. Then, the probability of staying healthy is computed using the wavelet-based PDF estimated in the offline phase. If the probability of the failure falls below the defined threshold, the failure will be detected. Figure 3.4.3 illustrates the PDF  $h(x)$  of the first selected PC ( $x$ ), and PDF  $h(y)$  of the second selected PC ( $y$ ). Figure 3.4.3 indicates that the blade stays healthy in 95% of time (blue region). However, whenever a fault occurs, the PCs starts to push away from the normal condition and the probability of healthy blade decreases sharply, falling into the faulty region (red region).

### 3.4.3 Methodology evaluation

To perform a comprehensive analysis of the proposed hybrid method, three metrics including the diagnosis accuracy (ACC), True Positive Rate (TPR) and False Positive Rate (FPR) are introduced as follows:

$$ACC = \frac{TP + TN}{TP + TN + FP + FN} \quad (3.4.1)$$

$$TPR = \frac{TP}{TP + FN} \quad (3.4.2)$$

$$FPR = \frac{FP}{TN + FP} \quad (3.4.3)$$

where  $TP$  and  $FP$  denote the number of true and false classified faults, respectively. Note that  $TN$  and  $FN$  is the number of true and false classified healthy conditions, respectively. Table 3.4.2 discusses the comparison of the proposed hybrid method and SVM

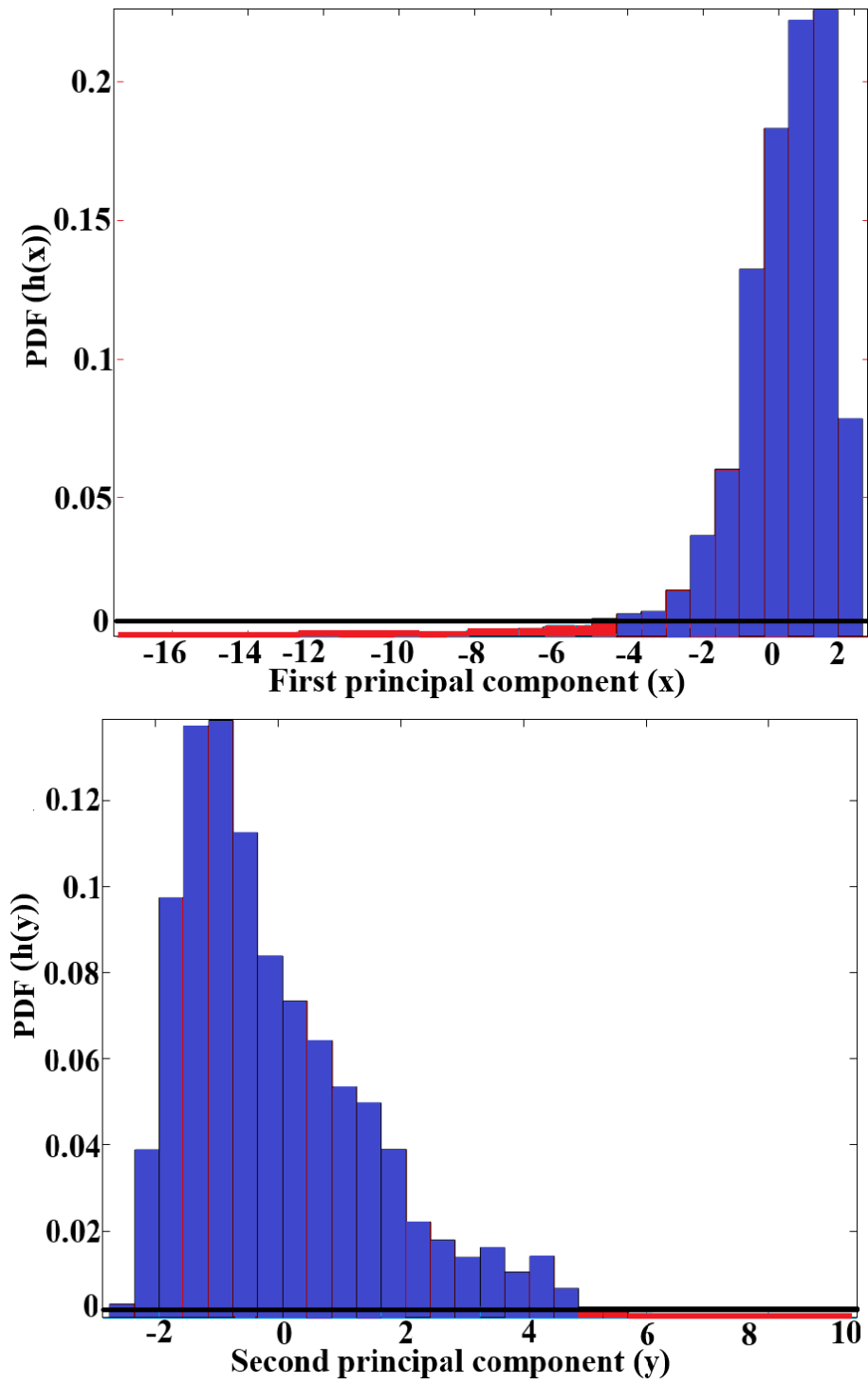


FIGURE 3.4.3: The PDF  $h(x)$  of the first selected PC ( $x$ ), and PDF  $h(y)$  of the second selected PC ( $y$ ).

technique. It is worth noting that 62 WTs are considered as the training set and the remainder as the test set. It is noted from Table 3.4.2 that the proposed method with recursive PCA correctly detect 95.7% of faults with only 33.3% of false classification as a fault, better than the proposed method with conventional PCA and SVM with 93.3% and 90.9% of true classification and 47.1% and 55.6% of false classification as a fault on training set, respectively. The proposed hybrid method with recursive PCA gives the most accurate detection (88.7%) compared to the proposed hybrid method with conventional PCA and SVM technique (82.3% and 77.4% accurate, respectively). Table 3.4.2 also confirms the same trend for the test set.

TABLE 3.4.2: Method evaluation

<b>fault detection method</b>	<b>ACC%</b>	<b>TPR%</b>	<b>FPR%</b>
The proposed method with Recursive PCA (training set)	88.7	95.7	33.3
SVM (training set)	77.4	90.9	55.6
The proposed method with conventional PCA (training set)	82.3	93.3	47.1
The proposed method with Recursive PCA (test set)	80.8	89.5	42.9
SVM (test set)	69.2	83.3	62.5
The proposed method with conventional PCA (test set)	73.1	84.2	57.1

Therefore, it is concluded that the proposed hybrid method provides a more reliable fault detection system by improving the accuracy and reducing the false alarm rate in comparison with the SVM technique. Here, we have also investigated the time response of the proposed hybrid method. The data from a wind turbine, *T72*, installed in 2011 is utilized to evaluate the time response of the detection system. A blade fault occurred in the WT *T72*. For additional qualitative insights into the characteristics of the turbine under study, the power curve of the WT *T72* with a faulty blade in October and November 2017 is shown in Figure 3.4.4. It is worth noting that the data points far from the normal condition might be due to turbine operational fault conditions (see red region). However, these data points could be due to noise, disturbances, or even false alarms, not a failure! Moreover, in the case of a failure, the time of occurrence of a failure cannot be detected from Figure 3.4.4.

Here, a comparison between the fault detection of the proposed method with recursive PCA, with conventional PCA, and SVM method is shown in Figure 3.4.5. Note that Y-axis denotes categorical output variables with two categories: an event of interest (coded as 0

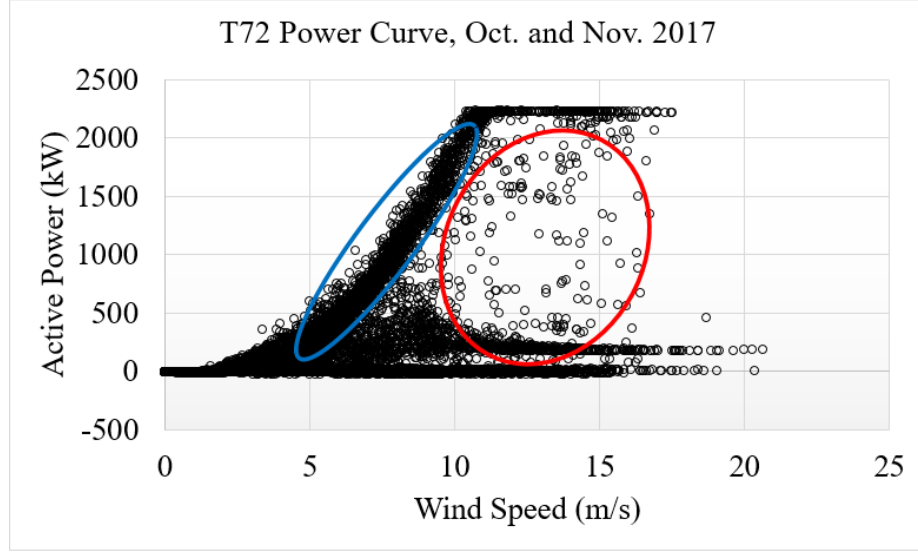


FIGURE 3.4.4: Power curve of wind Turbine T72 in October and November 2017

as a healthy state) or not (coded as 1 as a faulty state). Figure 3.4.5 shows that a blade fault in the WT *T72* was detected by the proposed hybrid fault detection method with recursive PCA on March 6<sup>th</sup> 2018 which indicates an earlier detection compared to SVM method (March 23<sup>rd</sup> 2018) and the proposed hybrid fault detection method with conventional PCA (March 16<sup>th</sup> 2018).

### 3.5 Conclusions and future work

This chapter proposed a new real-time hybrid fault detection strategy for wind turbine blades. The suggested fault detection system employed integrated GRNN-ESI, recursive PCA, and a wavelet-based PDF method to detect incipient faults in an early stage. The GRNN-ESI method dealt with the missing values, noise, and disturbances and, therefore, enhanced the accuracy of the proposed hybrid method. The recursive PCA captured the fault dynamics and reduced the false alarm rate. Afterward, the wavelet-based PDF method accurately estimated the density function of the principal components and detected incipient faults. Experimental test results with SCADA data from a wind farm in southwestern Ontario indicated that the proposed wavelet-based PDF with recursive PCA could not only enhance the reliability of the fault detection, by intensifying the accuracy and lowering the

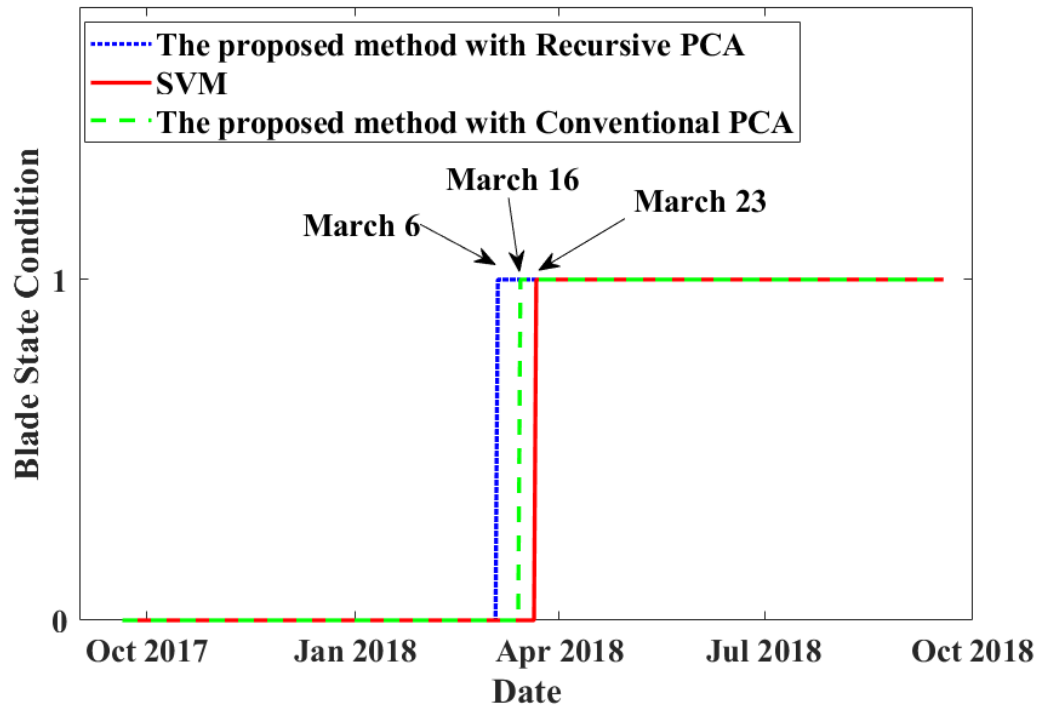


FIGURE 3.4.5: Blade fault detection in the WT *T72*

false alarm rate, but it also improved early detection of blade faults over the wavelet-based PDF with conventional PCA and SVM technique. Finally, some areas for further research are:

1. Expanding the proposed fault detection method by formulating new performance indices to determine the amount of damage to the blade surface.
2. Applying classification methods to identify the type of damage such as crack and erosions in the blade.

### 3.6 List of Abbreviations

AE	Acoustic Emission
ANFIS	Adaptive Neuro-fuzzy inference systems
ARMC	Autoregressive model Coefficient
DSF	Damage Sensitive Features
EKF	Extended Kalman filter
EM	Expectation–Maximization
EEMD	Ensemble Empirical mode decomposition
FDD	Fault detection and diagnosis
FL	Fuzzy logic
FPR	False Positive Rate
GA	Genetic Algorithm
GRNN-ESI	Generalized Regression Neural Network Ensemble for Single Imputation
KF	Kalman filter
MRA	Multi-Resolution Analysis
NN	Neural network
PC	Principal component
PCA	Principal component analysis
PDF	Probability density function
SAGA	Simulated Annealing Genetic Algorithm
SCADA	Supervisory Control and Data Acquisition
SHM	Structural Health Monitoring
SNS	Structural Neural System
SVM	Support Vector Machine
TCM	Turbine Condition Monitoring
TPR	True Positive Rate
UKF	Unscented Kalman Filter
WT	Wind Turbine

## REFERENCES

- [1] P. Qian, X. Ma, D. Zhang, and J. Wang, “Data-driven condition monitoring approaches to improving power output of wind turbines,” *IEEE Transactions on Industrial Electronics*, 2018.
- [2] Z. Hameed, Y. Hong, Y. Cho, S. Ahn, and C. Song, “Condition monitoring and fault detection of wind turbines and related algorithms: A review,” *Renewable and Sustainable energy reviews*, vol. 13, no. 1, pp. 1–39, 2009.
- [3] W. Yang, Z. Lang, and W. Tian, “Condition monitoring and damage location of wind turbine blades by frequency response transmissibility analysis,” *IEEE Transactions on Industrial Electronics*, vol. 62, no. 10, pp. 6558–6564, 2015.
- [4] X. Jin, W. Qiao, Y. Peng, F. Cheng, and L. Qu, “Quantitative evaluation of wind turbine faults under variable operational conditions,” *IEEE Transactions on Industry Applications*, vol. 52, no. 3, pp. 2061–2069, 2016.
- [5] M. Zhong, J. Guo, and Q. Cao, “On designing pmi kalman filter for ins/gps integrated systems with unknown sensor errors,” *IEEE Sensors Journal*, vol. 15, no. 1, pp. 535–544, 2015.
- [6] R. Ibrahim, S. Watson, S. Djurovic, and C. Crabtree, “An effective approach for rotor electrical asymmetry detection in wind turbine dfigs,” *IEEE Transactions on Industrial Electronics*, 2018.
- [7] H. Zhou, Z. Liu, and X. Yang, “Motor torque fault diagnosis for four wheel independent motor-drive vehicle based on unscented kalman filter,” *IEEE Transactions on Vehicular Technology*, vol. 67, no. 3, pp. 1969–1976, 2018.
- [8] F. Cheng, L. Qu, and W. Qiao, “Fault prognosis and remaining useful life prediction of wind turbine gearboxes using current signal analysis,” *IEEE Transactions on Sustainable Energy*, vol. 9, no. 1, pp. 157–167, 2018.



- [9] A. P. Singh, T. S. Kamal, and S. Kumar, "Development of ann-based virtual fault detector for wheatstone bridge-oriented transducers," *IEEE sensors journal*, vol. 5, no. 5, pp. 1043–1049, 2005.
- [10] M. Kordestani, A. Zanj, M. E. Orchard, and M. Saif, "A modular fault diagnosis and prognosis method for hydro-control valve system based on redundancy in multisensor data information," *IEEE Transactions on Reliability*, no. 99, pp. 1–12, 2018.
- [11] M. Rezamand, R. Carriveau, D. Ting, M. Davison, and J. J. Davis, "Aggregate reliability analysis of wind turbine generators," *IET Renewable Power Generation*, 2019.
- [12] S. Zidi, T. Moulahi, and B. Alaya, "Fault detection in wireless sensor networks through svm classifier," *IEEE Sensors Journal*, vol. 18, no. 1, pp. 340–347, 2018.
- [13] D. Agarwal and N. Kishor, "A fuzzy inference-based fault detection scheme using adaptive thresholds for health monitoring of offshore wind-farms," *IEEE Sensors Journal*, vol. 14, no. 11, pp. 3851–3861, 2014.
- [14] Y. Wang and X. Ma, "Optimal sensor selection for wind turbine condition monitoring using multivariate principal component analysis approach," in *18th International Conference on Automation and Computing (ICAC)*. IEEE, 2012, pp. 1–7.
- [15] M. Crespo-Ballesteros and M. Antoniou, "Automatic classification of wind turbine structural faults using doppler radar: Proof of concept study," in *2015 IEEE Radar Conference (RadarCon)*. IEEE, 2015, pp. 0286–0291.
- [16] F. Pozo, Y. Vidal, and Ó. Salgado, "Wind turbine condition monitoring strategy through multiway pca and multivariate inference," *Energies*, vol. 11, no. 4, p. 749, 2018.
- [17] X. Guo, Y. Zhao, and Y. Zhao, "Research on condition monitoring of wind turbines data visualization based on random forest," in *2016 International Conference on Smart Grid and Clean Energy Technologies (ICSGCE)*. IEEE, 2016, pp. 166–170.

- [18] N. Fang and P. Guo, “Wind generator tower vibration fault diagnosis and monitoring based on pca,” in *2013 25th Chinese Control and Decision Conference (CCDC)*. IEEE, 2013, pp. 1924–1929.
- [19] Y. Wang, X. Ma, and P. Qian, “Wind turbine fault detection and identification through pca-based optimal variable selection,” *IEEE Transactions on Sustainable Energy*, vol. 9, no. 4, pp. 1627–1635, 2018.
- [20] P. Bangalore, S. Letzgus, D. Karlsson, and M. Patriksson, “An artificial neural network-based condition monitoring method for wind turbines, with application to the monitoring of the gearbox,” *Wind Energy*, vol. 20, no. 8, pp. 1421–1438, 2017.
- [21] M. Schlechtingen and I. F. Santos, “Condition monitoring with wind turbine scada data using neuro-fuzzy normal behavior models,” in *ASME Turbo Expo 2012: Turbine Technical Conference and Exposition*. American Society of Mechanical Engineers, 2012, pp. 717–726.
- [22] Y. Li, G. Li, and J. Yan, “Fault diagnosis of wind turbine blades based on fuzzy theory,” in *2011 International Conference on Control, Automation and Systems Engineering (CASE)*. IEEE, 2011, pp. 1–3.
- [23] C.-S. Tsai, C.-T. Hsieh, and S.-J. Huang, “Enhancement of damage-detection of wind turbine blades via cwt-based approaches,” *IEEE Transactions on energy conversion*, vol. 21, no. 3, pp. 776–781, 2006.
- [24] P. Joosse, M. Blanch, A. Dutton, D. Kouroussis, T. Philippidis, and P. Vionis, “Acoustic emission monitoring of small wind turbine blades,” in *ASME 2002 Wind Energy Symposium*. American Society of Mechanical Engineers, 2002, pp. 401–411.
- [25] E. R. Jørgensen, K. K. Borum, M. McGugan, C. Thomsen, C. Debel, B. F. Sørensen *et al.*, “Full scale testing of wind turbine blade to failure-flapwise loading,” 2004.
- [26] B. Park, H. Sohn, C.-M. Yeum, and T. C. Truong, “Laser ultrasonic imaging and damage detection for a rotating structure,” *Structural Health Monitoring*, vol. 12, no. 5-6, pp. 494–506, 2013.

- [27] G. R. Kirikera, V. Shinde, M. J. Schulz, M. J. Sundaresan, S. Hughes, J. van Dam, F. Nkrumah, G. Grandhi, and A. Ghoshal, “Monitoring multi-site damage growth during quasi-static testing of a wind turbine blade using a structural neural system,” *Structural Health Monitoring*, vol. 7, no. 2, pp. 157–173, 2008.
- [28] A. Dutton, “Thermoelastic stress measurement and acoustic emission monitoring in wind turbine blade testing,” in *European Wind Energy Conference London*, 2004, pp. 22–25.
- [29] M. A. Rumsey and J. A. Paquette, “Structural health monitoring of wind turbine blades,” in *Smart Sensor Phenomena, Technology, Networks, and Systems 2008*, vol. 6933. International Society for Optics and Photonics, 2008, p. 69330E.
- [30] R. Bouhali, K. Tadjine, H. Bendjama, and M. N. Saadi, “Fault diagnosis of bladed disc using wavelet transform and ensemble empirical mode decomposition,” *Australian Journal of Mechanical Engineering*, pp. 1–11, 2018.
- [31] C. Q. G. Muñoz, A. A. Jiménez, and F. P. G. Márquez, “Wavelet transforms and pattern recognition on ultrasonic guides waves for frozen surface state diagnosis,” *Renewable Energy*, vol. 116, pp. 42–54, 2018.
- [32] M. Nithya, S. Nagarajan, and P. Navaseelan, “Fault detection of wind turbine system using neural networks,” in *Technological Innovations in ICT for Agriculture and Rural Development (TIAR), 2017 IEEE*. IEEE, 2017, pp. 103–108.
- [33] E. Lapira, D. Brisset, H. D. Ardakani, D. Siegel, and J. Lee, “Wind turbine performance assessment using multi-regime modeling approach,” *Renewable Energy*, vol. 45, pp. 86–95, 2012.
- [34] D. McLaughlin, P. Clive, and J. McKenzie, “Staying ahead of the wind power curve,” *Renewable Energy World Magazine*, 2010.
- [35] I. A. Gheyas and L. S. Smith, “A neural network-based framework for the reconstruction of incomplete data sets,” *Neurocomputing*, vol. 73, no. 16-18, pp. 3039–3065, 2010.

- [36] D. F. Specht, "A general regression neural network," *IEEE transactions on neural networks*, vol. 2, no. 6, pp. 568–576, 1991.
- [37] I. A. Gheyas and L. S. Smith, "Feature subset selection in large dimensionality domains," *Pattern recognition*, vol. 43, no. 1, pp. 5–13, 2010.
- [38] M. Morshedizadeh, M. Kordestani, R. Carriveau, D. S.-K. Ting, and M. Saif, "Power production prediction of wind turbines using a fusion of mlp and anfis networks," *IET Renewable Power Generation*, vol. 12, no. 9, pp. 1025–1033, 2018.
- [39] K. Salahshoor, M. Kordestani, and M. S. Khoshro, "Design of online soft sensors based on combined adaptive pca and rbf neural networks," in *2009 IEEE Symposium on Computational Intelligence in Control and Automation*. IEEE, 2009, pp. 89–95.
- [40] K. Baker, "Singular value decomposition tutorial," *The Ohio State University*, vol. 24, 2005.
- [41] W. Li, H. H. Yue, S. Valle-Cervantes, and S. J. Qin, "Recursive pca for adaptive process monitoring," *Journal of process control*, vol. 10, no. 5, pp. 471–486, 2000.
- [42] M. Kordestani, A. A. Safavi, and N. Sharafi, "Two practical performance indexes for monitoring the rhine–meuse delta water network via wavelet-based probability density function," *Neurocomputing*, vol. 177, pp. 469–477, 2016.
- [43] S. G. Mallat, "A theory for multiresolution signal decomposition: the wavelet representation," *IEEE transactions on pattern analysis and machine intelligence*, vol. 11, no. 7, pp. 674–693, 1989.
- [44] C. C. Ciang, J.-R. Lee, and H.-J. Bang, "Structural health monitoring for a wind turbine system: a review of damage detection methods," *Measurement science and technology*, vol. 19, no. 12, p. 122001, 2008.
- [45] J. A. Andrawus and L. Mackay, "Offshore wind turbine blade coating deterioration maintenance model," *Wind Engineering*, vol. 35, no. 5, pp. 551–560, 2011.

- [46] R. Li, W. L. Du, X. J. Shen, and F. X. Li, “Overview of fault detection and state diagnosis technology in wind turbine blades,” in *Applied Mechanics and Materials*, vol. 513. Trans Tech Publ, 2014, pp. 2983–2988.
- [47] W. Qiao and D. Lu, “A survey on wind turbine condition monitoring and fault diagnosis—part i: Components and subsystems,” *IEEE Transactions on Industrial Electronics*, vol. 62, no. 10, pp. 6536–6545, 2015.
- [48] X. Gong and W. Qiao, “Imbalance fault detection of direct-drive wind turbines using generator current signals,” *IEEE Transactions on energy conversion*, vol. 27, no. 2, pp. 468–476, 2012.
- [49] A. Sareen, C. A. Sapre, and M. S. Selig, “Effects of leading edge erosion on wind turbine blade performance,” *Wind Energy*, vol. 17, no. 10, pp. 1531–1542, 2014.

---

## CHAPTER 4

# *A Review of Health Monitoring and Failure Prognosis of Wind Turbine Bearings*

---

### 4.1 Introduction

Wind energy is playing an increasingly pivotal role in global energy systems. According to the Global Wind Energy Council (GWEC)'s report [1], wind energy capacity could reach almost 2.1 TW, supplying up to 20% of global electricity by 2030. Wind is also assuming a nascent and growing role in the expanding ancillary services market associated with evolving grids.

Wind Turbines (WTs) are complex machines, assembled combinations of numerous technologies, operating in challenging environments. As an integrated system, some of the components are more critical than others. So, it is essential to identify components with the highest failure rate and downtime. There have been some fundamental studies in recent decades on the reliability of wind farm components as reviewed below.

Shafiee et al. [2] showed that, for onshore machines, the most frequent failures are related to the tower, gearbox, rotor blades, rotor hub, and the transformer in that order respectively; whereas in offshore settings, the gearbox, rotor blades, generator, tower, and the transformer have the highest failure rates. Hahn et al. [3] indicated that generator, gearbox, drive train and rotor blade have the most downtime according to 1467 WT (below 1 MW) data in the period from 1989 until the end of 2004. In Stenberg and Holttinen [4],

a dataset from 72 operating wind turbines of Finland revealed that the gearbox, hydraulic system, brake, and generator had the most downtime over a period from 1996 to 2008. Reviews of these reliability summary studies reveal that the gearbox and generator failure rates are distinctly high. The downtime for these failures is among the highest of all wind turbine assemblies.

Numerous studies have sought to obtain the distribution of failures by subassembly in WTs [5, 6, 7, 8, 9, 10], they have illustrated that the bearings of gearboxes and generators have significant downtime and subsequently lead to more economic losses for the wind farm operator.

Wind turbine bearings can be subject to defects induced by corrosive, high-speed, and high temperature operating conditions. The performance degradation of a bearing is a continuous irreversible process. Once the bearing is placed in its housing, there are certain expectations of long-term healthy service life. Eventually, minor early faults can arise that grow gradually at the initiation. Then, a major bearing failure in wind turbines can cause catastrophic downtime due to time-consuming reactive maintenance practices. Such lost production directly affects the wind farm bottom line [6]. Bearing defects can be categorized into two groups including distributed and single-point defects. The distributed defect is characterized by degradation over large areas of the surface which become rough, irregular, or deformed. A typical example is the overall surface roughness caused by contamination or lack of lubricant. This type of fault is difficult to identify by distinct frequencies. On the contrary, a single-point defect is localized and can be defined by specific frequencies that typically appear in the machine vibration. A typical example of a localized defect is a pit or spall [11, 12].

Fault detection and failure prognosis, i.e., estimation of Remaining Useful Life (RUL) are a critical area of interest for researchers. For this purpose, appropriate Condition Monitoring Systems (CMS) are essential. Health state assessment can be carried out applying monitoring methods such as Vibration Analysis (VA), acoustic emission, Strain Measurement, Oil Analysis, and thermography. Data is provided at regular time periods using sensors and measurement systems. Defects can be detected and, then, predicted by monitoring and processing the real-time data. Finally, a proper maintenance approach can be sched-

uled based on the degradation trend of failure [13]. It is worth noting among all monitoring systems, VA is the most common method applied to bearings [14].

This chapter presents a literature review of vibration based bearing prognostics. Bearing failure prognosis is categorized, and the most recent literature is summarized and discussed. In each group, the principal concept is illustrated, and the pros and cons are given. Some directions for future studies are also provided.

The work is organized as follows: Section 4.2 demonstrates the definition of prognosis and its approaches. Bearings are described in Section 4.3. Section 4.4 provides a thorough review of bearing prognosis. Section 4.5 concludes the chapter with an emphasis on future research challenges.

## **4.2 Prognosis definition**

The main goal of prognosis is to evaluate how long a faulty component can work under reliable operating conditions, still achieving desired performance metrics [15].

Data-Driven Methods, which transform historical data into relevant models of the degradation's behavior, are widely used in bearing prognosis due to the existence of historical wind farm data. However, a complete set of failure data based on all operating conditions is required to develop thorough and accurate data-driven prognosis methods [16, 17].

## **4.3 Bearings**

Bearings are mechanical elements that play a critical role in the function of rotary machinery. They not only yield relative motion between two parts with minimum friction, such as shaft and housing but these parts also transfer loads from the sources to the structure supporting them [18]. A bearing that transfers loads via rolling elements is expressed as a rolling bearing. Rolling element bearings are categorized into two classes: ball bearings, which transmit the load over a tiny contact surface with the raceway, and roller bearings, which transfer the load via line contact with the raceway. Roller bearings, can support larger loads than ball bearings. Therefore, heavy engineering applications employ roller



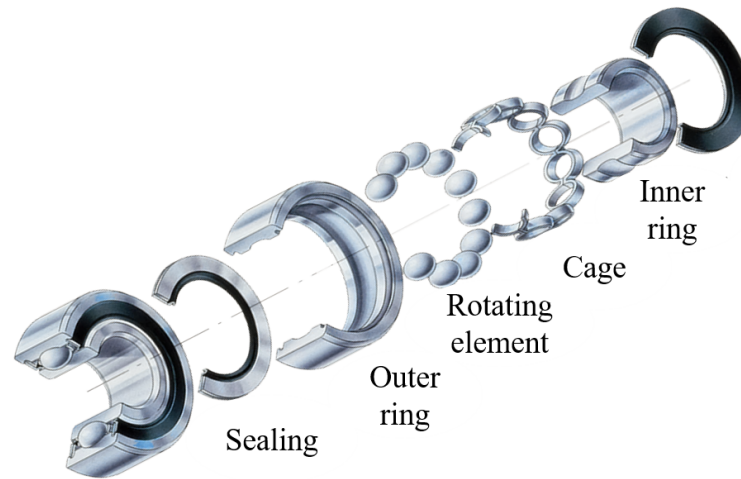


FIGURE 4.3.1: Rolling bearings components

bearings. Rolling bearings as shown in Figure 4.3.1, are comprised of four primary components including rolling elements, inner ring, outer ring, and cage or separator. The guide ring and seals are employed only in some particular bearings. The inner ring is installed on the shaft of the machine, whereas the outer ring is fixed in the housing of the device. The rolling elements, either balls or rollers, rotate against the inner and outer ring raceways and transfer the load acting on the bearing through small surface contacts separated by a thin lubricating film [19, 20]. The cage keeps the rolling elements apart to prevent metal-to-metal contact between them during operation and to decrease the frictional heat generated in the bearing [21].

In the next section, the literature on modeling methods for bearing prognosis is investigated, principally those that are related to vibration-based prognostics of bearings.

## 4.4 Review of bearing prognosis

Some common categories for bearing failure prognosis are studied in the following.

#### 4.4.1 Intelligent method-based prognostics

In this section, intelligent prognostic methods are introduced, and various studies on artificial intelligence failure prognosis of wind turbine bearings are reviewed.

Artificial Neural Networks (ANNs) estimate the RUL of a component using an input-output representative pattern, known as a black box model, derived from observational data. ANNs provide a flexible tool for learning and recognizing system failures due to their ability in learning and generalizing nonlinear relationships between input data and output data [22].

Networks consist of nodes connected in a layered format. A typical neural network is comprised of a single input layer, one or more hidden layers and an output layer, each including one or more nodes. Connections between nodes in adjacent layers are weighted. An activation function is associated with each node that defines if and how information is transferred to the following nodes. Estimated values of each node's function are then used as inputs to any subsequent nodes[23, 24].

ANNs are capable of handling noisy and incomplete data, and once trained can help with prediction and generalization at a high rate [25, 26]. ANNs are effective and efficient at modeling complex non-linear systems. However, they require a significant amount of data for training data that should be representative of the real data range and its variability [15].

In Malhi et al. [27], vibration signals from a defect-seeded rolling bearing were pre-processed using a continuous wavelet transform. The preprocessed data were employed as candidate inputs to a Recurrent Neural Network (RNN) and, then were clustered for effective representation into similar stages of bearing defect propagation. Analysis indicated that the proposed method is more accurate in predicting bearing defect progression than the incremental training technique.

An approach to predict the RUL of bearings in a wind turbine gearbox was proposed by Teng et al. [28]. They took an artificial neural network to train data-driven models and to predict short-term tendencies of feature series. By combining the predicted and training features, a polynomial curve reflecting the long-term degradation process of bearings

was fitted. By determining the intersection between the fitted curve and the pre-defined threshold, the RUL was deduced. The results showed that the combination of the time and frequency features leads to more accurate prognostic results than those available from the individual features.

Xie and Zhang [29] developed a fault prognosis scheme employing an Echo State Network (ESN) and Recurrent Multilayer Perceptron (RMLP), based on the vibration signal of rotating machinery. Both ESN and RMLP are functional forms of a recurrent neural network. The experimental outcomes on faulty bearings demonstrated that these prognostic methods are capable of enhancing the bearing performance forecast within a relatively short time interval and even with limited data availability. It was also indicated that the accuracy of fault prognosis improved considerably.

In Guo et al. [30], an RNN based Health Indicator (RNN-HI) for RUL prediction of bearings was proposed. The performance of the RNN-HI was validated through two experimental bearing data sets. The results indicated that the ability of RNN-HI to obtain better performance than a self-organization map-based method. Cui et al. [31] employed an RNN for rolling bearing fault prognosis. Their results showed that RNN had good results in fault prognosis compared to the traditional methods like probability trend analysis.

A study of wavelet neural network classifier bearing fault diagnosis was presented by Karim et al. [32]. In this work, the statistical features of vibration signals such as standard deviation, kurtosis, and wavelet energy were employed as input to an ANN classifier. The results showed that these parameters could be applied as an operational status indicator to distinguish between a safe operational mode and a defective one. Kramti et al. [33] developed an Elman Neural Network (ENN) architecture for direct RUL estimation of a High-Speed Shaft Bearing (HSSB) validated by use of real measured data. The proposed method indicated accurate estimation capability even with noisy signals and harsh environmental conditions.

Senanayaka et al. [34] used an autoencoder and RNN-based prediction algorithm for the prognosis of bearing life. A two-stage approach using Deep Neural Networks (DNN) is proposed in Xia et al. [35] to estimate the RUL of bearings. A denoising auto encoder-based DNN was employed to classify the acquired signals into different degradation states.

Then, regression models based on shallow neural networks were constructed for each health state. The proposed approach obtained satisfactory prediction performance on a real bearing degradation dataset with different working conditions.

Li et al. [36] proposed an intelligent RUL prediction method based on deep learning. Multi-scale feature extraction was executed employing convolutional neural networks. Experiments on a popular rolling bearing dataset showed a high accuracy on the RUL prediction. A Health Index (HI) based Hierarchical Gated Recurrent Unit Network (HGRUN) was proposed by Li et al. [37] for rolling bearing health prognosis. The HGRUN was formed by stacking various hidden layers. An open experimental bearing data was practiced to validate the capacity of the proposed approach. The results proved that HGRUN outperforms the other techniques including Back-Propagation (BP) neural network, Support Vector Machine (SVM), and basic Deep Belief Network (DBN).

In Deutsch and He [38], a deep learning-based method was developed through the combination of a DBN and a Feedforward Neural Network (FNN) algorithm for RUL forecasting of rotating equipment. The proposed DBN FNN algorithm benefits from the feature learning ability of the DBN and the prediction power of the FNN. The test result indicated the promising RUL prediction performance of the deep learning-based DBN FNN.

Adaptive Neuro-Fuzzy Inference Systems (ANFIS) method, a combination of fuzzy logic and NNs, constructs a hybrid intelligent system and benefits from the potentials of both techniques including the simplicity and strength of NNs and the reasoning of fuzzy systems. ANFIS forms a series of fuzzy if-then rules with relevant membership functions to provide the specified input-output pairs. The result contributes to a robust framework for addressing practical classification problems [39, 40, 41].

A machine condition prognosis approach based on ANFIS was proposed by Chen et al. [42] to model a fault propagation trend. The high-order particle filtering was, then, employed to carry out the prediction. The results of experimental data from a faulty bearing demonstrated a higher prediction accuracy compared to RNNs. A methodology based on a distributed features forecasting approach using ANFIS models was developed by Zurita et al. [43]. The proposed method was validated by means of an accelerated bearing degradation experimental platform.

TABLE 4.4.1: Summary of intelligent method-based prognostics literature review

Reference	Architecture	Results
Malhi et al. [27]	RNN	Mean Square Error (MSE) = 0.04
Teng et al. [28]	ANN	Error = 12.78%
Xie and Zhang [29]	ESN	Root Mean Square Error (RMSE) = 0.0136
Xie and Zhang [29]	RMLP	RMSE = 0.0262
Guo et al. [30]	RNN-HI	Mean of error = 23.24%
Karim et al. [32]	ANN	MSE = $10^{-5}$
Kramti et al. [33]	ENN	MSE = 0.0023
Senanayaka et al. [34]	DNN	Error = 26.25%
Li et al. [36]	DNN	Mean Absolute Error (MAE) = 30.4%
Li et al. [37]	HGRUN	Maximum of Absolute Error (MaxAE) = 18.79%
Chen et al. [42]	ANFIS	RMSE = 0.0812
Zurita et al. [43]	ANFIS	Error = 14.2%
Cheng et al. [44]	ANFIS	Average RMSE = 0.0503
Soualhi et al. [45]	NFN	RMSE = 0.000428

Cheng et al. [44] introduced a case-based data-driven prognostic framework using the ANFIS. First, large historical data was processed to build an ANFIS model-case library. Then, the fault prognosis of a new machinery system was implemented by applying the suitable ANFIS model extracted from the model-case library. The suggested framework was examined by using the experimental data of bearing faults obtained from a bearing test rig. It was shown that the prognostic framework has better fault prognostic accuracy compared to the traditional data-driven systems.

In Soualhi et al. [45], a time series forecasting model, neo-fuzzy neuron, was proposed to predict the degradation of bearings. The neo-fuzzy neuron (NFN) is an intelligent tool that contributes to modeling complex systems by the simplicity of its structure, which is comprised of a single neuron. The Root Mean Square (RMS) extracted from vibration signals was employed as an input of the neo-fuzzy neuron in order to determine the growth of the bearing's degradation in time. A comparative study between the neo-fuzzy neuron and ANFIS was conducted to evaluate their prediction capabilities. The experimental results illustrated that the neo-fuzzy model could track the degradation of bearings. The details of these works are shown in Table 4.4.1.

#### 4.4.2 Bayesian network-based techniques

Bayesian networks are a type of probabilistic open-chain graphical model for estimating probabilities. A Bayesian network is comprised of nodes, which correspond to random variables that can take on distinct states. These are connected by directional arcs representing conditional dependencies between nodes [46]. A Bayesian network can be utilized to assess the likelihood of different scenarios being the root cause of an event, or in the case of time series modeling, determine probabilities associated with a particular future event [47].

In Hong and Zhou [48], a potential Bayesian machine learning method called Gaussian Process Regression (GPR) for bearing degradation evaluation was proposed. From the test results, it was shown that the GPR model application in bearing prognosis could achieve higher performance compared with the Wavelet Neural Network (WNN).

The most common Bayesian techniques used in engineering prognostics consist of Markov models, Kalman filters, and Particle filters.

Markov models aim at estimating probabilities of future failure by determining probabilities associated with each state and probabilities associated with transitioning from one state to another. A primary characteristic of all Markov models is that future states are only dependent on the immediately prior state. For Markov prognostics purposes, the following assumptions are considered [15].

- Transition probabilities are independent of time (i.e., a constant failure rate).
- The waiting time in a distinct state has an exponential trend.
- The sum of all transition probabilities for leaving one state and entering different states must be equal to one.

On the other hand, Semi-Markov models assume that the time spent in a particular state can be attributed to any distribution. This implies that the sum of probabilities for each state transitioning into other different states can be less than one. Thus, they are more advantageous for predicting RUL than traditional Markov chains. Despite Markov and Semi-Markov models' explicit flexibility in modeling a number of various system designs

and failure scenarios, the primary drawback is the underlying assumption of a constant failure rate, which is quite idealistic [49, 50]. This can be addressed by employing the hidden and semi-hidden Markov variants.

The Hidden Markov Model (HMM) and Semi-Hidden Markov Model (SHMM) are an extension of Markov chains in which not all states are directly observable and thus corresponding transition probabilities are not directly assignable. An HMM is characterized by the number of model states, the number of distinct observation symbols per state, a state transition probability distribution, an observation symbol probability distribution, and an initial state distribution [15]. The stochastic model is trained with failure data to overcome the lack of transition information to and from hidden states.

The main benefit of HMM is its capability in the modeling of both spatial and temporal phenomena, so time-series data can be analyzed without a physical understanding of the failure, so long as enough data is available for training. A weakness of all forms of the Markov model is that it is computationally expensive, even for the simplest models with few states. The number of calculations to evaluate how well the model fits the observation data set is proportional to the number of states squared [51].

A fault diagnosis using an HMM method was developed for rolling bearings in Zhang and Kang [52]. Afterward, failure prognosis was further implemented based on a Hierarchical Hidden Markov Model (HHMM). Their research work indicated that the accuracy of the method depended on the sample size of historical data. In Chen et al. [53], a Multi-Sensor Hidden Semi-Markov Model was proposed; which is an extension of classical hidden semi-Markov models. The proposed prognostic methodology was validated on a practical bearing application. The experimental results revealed that the prognostic method was promising to achieve more reliable performance than classical hidden semi-Markov models.

Le et al. [54] developed a multibranch HSMM to deal with a multi-modes deterioration mechanism. The results, based on deterioration data of a bearing under different operation conditions, indicated that the proposed multibranch HSMM provided accurate prediction in the detection of deterioration modes.

The Kalman filter is a recursive processing method applied to determine the unknown

state of a dynamic system from a set of noisy measurements based on mean squared error minimization. The Kalman filter accomplishes this goal through linear projections. These are based on the assumption that process noise and measurement noise are Gaussian, white, independent of each other, and additive [15].

Singleton et al. [55] applied an Extended Kalman Filter (EKF) for anticipating the RUL of bearings. For this purpose, an affine function that best approximates the fault degradation is determined and utilized to learn the parameters of the EKF. Then, the learned EKF is employed to examine data to forecast the RUL of bearing faults under different operating conditions. Bearing vibration data from the "PRONOSTIA platform", an experimental platform for bearings accelerated degradation tests, was applied to the proposed algorithm. This showed the convergence of the algorithm along with its behavior for different conditions. In Lim and Mba [56], Switching Kalman Filter (SKF) was introduced for fault diagnosis and prognosis of a gearbox bearing. For this purpose, it was presumed that the degradation trend would grow through time and the various deterioration processes were modeled applying a Kalman filter each. The SKF would then practice various models. From there the most probable one would be selected from the Condition Monitoring (CM) data through the employment of Bayesian estimation for the RUL forecast. The experimental results showed that the developed approach was a promising tool to improve maintenance decision-making.

Particle Filters (PFs) are alternatives to KF for determining the posterior distribution. These are not restricted by linearity or Gaussian noise assumptions. They are especially helpful with conditions where the posterior distribution is multivariate and non-standard. Whereas Kalman filters determine the posterior Probability Density Function (PDF) by extrapolating from the previous state, particle filters use Sequential Importance Sampling (SIS) to predict the entire next state in every iteration of the filter [15].

A stochastic modeling method based on particle filter for bearing remaining life prediction was proposed by Wang et al. [57]. Experiments were conducted on a customized bearing test rig to illustrate the effectiveness of the developed approach. Chen et al. [58] presented a generic particle-filtering-based framework with application in bearing spalling fault diagnosis and failure prognosis. The results suggested that the system was capable of



TABLE 4.4.2: Summary of Bayesian network-based techniques literature review

Reference	Architecture	Results
Hong and Zhou [48]	GPR	Relative Error (RE) = 6.32%
Zhang and Kang [52]	HHMM	Error = 13.64%
Le et al. [54]	Multi-branch HSMM	Average RMSE = 64.72
Singleton et al. [55]	EKF	Mean error of OPs = 32.8%, 73.2%, 44%
Lim and Mba [56]	SKF	Error = 13.3%
Wang et al. [57]	PF	Error = 3.0%
Chen et al. [58]	Generic PF	low MSE = $10^{-2}$

meeting performance requirements. The details of these efforts are shown Table 4.4.2.

### 4.4.3 Hybrid prognostic techniques

Hybrid failure prognosis methods are constructed using a combination of various prognostic approaches [59].

In Satish and Sarma [60], a combination of neural networks and fuzzy logic was proposed to develop a Fuzzy BP network for identifying the present state of the bearing and predict its remaining useful life. The results confirmed that the hybrid approach is well suited for evaluating the present state of the bearing and the time available for the replacement of the bearing. In Caesarendra et al. [61], a combination of Vector Machine (VM), Logistic Regression (LR), and autoregressive moving average (ARMA)/generalized autoregressive conditional heteroscedastic (GARCH) models was proposed to assess bearing failure degradation as shown in Figure 4.4.1. The results confirmed the ability of the proposed method for bearing failure degradation assessment.

In Sun et al. [62], an SVM-based model for bearing prognosis was proposed. In this model, Principal Component Analysis (PCA) was employed for feature extraction from a vibration signal, and the SVM parameters were optimized using Particle Swarm Optimization (PSO). The expected result based on bearing run-to-failure experimental data confirmed that the proposed model was more accurate than the classic models.

Chen et al. [63] proposed an approach for bearing prognosis based on Neuro-Fuzzy Systems (NFSs) and Bayesian algorithms. The NFS was used as a prognostic model to determine degradation with time. A Bayesian algorithm was employed to update the degree

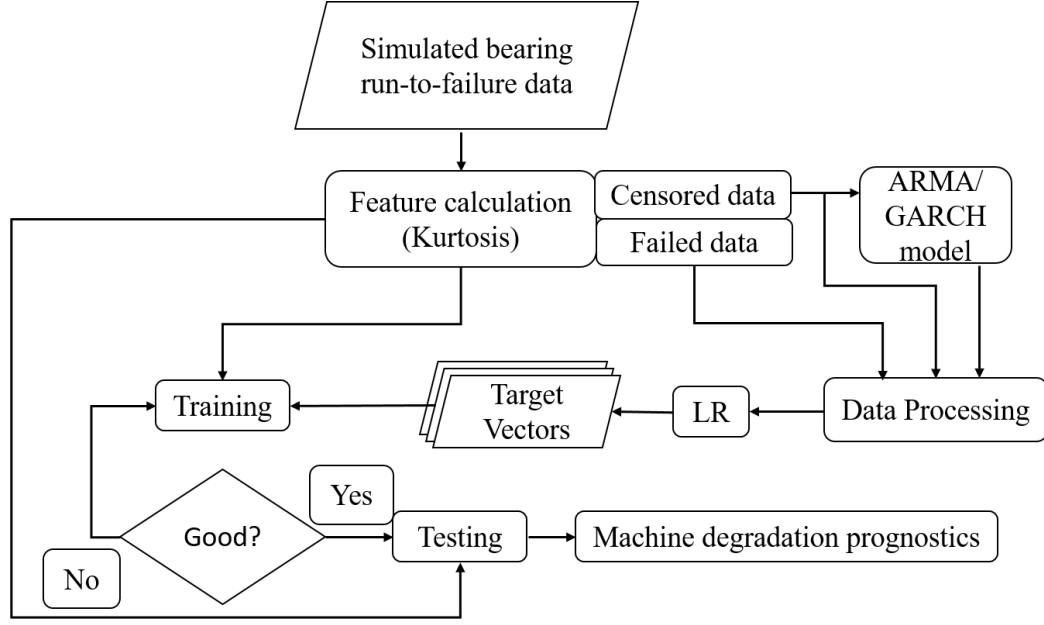


FIGURE 4.4.1: A combination of VM, LR and ARMA GARCH for bearings RUL estimation [61]

of confidence in the forecasting estimations. The experimental test results confirmed that the proposed failure prognosis approach could predict bearing conditions more accurately compared to recurrent neural networks, NFSs, and recurrent NFSs techniques. In Dong and Luo [64], an approach to determine bearing degradation was developed based on a combination of PCA and an optimized Least-Squares Support Vector Machine (LSSVM) method as shown in Figure 4.4.2. Firstly, PCA was employed to decrease the dimension of the extracted features. Then, the LSSVM model was formed and trained based on the extracted features for bearing degradation trend estimation. The Pseudo Nearest Neighbor (PNN) and the PSO were applied for the input number of the model estimation and the LS-SVM parameters selection, respectively. The experimental results confirmed the effectiveness of the methodology.

A hybrid approach for prognostics based on the Least Squares Support Vector Regression (LSSVR), and the HMM was proposed by Liu et al. [65]. Features extracted from vibration signals were utilized to train HMMs. The LSSVR algorithm was employed to predict feature trends. The predicted features probabilities for each HMM were estimated using forward or backward algorithms. Then, these probabilities helped with determining

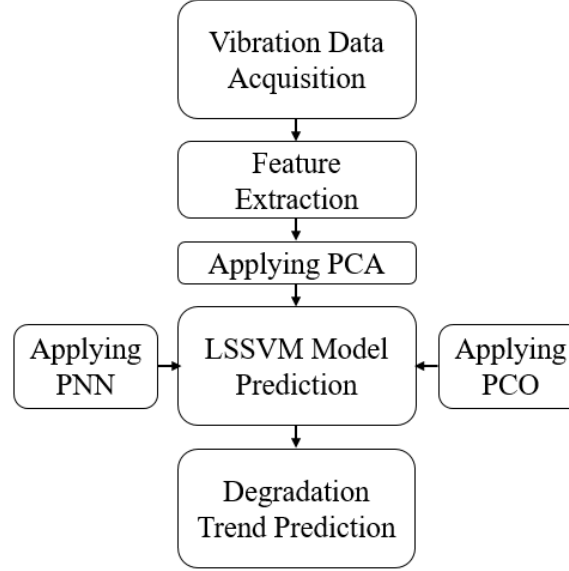


FIGURE 4.4.2: A combination of PCA and LSSVM for bearings RUL estimation [64]

future health states and anticipating the RUL. A test was conducted using bearing vibration signals to validate the proposed method. The results illustrated that the LSSVR/HMM approach predicted faults before their occurrence.

Hong et al. [66] proposed a combination of Wavelet Packet Decomposition (WPD), Empirical Mode Decomposition (EMD) and Self-Organizing Map (SOM) neural network techniques as shown in Figure 4.4.3 for assessing the state of the bearing's degradation and estimating the RUL. A health indicator named Confidence Value (CV) was derived from the SOM network. The results indicated that the CV could effectively identify the degradation stage and help to estimate the RUL accurately. Later, the CV change rate was used to classify degradation stages into normal, slight degradation, severe degradation, and failure stages. Then, the corresponding prognosis models are chosen to determine the health trend and RUL. The proposed hybrid approach enhanced accuracy when entering the severely degraded stage compared to the traditional single method such as Wavelet Neural Network [67].

Soualhi et al. [68] presented a methodology which combines HMM, the multistep time series prediction, and the ANFIS for providing the imminence of the next degradation state and estimating the remaining time before the next degradation state. The experimental results showed the proposed methodology potential for the detection, diagnosis, and prog-

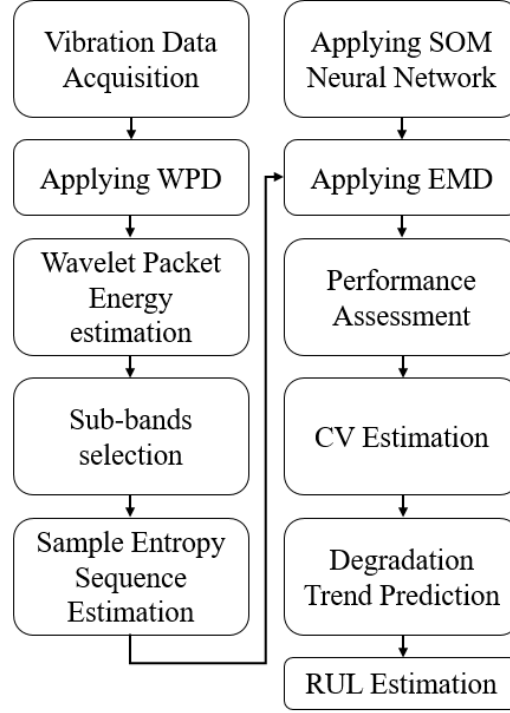


FIGURE 4.4.3: A combination of WPD, EMD and SOM neural network techniques for bearings RUL estimation [66]

nosis of faults in roller bearings. A combination of Simplified Fuzzy Adaptive Resonance Theory Map (SFAM) neural network and Weibull Distribution (WD) was developed by Ali et al. [69] for bearing prognosis. Experimental results showed that the capability of the proposed method to learn nonlinear time series and to reliably estimate the RUL of rolling element bearings based on vibration signals.

In Soualhi et al. [70], an approach that combines the Hilbert Huang Transform (HHT) to extract feature indexes from raw vibration signals, an SVM to detect the degradation states, and the Support Vector Regression (SVR) for the estimation of the RUL of ball bearings was proposed. The experimental results confirmed that the use of the HHT, the SVM, and the SVR is a suitable strategy to enhance the detection, diagnosis, and prognosis of bearing degradation. Wang et al. [71] proposed a two-stage strategy prognosis including, first, estimation of degradation by determining the deviation of extracted features from a known healthy state and, then, estimating the RUL of the bearing using an enhanced Kalman filter and an Expectation–Maximization (EM) algorithm. The results confirmed that their proposed approach can provide higher estimation accuracy and narrower PDFs in

comparison with Gebraeel's model [72] and Si's model [73].

Zhao et al. [74] presented a feature extraction system for vibration-based bearing prognosis using Time-Frequency Representation (TFR) and supervised dimensionality reduction. A combination of TFR, Gaussian pyramid and Local Binary Pattern (LBP) was used to evaluate lifetime information represented by highly dimensional features. The RULs are determined by employing simple Multiple Linear Regressions (MLRs). The experimental results demonstrated that the proposed method outperforms techniques employing traditional statistical features and PCA.

In Jin et al. [75], a health index was proposed to detect bearing health states. A non-linear form was developed to track the bearings' degradation process, and an extended Kalman filter was employed for the RUL prediction. Experimental bearing life data was utilized to verify the effectiveness of the proposed anomaly detection and fault prognosis strategy. This showed that the advance warning of bearing failure can be obtained, and ongoing maintenance can be scheduled by identifying the anomaly successfully. Lu et al. [76] proposed a prediction method based on LSSVM and PCA to determine the slewing bearing's degradation trend. The proposed method was shown to be more accurate and efficient over conventional slewing bearing failure prognosis strategies.

Jiang et al. [77] proposed an evaluation approach for bearing performance degradation using a combination of HMM and Nuisance Attribute Projection (NAP) as shown in Figure 4.4.4. It was illustrated that the NAP could remove the impact of nuisance attributes and the new feature space calculated by the NAP was barely affected by other interference occurring during operation. The experimental results showed that their approach improved the accuracy of the bearing performance assessment system.

A prognostic method based on vibration signals including health monitoring methodology for wind turbine high-speed shaft bearing was proposed by Saidi et al. [78] using a Spectral Kurtosis (SK) data-driven approach. It was shown that SK-derived features could provide an early warning for bearing defects and help with the evaluation of bearing degradation. Aye and Heyns [79] proposed an optimal GPR, an integration of mean and covariance functions, for capturing the bearing degradation trend. The GPR also captured the irregularities within the data and, subsequently, improved the RUL estimation for

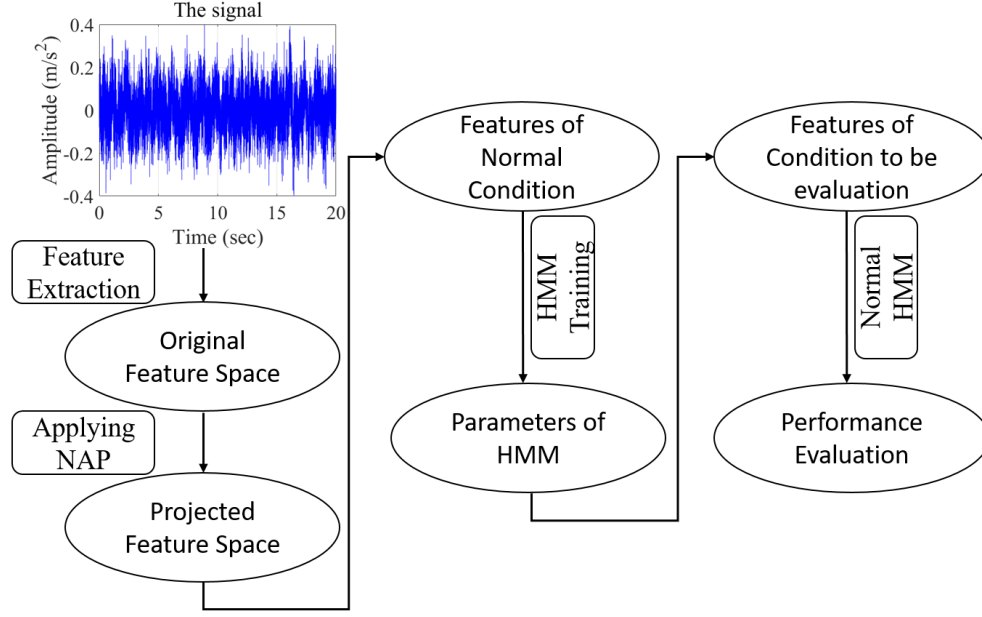


FIGURE 4.4.4: A combination of HMM and NAP bearing performance descending evaluation [77]

slow speed bearings. The experimental outcomes indicated that their model demonstrated improvement over simpler GPR models.

In Lu et al. [80], a prognostic algorithm applying a combination of the Variable Forgetting Factor Recursive Least-Square (VFF-RLS), an Auto-Regressive and Moving-Average (ARMA) model was proposed. To demonstrate the capability of the proposed methodology, the accuracy of the prediction of the proposed model is examined utilizing bearing experimental data compared to an auto-regressive integrated moving average model without adaptation. Results confirmed accurate predictions of the hybrid prognostic method over the ARIMA model. Elforjani et al. [81] proposed Signal Intensity Estimator (SIE) as a new indicator to detect individual types of early fault in real-world wind turbine bearings. This study indicated the ability of the proposed indicator to accurately estimate the RUL for wind turbine bearings in a combination of regression trees (RT) and multilayer artificial neural network (ANN) models. The experimental results demonstrated that SIE has an advantage over the other fault indicators such as Crest Factor (CF) and Kurtosis (KU) if sufficient data are provided.

A hybrid approach, Local Feature-based Gated Recurrent Unit (LFGRU) network, that combines handcrafted feature design with automatic feature learning for machine health

monitoring is proposed in Zhao et al. [82]. Experiments on incipient bearing fault detection and gearbox fault diagnosis indicated the effectiveness of the proposed LFGRU. Ahmad et al. [83] presented a hybrid method that employed regression-based adaptive predictive techniques to learn the degradation trend to project the RUL of a bearing. The approach applied a gradient-based method to determine the Time to Start Prediction (TSP) accurately using linear regression analysis which contributes to relatively more accurate RUL predictions.

A deep feature optimization fusion method was proposed by Zhao et al. [84] to extract centrifugal pump bearing degradation features from large amounts of vibration data. It benefited from the capability of deep neural networks (DNN) in extracting highly abstracted features that correlate well with bearing degradation. The detailed experiments on real datasets showed that the developed method has an advantage over other methods and creates degradation trajectories with potential predictive capabilities, therefore enhancing the accuracy of RUL prediction.

Elforjani and Shanbr [85] employed the combination of SVMR, multilayer artificial neural network models, and GPR to estimate the RUL of slow speed bearings by correlating features with the corresponding natural wear throughout a series of laboratory experiments. It was concluded that neural networks model with a back propagation learning algorithm outperformed the other models in predicting the RUL for slow speed bearings. This was true when the appropriate network structure was chosen and enough data was provided. Qiu et al. [86] presented a prognostic procedure by combining an HI and PF to determine the bearing RUL. The process included applying the Structural Information of the Spectrum (SIOS) algorithm to build the HI called SIOS-based Indicator (SIOSI) for bearing deterioration monitoring. Then, they assessed the Initial Degradation Point (IDP) through an index calculated with a self-zero space observer and predicted the bearing RUL using the SIOSI and an PF-based algorithm that was aided by a degradation model. Experimental results have shown that the bearing RUL could be acceptably anticipated by the proposed method, and its performance was superior to conventional prognostic methods.

Rai et al. [87] introduced a data-driven prognosis approach based on a Nonlinear Auto-Regressive Exogenous (NARX) neural network model that utilized a wavelet-filter tech-

nique for bearing RUL estimation. In time domain modeling, an NARX is a nonlinear autoregressive model that has exogenous inputs. This implies that the model links the current value of a time series to past values of the same series and current and past values of the driving (exogenous) series [88]. As shown in Figure 4.4.5 the approach was comprised of several steps as follows.

- In order to boost the impulsive aspects of bearing signals and enhance the quality of fault feature extraction, the vibration signals provided by an experimental test rig were preprocessed with the proposed wavelet-filter.
- To address the highly non-monotonic behavior of the extracted features due to the bearing degradation, an HI based on Mahalanobis Distance (MD) criterion [89, 90] and Cumulative Sum (CUMSUM) chart [91] was introduced.
- The NARX neural network was developed as a Time Delay Neural Network (TDNN) model which was trained by the introduced HI and bearing age as inputs, and bearing life percentage as output for bearing RUL estimation.

The results confirmed that the proposed method could accurately predict the RUL of bearings and outperformed the application of the self-organizing map-based indicator.

In Deutsch and He [38], a deep learning-based method was developed through the combination of a DBN and a Feedforward Neural Network (FNN) algorithm for RUL forecasting of rotating equipment. The proposed DBN FNN algorithm benefits from the feature learning ability of the DBN and the prediction power of the FNN. The test result indicated the promising RUL prediction performance of the deep learning-based DBN FNN. Hu et al. [92] presented a real-time performance degradation model based on temperature characteristic parameters for failure prognosis of wind turbine bearings. Here a combination of the Wiener process for establishing the performance degradation model, the maximum likelihood estimation method for obtaining the parameters of the developed model, and an inverse Gaussian distribution approach for RUL prediction was employed to achieve this. The comparison of the predicted RUL and actual RUL revealed that the hybrid prediction method was correct and effective. Furthermore, the proposed method can be utilized in CM of the wind turbine bearings for the Prognostics and health management (PHM).



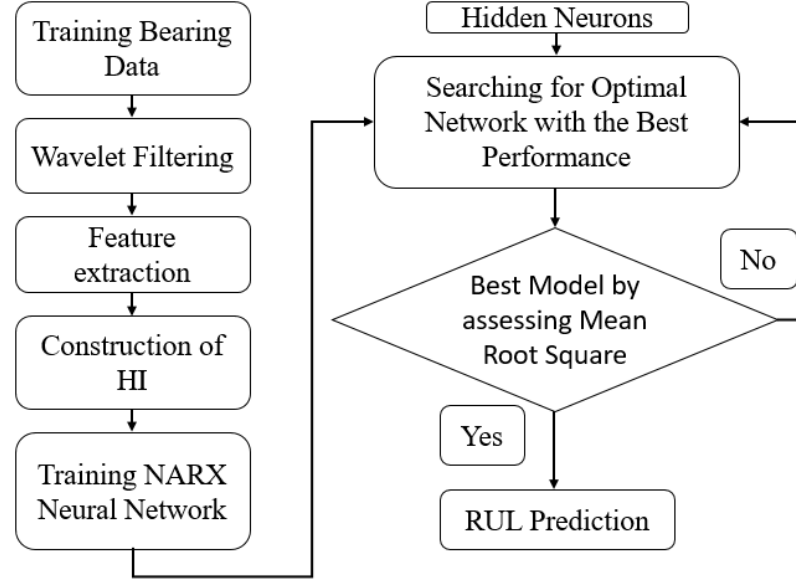


FIGURE 4.4.5: Flowchart for prognosis approach based on a NARX neural network model in association with a wavelet-filter technique for bearing RUL estimation [87]

Hemmer et al. [93] suggested a framework based on three fault classifiers of Convolutional Neural Network (CNN), SVM, and sparse autoencoder-based SVM utilizing transfer learning. The effectiveness of the proposed technique was examined employing vibration and acoustic emission signal datasets from roller bearings with artificial damage. The survey showed the ability of the combination of a trained CNN and SVM for extracting features and classification, respectively, in detecting faults in roller bearings based on robustness, easy implementation, and computational weight. However, the combination of a trained CNN and sparse autoencoder for extracting features and, then, decreasing dimensions of extracted features increased the computational weight and complexity as well as reducing the accuracy. The details of these efforts are shown in Table 4.4.3.

## 4.5 Conclusions and Future Guidelines

This study provided a review of recent modeling developments for wind turbine bearing prognosis. Basic definitions and elemental bearing reliability concepts were also discussed. The pros and cons of each prognosis method have also been highlighted. Our review has illustrated that hybrid methods are now the leading tools for turbine bearing failure pre-

TABLE 4.4.3: Summary of hybrid prognostic techniques literature review

Reference	Architecture	Results
Satish and Sarma [60]	Fuzzy BP network	MaxAE = 27.2%
Sun et al. [62]	SVM/PCA/PSO	Error = 3.2%
Chen et al. [63]	NFS/Bayesian	Average RMSE = 0.0506
Dong and Luo [64]	PCA/LSSVM/PNN/PSO	RMSE = 0.000118
Liu et al. [65]	LSSVR/HMM	MaxAE = 43.75%
Hong et al. [66]	WPD/EMD/SOM	MaxAE = 51.8%
Ali et al. [69]	SFAM neural network/WD	Error = 2.23%
Soualhi et al. [70]	HHT/SVM/SVR	MaxAE = 1.25%
Wang et al. [71]	Enhanced KF/EM algorithm	Error = 12.09%
Jin et al. [75]	Autoregressive model/EKF	RMSE = 0.865
Lu et al. [76]	LSSVM/PCA/PSO	RMSE = 0.1148
Aye and Heyns [79]	GPR	RMSE = 0.0069
Lu et al. [80]	VFF-RLS/ARMA	MSE = 0.0164
Zhao et al. [82]	LFGRU	Error = 6.8%
Ahmad et al. [83]	Regression-based hybrid method	MaxAE = 32.1%
Qiu et al. [86]	SIOS/PF	MaxAE = 13.42%
Rai et al. [87]	NARX	MSE = 0.0059
Hemmer et al. [93]	CNN/SVR/Sparse autoencoder-based SVM	MaxAE = 27%

diction because of their higher accuracy over individual prognosis methods. Beyond this, there are a number of challenges that merit further study. We summarize them as follows.

#### 1. Considering operating conditions in monitoring methods.

Bearing prognostic studies have largely been executed over constant environmental (operating) conditions, and the prognostic techniques are developed using monitoring methods such as VA [36, 74, 83]. However, it is vital to also consider varying operating conditions which can include environmental variables like wind speed and ambient temperature. It should be recognized that damage progression can be a function of the stress and loading applied to bearings, which subsequently affect the RUL estimation, i.e., classification of operating conditions based on the severity of an environmental condition.

#### 2. Investigating component interactions for the prognosis task.

Almost all studies reviewed were for individual bearings [33, 57]. However, component interactions should also be considered in the degradation process (for instance, the interaction between bearings and gears in a gearbox). More signal processing procedures could also be applied to the machine degradation process to differentiate bearing fault signals from other component signals.

### **3. Applying hybrid methods for the prognosis task.**

Hybrid methods use a combination of various prognosis techniques which can lead to higher accuracy compared to individually employed prognosis methods [60, 42]. Hence, it is beneficial to construct more hybrid methods to continue to achieve improved accuracies.

### **4. Application of Bayesian methods.**

Bayesian approaches intrinsically consider probability theory which may be more appropriate for RUL prediction owing to the probabilistic characteristics of the RUL task [48, 63]. Therefore, additional emphasis should be applied to the Bayesian style of analysis.

## 4.6 List of Abbreviations

AE	Absolute error
ANFIS	Adaptive Neuro-fuzzy inference systems
ANN	Artificial Neural Network
ARMA	Autoregressive moving average
BP	Back Propagation
CM	Condition monitoring
CNN	Convolutional neural network
CUMSUM	cumulative sum
CV	Confidence value
DBN	Deep belief network
DNN	Deep neural network
EKF	Extended Kalman filter
EM	expectation–maximization
EMD	Empirical mode decomposition
ENN	Elman neural network
ESN	Echo state network
FDP	Fault diagnosis and prognosis
FL	Fuzzy logic
FNN	Feedforward neural network
GPR	Gaussian process regression
GWEC	Global Wind Energy Council
HGRUN	Hierarchical gated recurrent unit network
HHHM	Hierarchical Hidden Markov model
HHT	Hilbert Huang transform
HI	Health indicator
HSSB	High-speed shaft bearing
HMM	Hidden Markov model
IDP	Initial degradation point
KF	Kalman filter
LBP	Local binary pattern

LFGRU	Local feature-based gated recurrent unit
LR	Logistic regression
LSSVM	Least squares support vector machine
LSSVR	least squares support vector regression
MAE	Mean absolute error
MD	Mahalanobis distance
MLP	Multilayer perceptron
MLR	Multiple linear regression
MSE	Mean Square Error
MaxAE	Maximum of absolute error
NARX	Nonlinear autoregressive exogenous
NAP	Nuisance attribute projection
NFN	Neo-fuzzy neuron
NFS	Neuro-fuzzy system
NN	Neural network
PCA	Principal component analysis
PCO	Pseudo nearest neighbor
PDF	Probability density function
PF	Particle filter
PNN	Particle swarm optimization
PHM	Prognostics and health management
RLS	Recursive least-square
RMLP	Recurrent multilayer perceptron
RNN	Recurrent neural network
RMSE	Root mean square error
SKF	Switching Kalman Filter
SK	Spectral kurtosis
SFAM	Simplified fuzzy adaptive resonance theory map
SHMM	Semi-hidden Markov model
SIOS	Structural information of the spectrum
SIOSI	SIOS-based indicator

SOM	Self-organizing map
SVM	Support vector machine
SVMR	Support vector machine regression
SVR	Support vector regression
TDNN	time delay neural network
TFR	Time-frequency representation
TSP	Time to start prediction
VA	Vibration analysis
VFF	variable forgetting factor
VM	Vector machine
WD	Weibull distribution
WPD	Wavelet packet decomposition

## REFERENCES

- [1] G. W. E. Council. (2016) Wind power to dominate power sector growth. [Online]. Available: <https://gwec.net/publications/global-wind-energy-outlook/global-wind-energy-outlook-2016/>
- [2] M. Shafiee and F. Dinmohammadi, “An fmea-based risk assessment approach for wind turbine systems: a comparative study of onshore and offshore,” *Energies*, vol. 7, no. 2, pp. 619–642, 2014.
- [3] B. Hahn, M. Durstewitz, and K. Rohrig, “Reliability of wind turbine—experiences of 15 years with 1500 wts,” *Institut für Solare Energieversorgungstechnik (ISET): Hesse, Germany*, 2005.
- [4] A. Stenberg and H. Holttinen, “Analysing failure statistics of wind turbines in finland,” in *European Wind Energy Conference, April*, 2010, pp. 20–23.
- [5] B. Nivedh, “Major failures in the wind turbine components and the importance of periodic inspections,” *Wind Insid*, 2014.
- [6] S. Sankar, M. Nataraj, and P. V. Raja, “Failure analysis of bearing in wind turbine generator gearbox,” *Journal of Information Systems and Communication*, vol. 3, no. 1, p. 302, 2012.
- [7] M. Whittle, “Wind turbine generator reliability: An exploration of the root causes of generator bearing failures,” Ph.D. dissertation, Durham University, 2013.
- [8] M. Whittle, J. Trevelyan, W. Shin, and P. Tavner, “Improving wind turbine drivetrain bearing reliability through pre-misalignment,” *Wind Energy*, vol. 17, no. 8, pp. 1217–1230, 2014.
- [9] H. D. M. de Azevedo, A. M. Araújo, and N. Bouchonneau, “A review of wind turbine bearing condition monitoring: State of the art and challenges,” *Renewable and Sustainable Energy Reviews*, vol. 56, pp. 368–379, 2016.

- [10] N. Chen, R. Yu, Y. Chen, and H. Xie, "Hierarchical method for wind turbine prognosis using scada data," *IET Renewable Power Generation*, vol. 11, no. 4, pp. 403–410, 2016.
- [11] M. Blodt, P. Granjon, B. Raison, and G. Rostaing, "Models for bearing damage detection in induction motors using stator current monitoring," *IEEE transactions on industrial electronics*, vol. 55, no. 4, pp. 1813–1822, 2008.
- [12] J. R. Stack, T. G. Habetler, and R. G. Harley, "Fault classification and fault signature production for rolling element bearings in electric machines," *IEEE Transactions on Industry Applications*, vol. 40, no. 3, pp. 735–739, 2004.
- [13] P. Tchakoua, R. Wamkeue, M. Ouhrouche, F. Slaoui-Hasnaoui, T. A. Tameghe, and G. Ekemb, "Wind turbine condition monitoring: State-of-the-art review, new trends, and future challenges," *Energies*, vol. 7, no. 4, pp. 2595–2630, 2014.
- [14] F. P. G. Márquez, A. M. Tobias, J. M. P. Pérez, and M. Papaelias, "Condition monitoring of wind turbines: Techniques and methods," *Renewable Energy*, vol. 46, pp. 169–178, 2012.
- [15] J. Sikorska, M. Hodkiewicz, and L. Ma, "Prognostic modelling options for remaining useful life estimation by industry," *Mechanical systems and signal processing*, vol. 25, no. 5, pp. 1803–1836, 2011.
- [16] M. Kordestani, M. F. Samadi, M. Saif, and K. Khorasani, "A new fault diagnosis of multifunctional spoiler system using integrated artificial neural network and discrete wavelet transform methods," *IEEE Sensors Journal*, vol. 18, no. 12, pp. 4990–5001, 2018.
- [17] M. Kordestani, A. Zanj, M. E. Orchard, and M. Saif, "A modular fault diagnosis and prognosis method for hydro-control valve system based on redundancy in multisensor data information," *IEEE Transactions on Reliability*, no. 99, pp. 1–12, 2018.



- [18] N. Jammu and P. Kankar, "A review on prognosis of rolling element bearings," *International Journal of Engineering Science and Technology*, vol. 3, no. 10, pp. 7497–7503, 2011.
- [19] A. Alwodai, T. Wang, Z. Chen, F. Gu, R. Cattley, and A. Ball, "A study of motor bearing fault diagnosis using modulation signal bispectrum analysis of motor current signals," *Journal of signal and information processing*, vol. 4, no. 03, p. 72, 2013.
- [20] SKF. (2018) Components and materials. [Online]. Available: <http://www.skf.com/group/products/bearings-units-housings/principles/general-bearing-knowledge/bearing-basics/components-and-materials/index.html>
- [21] A. Shrivastava and S. Wadhwani, "Vibration signature analysis for ball bearing of three phase induction motor," *IOSR Journal of Electrical and Electronics Engineering (IOSRJEEE)*, vol. 1, no. 3, pp. 2278–1676, 2012.
- [22] Y. Lei, *Intelligent fault diagnosis and remaining useful life prediction of rotating machinery*. Butterworth-Heinemann, 2016.
- [23] M. Morshedizadeh, M. Kordestani, R. Carriveau, D. S. Ting, and M. Saif, "Improved power curve monitoring of wind turbines," *Wind engineering*, vol. 41, no. 4, pp. 260–271, 2017.
- [24] M. Morshedizadeh, M. Kordestani, R. Carriveau, D. S.-K. Ting, and M. Saif, "Power production prediction of wind turbines using a fusion of mlp and anfis networks," *IET Renewable Power Generation*, vol. 12, no. 9, pp. 1025–1033, 2018.
- [25] A. Zameer, J. Arshad, A. Khan, and M. A. Z. Raja, "Intelligent and robust prediction of short term wind power using genetic programming based ensemble of neural networks," *Energy conversion and management*, vol. 134, pp. 361–372, 2017.
- [26] M. C. Mabel and E. Fernandez, "Analysis of wind power generation and prediction using ann: A case study," *Renewable energy*, vol. 33, no. 5, pp. 986–992, 2008.

- [27] A. Malhi, R. Yan, and R. X. Gao, “Prognosis of defect propagation based on recurrent neural networks,” *IEEE Transactions on Instrumentation and Measurement*, vol. 60, no. 3, pp. 703–711, 2011.
- [28] W. Teng, X. Zhang, Y. Liu, A. Kusiak, and Z. Ma, “Prognosis of the remaining useful life of bearings in a wind turbine gearbox,” *Energies*, vol. 10, no. 1, p. 32, 2016.
- [29] Y. Xie and T. Zhang, “The application of echo state network and recurrent multilayer perceptron in rotating machinery fault prognosis,” in *2016 IEEE Chinese Guidance, Navigation and Control Conference (CGNCC)*. IEEE, 2016, pp. 2286–2291.
- [30] L. Guo, N. Li, F. Jia, Y. Lei, and J. Lin, “A recurrent neural network based health indicator for remaining useful life prediction of bearings,” *Neurocomputing*, vol. 240, pp. 98–109, 2017.
- [31] Q. Cui, Z. Li, J. Yang, and B. Liang, “Rolling bearing fault prognosis using recurrent neural network,” in *2017 29th Chinese Control And Decision Conference (CCDC)*. IEEE, 2017, pp. 1196–1201.
- [32] B. Karim and L. Abderrazak, “A statistical parameters and artificial neural networks application for rolling element bearing fault diagnosis using wavelet transform pre-processing.” *ICEE-B*, 10 2017, pp. 1–6.
- [33] S. E. Kramti, J. B. Ali, L. Saidi, M. Sayadi, and E. Bechhoefer, “Direct wind turbine drivetrain prognosis approach using elman neural network,” in *2018 5th International Conference on Control, Decision and Information Technologies (CoDIT)*. IEEE, 2018, pp. 859–864.
- [34] J. S. L. Senanayaka, H. Van Khang, and K. G. Robbersmyr, “Autoencoders and recurrent neural networks based algorithm for prognosis of bearing life,” in *2018 21st International Conference on Electrical Machines and Systems (ICEMS)*. IEEE, 2018, pp. 537–542.
- [35] M. Xia, T. Li, T. Shu, J. Wan, Z. Wang *et al.*, “A two-stage approach for the remaining

- useful life prediction of bearings using deep neural networks,” *IEEE Transactions on Industrial Informatics*, 2018.
- [36] X. Li, W. Zhang, and Q. Ding, “Deep learning-based remaining useful life estimation of bearings using multi-scale feature extraction,” *Reliability Engineering & System Safety*, vol. 182, pp. 208–218, 2019.
- [37] X. Li, H. Jiang, X. Xiong, and H. Shao, “Rolling bearing health prognosis using a modified health index based hierarchical gated recurrent unit network,” *Mechanism and Machine Theory*, vol. 133, pp. 229–249, 2019.
- [38] J. Deutsch and D. He, “Using deep learning-based approach to predict remaining useful life of rotating components,” *IEEE Transactions on Systems, Man, and Cybernetics: Systems*, vol. 48, no. 1, pp. 11–20, 2018.
- [39] M. Morshedizadeh, M. Kordestani, R. Carriveau, D. S.-K. Ting, and M. Saif, “Application of imputation techniques and adaptive neuro-fuzzy inference system to predict wind turbine power production,” *Energy*, vol. 138, pp. 394–404, 2017.
- [40] K. Salahshoor, M. Kordestani, and M. S. Khoshro, “Fault detection and diagnosis of an industrial steam turbine using fusion of svm (support vector machine) and anfis (adaptive neuro-fuzzy inference system) classifiers,” *Energy*, vol. 35, no. 12, pp. 5472–5482, 2010.
- [41] M. Mostafaei, H. Javadikia, and L. Naderloo, “Modeling the effects of ultrasound power and reactor dimension on the biodiesel production yield: Comparison of prediction abilities between response surface methodology (rsm) and adaptive neuro-fuzzy inference system (anfis),” *Energy*, vol. 115, pp. 626–636, 2016.
- [42] C. Chen, B. Zhang, G. Vachtsevanos, and M. Orchard, “Machine condition prediction based on adaptive neuro-fuzzy and high-order particle filtering,” *IEEE Transactions on Industrial Electronics*, vol. 58, no. 9, pp. 4353–4364, 2011.

- [43] D. Zurita, J. A. Carino, M. Delgado, and J. A. Ortega, “Distributed neuro-fuzzy feature forecasting approach for condition monitoring,” in *Proceedings of the 2014 IEEE Emerging Technology and Factory Automation (ETFA)*. IEEE, 2014, pp. 1–8.
- [44] F. Cheng, L. Qu, and W. Qiao, “A case-based data-driven prediction framework for machine fault prognostics,” in *2015 IEEE Energy Conversion Congress and Exposition (ECCE)*. IEEE, 2015, pp. 3957–3963.
- [45] A. Soualhi, G. Clerc, H. Razik, and F. Rivas, “Long-term prediction of bearing condition by the neo-fuzzy neuron,” in *2013 9th IEEE International Symposium on Diagnostics for Electric Machines, Power Electronics and Drives (SDEMPED)*. IEEE, 2013, pp. 586–591.
- [46] S. Dey and J. Stori, “A bayesian network approach to root cause diagnosis of process variations,” *International Journal of Machine Tools and Manufacture*, vol. 45, no. 1, pp. 75–91, 2005.
- [47] M. Kordestani, M. F. Samadi, M. Saif, and K. Khorasani, “A new fault prognosis of mfs system using integrated extended kalman filter and bayesian method,” *IEEE Transactions on Industrial Informatics*, 2018.
- [48] S. Hong and Z. Zhou, “Application of gaussian process regression for bearing degradation assessment,” in *2012 6th International Conference on New Trends in Information Science, Service Science and Data Mining (ISSDM2012)*. IEEE, 2012, pp. 644–648.
- [49] M. Rausand and A. Høyland, *System reliability theory: models, statistical methods, and applications*. John Wiley & Sons, 2004, vol. 396.
- [50] P. O’Connor and A. Kleyner, *Practical reliability engineering*. John Wiley & Sons, 2012.
- [51] Q. Miao and V. Makis, “Condition monitoring and classification of rotating machinery using wavelets and hidden markov models,” *Mechanical systems and signal processing*, vol. 21, no. 2, pp. 840–855, 2007.

- [52] X.-H. Zhang and J.-S. Kang, “Hidden markov models in bearing fault diagnosis and prognosis,” in *Computational Intelligence and Natural Computing Proceedings (CINCP)*, 2010 Second International Conference on, vol. 2, 2010, p. 364.
- [53] Z. Chen, Y. Yang, Z. Hu, and Q. Zeng, “Fault prognosis of complex mechanical systems based on multi-sensor mixtured hidden semi-markov models,” *Proceedings of the Institution of Mechanical Engineers, Part C: Journal of Mechanical Engineering Science*, vol. 227, no. 8, pp. 1853–1863, 2013.
- [54] T. T. Le, C. Berenguer, and F. Chatelain, “Multi-branch hidden semi-markov modeling for rul prognosis,” in *2015 Annual Reliability and Maintainability Symposium (RAMS)*. IEEE, 2015, pp. 1–6.
- [55] R. K. Singleton, E. G. Strangas, and S. Aviyente, “Extended kalman filtering for remaining-useful-life estimation of bearings,” *IEEE Transactions on Industrial Electronics*, vol. 62, no. 3, pp. 1781–1790, 2015.
- [56] C. K. R. Lim and D. Mba, “Switching kalman filter for failure prognostic,” *Mechanical Systems and Signal Processing*, vol. 52, pp. 426–435, 2015.
- [57] J. Wang and R. X. Gao, “Multiple model particle filtering for bearing life prognosis,” in *2013 IEEE Conference on Prognostics and Health Management (PHM)*. IEEE, 2013, pp. 1–6.
- [58] C. Chen, D. Brown, C. Sconyers, G. Vachtsevanos, B. Zhang, and M. E. Orchard, “A. net framework for an integrated fault diagnosis and failure prognosis architecture,” in *2010 IEEE AUTOTESTCON*. IEEE, 2010, pp. 1–6.
- [59] L. Liao and F. Köttig, “Review of hybrid prognostics approaches for remaining useful life prediction of engineered systems, and an application to battery life prediction,” *IEEE Transactions on Reliability*, vol. 63, no. 1, pp. 191–207, 2014.
- [60] B. Satish and N. Sarma, “A fuzzy bp approach for diagnosis and prognosis of bearing faults in induction motors,” in *IEEE Power Engineering Society General Meeting, 2005*. IEEE, 2005, pp. 2291–2294.

- [61] W. Caesarendra, A. Widodo, P. H. Thom, B.-S. Yang, and J. D. Setiawan, “Combined probability approach and indirect data-driven method for bearing degradation prognostics,” *IEEE Transactions on Reliability*, vol. 60, no. 1, pp. 14–20, 2011.
- [62] C. Sun, Z. Zhang, and Z. He, “Research on bearing life prediction based on support vector machine and its application,” in *Journal of Physics: Conference Series*, vol. 305, no. 1. IOP Publishing, 2011, p. 012028.
- [63] C. Chen, B. Zhang, and G. Vachtsevanos, “Prediction of machine health condition using neuro-fuzzy and bayesian algorithms,” *IEEE Transactions on instrumentation and Measurement*, vol. 61, no. 2, pp. 297–306, 2012.
- [64] S. Dong and T. Luo, “Bearing degradation process prediction based on the pca and optimized ls-svm model,” *Measurement*, vol. 46, no. 9, pp. 3143–3152, 2013.
- [65] Z. Liu, Q. Li, X. Liu, and C. Mu, “A hybrid lssvr/hmm-based prognostic approach,” *Sensors*, vol. 13, no. 5, pp. 5542–5560, 2013.
- [66] S. Hong, Z. Zhou, E. Zio, and K. Hong, “Condition assessment for the performance degradation of bearing based on a combinatorial feature extraction method,” *Digital Signal Processing*, vol. 27, pp. 159–166, 2014.
- [67] S. Hong, Z. Zhou, E. Zio, and W. Wang, “An adaptive method for health trend prediction of rotating bearings,” *Digital Signal Processing*, vol. 35, pp. 117–123, 2014.
- [68] A. Soualhi, H. Razik, G. Clerc, and D. D. Doan, “Prognosis of bearing failures using hidden markov models and the adaptive neuro-fuzzy inference system,” *IEEE Transactions on Industrial Electronics*, vol. 61, no. 6, pp. 2864–2874, 2014.
- [69] J. B. Ali, B. Chebel-Morello, L. Saidi, S. Malinowski, and F. Fnaiech, “Accurate bearing remaining useful life prediction based on weibull distribution and artificial neural network,” *Mechanical Systems and Signal Processing*, vol. 56, pp. 150–172, 2015.

- [70] A. Soualhi, K. Medjaher, and N. Zerhouni, "Bearing health monitoring based on hilbert–huang transform, support vector machine, and regression," *IEEE Transactions on Instrumentation and Measurement*, vol. 64, no. 1, pp. 52–62, 2015.
- [71] Y. Wang, Y. Peng, Y. Zi, X. Jin, and K.-L. Tsui, "A two-stage data-driven-based prognostic approach for bearing degradation problem," *IEEE Transactions on Industrial Informatics*, vol. 12, no. 3, pp. 924–932, 2016.
- [72] N. Z. Gebraeel, M. A. Lawley, R. Li, and J. K. Ryan, "Residual-life distributions from component degradation signals: A bayesian approach," *IiE Transactions*, vol. 37, no. 6, pp. 543–557, 2005.
- [73] X.-S. Si, W. Wang, C.-H. Hu, M.-Y. Chen, and D.-H. Zhou, "A wiener-process-based degradation model with a recursive filter algorithm for remaining useful life estimation," *Mechanical Systems and Signal Processing*, vol. 35, no. 1-2, pp. 219–237, 2013.
- [74] M. Zhao, B. Tang, and Q. Tan, "Bearing remaining useful life estimation based on time–frequency representation and supervised dimensionality reduction," *Measurement*, vol. 86, pp. 41–55, 2016.
- [75] X. Jin, Y. Sun, Z. Que, Y. Wang, and T. W. Chow, "Anomaly detection and fault prognosis for bearings," *IEEE Transactions on Instrumentation and Measurement*, vol. 65, no. 9, pp. 2046–2054, 2016.
- [76] C. Lu, J. Chen, R. Hong, Y. Feng, and Y. Li, "Degradation trend estimation of slewing bearing based on lssvm model," *Mechanical Systems and Signal Processing*, vol. 76, pp. 353–366, 2016.
- [77] H. Jiang, J. Chen, and G. Dong, "Hidden markov model and nuisance attribute projection based bearing performance degradation assessment," *Mechanical Systems and Signal Processing*, vol. 72, pp. 184–205, 2016.
- [78] L. Saidi, J. B. Ali, E. Bechhoefer, and M. Benbouzid, "Wind turbine high-speed shaft bearings health prognosis through a spectral kurtosis-derived indices and svr," *Applied Acoustics*, vol. 120, pp. 1–8, 2017.

- [79] S. Aye and P. Heyns, “An integrated gaussian process regression for prediction of remaining useful life of slow speed bearings based on acoustic emission,” *Mechanical Systems and Signal Processing*, vol. 84, pp. 485–498, 2017.
- [80] Y. Lu, Q. Li, Z. Pan, and S. Y. Liang, “Prognosis of bearing degradation using gradient variable forgetting factor rls combined with time series model,” *IEEE Access*, vol. 6, pp. 10 986–10 995, 2018.
- [81] M. Elforjani, S. Shanbr, and E. Bechhoefer, “Detection of faulty high speed wind turbine bearing using signal intensity estimator technique,” *Wind Energy*, vol. 21, no. 1, pp. 53–69, 2018.
- [82] R. Zhao, D. Wang, R. Yan, K. Mao, F. Shen, and J. Wang, “Machine health monitoring using local feature-based gated recurrent unit networks,” *IEEE Transactions on Industrial Electronics*, vol. 65, no. 2, pp. 1539–1548, 2018.
- [83] W. Ahmad, S. A. Khan, and J.-M. Kim, “A hybrid prognostics technique for rolling element bearings using adaptive predictive models,” *IEEE Transactions on Industrial Electronics*, vol. 65, no. 2, pp. 1577–1584, 2018.
- [84] L. Zhao and X. Wang, “A deep feature optimization fusion method for extracting bearing degradation features,” *IEEE Access*, vol. 6, pp. 19 640–19 653, 2018.
- [85] M. Elforjani and S. Shanbr, “Prognosis of bearing acoustic emission signals using supervised machine learning,” *IEEE Transactions on Industrial Electronics*, vol. 65, no. 7, pp. 5864–5871, 2018.
- [86] M. Qiu, W. Li, F. Jiang, and Z. Zhu, “Remaining useful life estimation for rolling bearing with sios-based indicator and particle filtering,” *IEEE Access*, vol. 6, pp. 24 521–24 532, 2018.
- [87] A. Rai and S. Upadhyay, “The use of md-cumsum and narx neural network for anticipating the remaining useful life of bearings,” *Measurement*, vol. 111, pp. 397–410, 2017.



- [88] S. A. Billings, *Nonlinear system identification: NARMAX methods in the time, frequency, and spatio-temporal domains*. John Wiley & Sons, 2013.
- [89] R. De Maesschalck, D. Jouan-Rimbaud, and D. L. Massart, “The mahalanobis distance,” *Chemometrics and intelligent laboratory systems*, vol. 50, no. 1, pp. 1–18, 2000.
- [90] J. Lin and Q. Chen, “Fault diagnosis of rolling bearings based on multifractal detrended fluctuation analysis and mahalanobis distance criterion,” *Mechanical Systems and Signal Processing*, vol. 38, no. 2, pp. 515–533, 2013.
- [91] D. M. Hawkins and D. H. Olwell, *Cumulative sum charts and charting for quality improvement*. Springer Science & Business Media, 2012.
- [92] Y. Hu, H. Li, P. Shi, Z. Chai, K. Wang, X. Xie, and Z. Chen, “A prediction method for the real-time remaining useful life of wind turbine bearings based on the wiener process,” *Renewable energy*, vol. 127, pp. 452–460, 2018.
- [93] M. Hemmer, H. Van Khang, K. Robbersmyr, T. Waag, and T. Meyer, “Fault classification of axial and radial roller bearings using transfer learning through a pretrained convolutional neural network,” *Designs*, vol. 2, no. 4, p. 56, 2018.

---

## CHAPTER 5

# *An Integrated Feature-based Failure Prognosis Method for Wind Turbine Bearings*

---

### 5.1 Introduction

turbines are complex machines functioning in challenging environments. They embody technologies from aeronautics, mechanical engineering, hydraulics, electrical and electronic engineering, automation, information technologies, as well as civil engineering infrastructure.

As such, for an integrated system, some of the components are more critical than the others, so, for a wind turbine, it is necessary to rank components based on failure rate and downtime. There have been some seminal efforts in recent decades on the reliability of wind farm components as reviewed below.

Nivedh [1] illustrated that the bearings of gearboxes and generators have significant downtime and subsequently lead to more economic losses for the wind farm operator. Review of the reliability summary studies reveals the gearbox and generator failure rates are distinctly high. The downtime for these failures is among the highest of all wind turbine assemblies.

Bearings are critical subassemblies in wind turbines that are prone to faults caused by the corrosive, high temperature, and high-speed environments in which they usually operate. The performance deterioration of a bearing is an irreversible and typically continuous

process. Once the bearing is fixed in its housing, there are hopeful expectations of long, trouble-free service life. Ultimately, minor early faults can emerge that grow slowly at initiation, then hasten with operating time leading to a complete failure. Major bearing failure in wind turbines can create significant downtime from time-consuming reactive maintenance practices. Such lost production directly impacts the wind farm bottom line [2]. Therefore, fault detection and failure prognosis, i.e., estimation of remaining useful life (RUL) and the risk for one or more existing failure modes are a primary area of interest for researchers [3]. Proper condition-monitoring systems (CMS) are an essential component of this pursuit [4]. Continuous health state evaluation can be conducted using monitoring techniques, including vibration analysis (VA), acoustics emission (AE), oil analysis, strain measurement, and thermography. Data are collected at regular time intervals using sensors and measurement systems. By monitoring and processing the real-time data, faults can be detected and, then, predicted. Finally, an appropriate maintenance strategy can be chosen based on the progress of a failure. It is worth noting among all monitoring techniques, vibration analysis (VA) is the most popular technology applied in WT, especially for rotating equipment [5].

Bearing failure prognosis has recently become an essential topic of research. A prognosis method via robust regression-based curve fitting techniques was developed in Siegel et al. [6] for oil-cooler helicopter bearing system. Various algorithms in the proposed prediction framework, including feature extraction and selection, health assessment, and RUL forecasting were investigated in their study. A prognosis method was introduced by Ahmad et al. [7] using regression-based techniques to learn the degradation trend and project the RUL of bearings. This RUL approach applied a gradient-based method to determine a time to start prediction (TSP) using linear regression analysis, which produces a relatively more accurate RUL prediction. In Chen et al. [8], a Multi-Sensor Hidden Semi-Markov Model, an extension of classical hidden semi-Markov models, was proposed. The proposed prognostic methodology was validated on a practical bearing application. The experimental results revealed that the prognostic method was promising to achieve more reliable performance than classical hidden semi-Markov models. A model-based prognosis method was proposed in Singleton et al. [9] by applying an extended Kalman filter to anticipate the RUL of bearings. An analytical function that best approximated the growth of the failure

was employed to determine the parameters of the extended Kalman filter. Qiu et al. [10] presented a new prognostic method by implementing particle filtering (PF) to determine bearing RUL. The process applied the structural information of the spectrum (SIOS) algorithm to build a new health indicator for bearing deterioration monitoring. Then, the RUL was predicted using the PF method with the help of the SIOS-based indicator.

In Caesarendra et al. [11], a combination of Vector Machine, Logistic Regression, and autoregressive moving average/generalized autoregressive conditional heteroscedastic models was proposed to assess bearing failure degradation. The results confirmed the ability of the proposed method for bearing failure degradation assessment. Chen et al. [12] proposed an approach for bearing prognosis based on Neuro-Fuzzy System (NFS) and Bayesian algorithms. The NFS was used as a prognostic model to determine degradation path over time. Then, a Bayesian algorithm was employed to update the degree of confidence in the RUL prediction. Experimental test results confirmed that the proposed failure prognosis approach could predict bearing conditions more accurately in comparison with the recurrent neural networks, the NFS, and the recurrent NFSs techniques. A integrated prognosis method was developed by Cheng et al. [13] for a gearbox. Here an ANFIS was used to estimate the degradation function of the failure. Then, a particle filtering (PF) approach was applied to predict the RUL of the gearbox based on the learned degradation function. Soualhi et al. [14] presented a prognosis method which combines Hidden Markov Model (HMM), the multistep time series prediction, and the adaptive neuro-fuzzy inference system (ANFIS) to provide the imminence of the next degradation state and estimate the remaining time before the next degradation state. The experimental results showed the proposed methodology potential for the detection, diagnosis, and prognosis of faults in roller bearings.

A two-stage approach using Deep Neural Networks (DNN) was proposed in Xia et al. [15] to estimate the RUL of bearings. A denoising auto encoder-based DNN was employed to classify the acquired signals into different degradation states. Then, regression models based on shallow neural networks were constructed for each health state. The proposed approach obtained satisfactory prediction performance on a real bearing degradation dataset with different working conditions. Wang et al. [16] developed a generalized nonlin-

ear degradation approach with deterministic and stochastic parameters. The deterministic parameters were determined using the maximum-likelihood estimation method, while the stochastic parameter in the degradation trend was updated by the Bayesian method utilizing a new piece of degradation measurement. The experimental results confirmed that the proposed method outperforms Gebraeel's and Si's approaches. In Soualhi et al. [17], a prognosis approach that combines the Hilbert Huang Transform (HHT) to extract feature indexes from raw vibration signals, an SVM to detect the degradation states, and the Support Vector Regression (SVR) for the estimation of the RUL of ball bearings was proposed. The experimental results confirmed that the use of the HHT, the SVM, and the SVR is a suitable strategy to enhance the detection, diagnosis, and prognosis of bearing degradation. An integrated prognosis approach using support vector machine regression, multilayer artificial neural network model, and Gaussian process regression was introduced in Elforjani and Shanbr [18] to estimate the RUL of slow speed bearings. The proposed RUL method utilized correlating AE features with the corresponding natural wear throughout series of laboratory experiments.

Fault diagnosis is a well-known task, and it has been widely considered [19, 20, 21, 22]. However, fault prognosis is a relatively new subject, which is often more challenging owing to the uncertainty inherent in the potential for multiple failure degradation paths [23]. To overcome this difficulty, an innovative fusion method is developed in this paper for fault prognosis. The study presented here is driven by data harvested from the turbine. Hypotheses about the system description and data collection are here provided.

- Integrated Circuit-Piezoelectric (ICP) accelerometers sensors are used to record the vibration signals here leveraged for failure prognosis.
- Measurement data is recorded and processed by a device known as the “M-system” that is located in the nacelle of the turbine. Measurements are forwarded to the Turbine Condition Monitoring (TCM) site server located at wind farm substations and can be real-time available through the TCM site server.

The objective of this research is to predict the RUL of various bearings in wind turbines. To achieve this, we design a novel real-time failure prognosis based on a combination of

signal processing and an adaptive Bayesian algorithm. First, signal processing is engaged to extract characteristic features from the data. Next, feature selection and de-noising methods are employed to identify nonlinear dynamics symptomatic of degradation. Then for each selected feature, an RUL is predicted by means of an adaptive Bayesian algorithm. Finally, a fusion of various RULs is integrated into a common framework using an ordered weighted averaging (OWA) operator to provide the RUL of the bearings.

The main contributions of this study are as follows:

- A notable contribution is in the engagement of a fusion method that utilizes an OWA operator which combines the RULs obtained from various features, to produce a more accurate RUL prediction.
- Another contribution is in application of proposed signal processing method which accurately captures the dynamics of the failures through strategic feature extraction and feature selection. Moreover, de-noising of the signals by way of discrete wavelet transforms reduce the level of the noise and leads to more reliable results.
- Additional novelty is revealed in the application of the adaptive Bayesian algorithm. An affine function of time is identified in the performance degradation data obtained from the characteristic features via a sliding window. The proposed Bayesian algorithm is suitable for modeling the uncertainty inherent in the prediction horizon of the bearings and is suitable for online implementation.

A comprehensive study using a ten-year historical data on three wind farms in Canada are conducted. Experimental test results indicate a higher accuracy of the OWA-based prognosis approach in comparison with the other feature-based methods and also Choquet integral fusion technique.

This chapter is organized as follows: Section 5.2 demonstrates the description of the wind turbine drivetrain, bearings and the type of failures. A brief theory of the proposed fault prognosis method is provided in Section 5.3. Design implementations and experimental test results are presented in 5.4. Finally, a summary of results is provided in Section 5.5.

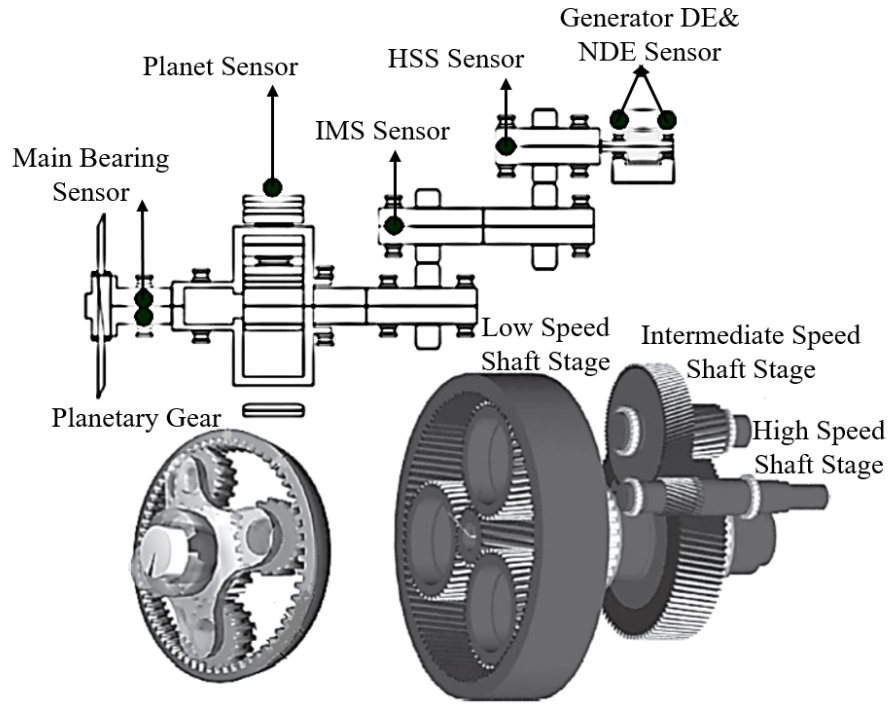


FIGURE 5.2.1: Wind turbine drivetrain Schematic including gearbox and Sensor Configuration

## 5.2 Wind Turbine Drivetrain

This section illustrates the wind turbine drivetrain and its components. The schematic of a wind turbine drivetrain that includes a rotor, gearbox, and generator is shown in Figure 5.2.1. Attached to three blades, the rotor transforms wind energy into low-speed mechanical energy which in turn is accelerated by the gearbox to produce power in the generator. For sizeable gear-driven wind turbines, most manufacturers employ a three-stage pattern as shown in Figure 5.2.1. The low-speed shaft (LSS) planetary gear stage includes the planetary gears in a planet carrier coaxial with a sun gear and a ring gear. Both the intermediate-speed shaft (IMS) stage and high-speed shaft (HSS) use parallel helical gears [24].

Bearings have several applications in a wind turbine, including yaw, pitch, generator, main-shaft, and gearbox bearings, which mount in the nacelle. The main-shaft bearings support the shaft that holds the hub and rotor. The generator bearings provide insulation against electric currents which reduce the risk of premature bearing failures due to erosion from electrical currents [25].

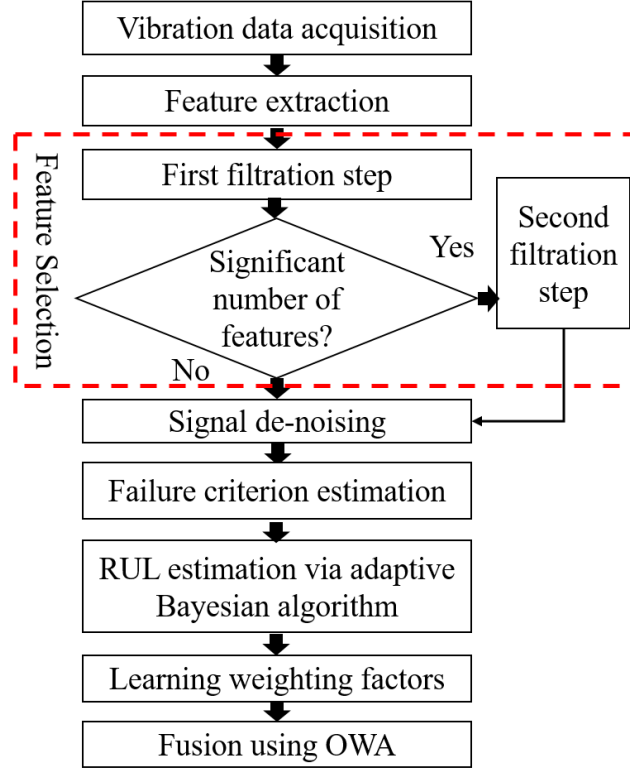


FIGURE 5.3.1: The block diagram of the proposed failure prognosis method.

The vibration data used in this study is provided by accelerometers that monitor the planet, main-shaft bearing, IMS, HSS, generator drive end (DE) and non-drive end (NDE) are shown in Figure 5.2.1. In the following subsection, wind turbine bearings are explained.

### 5.3 A preliminary theory of the proposed fault prognosis method

This section introduces the preliminary theory of the proposed fault prognosis. Figure 5.3.1 shows the block diagram of the proposed failure prognosis method.

The proposed failure prognosis method includes feature extraction, two-step feature selection, signal de-noising, adaptive Bayesian algorithm, and fusion units. In the following, different bearing failure types are discussed, and brief underlying theories of the proposed techniques are presented.



### 5.3.1 The bearing failures

Bearing failures can be classified into two categories of distributed and localized defects. The distributed type describes degradation over large areas of the surface that have become rough, irregular, or deformed. A typical example is the overall surface roughness caused by contamination or lack of lubricant. This type of failure is difficult to predict and to characterize by distinct frequencies. On the contrary, a single-point defect is localized and can be characterized by distinct frequencies, which typically appear in the machine vibration. A representative example of a localized defect is a pit or spall. Depending on which component the bearing has affected, the single point defects can be categorized as follows [20, 26]:

- Inner raceway defect
- Outer raceway defect
- Rolling element defect
- Cage defect

### 5.3.2 Feature extraction

For monitoring dynamic elements, in particular, rolling element bearings, the measured input signals for a condition monitoring system typically consists of vibration signals. In order to identify the dynamics of bearing failure, vibration signals are analyzed with signal processing methods which result in several feature categories. Some of the feature categories are listed as follows:

- Time domain statistical features: They utilize time domain characteristics of signals to extract features. The most relevant time domain features are [27]:
  - 1) Root mean square (RMS): Helps with distinguishing the differences between vibration signals.
  - 2) Variance: Estimates the distribution of a signal around a reference mean value.

3) Skewness: Determines whether a signal is negatively or positively skewed.

4) Kurtosis: Estimates the peak value of the probability density function (PDF) and can reveal if the signal is impulsive.

- Fast Fourier transform (FFT) based features: Convert signals from time to frequency domain and utilize the frequency domain characteristics of signals to obtain features [6].

### 5.3.3 Feature selection

In the feature extraction step, all potential features are obtained from the recorded vibration data. However, applying all the features for failure prognosis is not beneficial. It may increase the computational complexity of the system or even lead to reduced accuracy. In these cases, a subset of the proper features must be selected.

There are many feature selection techniques in the literature. The Filter method and Wrapper method are two popular examples. Filter-based feature selections employ a statistical metric to rank each feature. In this method, all the features are sorted based on the metric. Then, the highest ranked features will be selected. These methods often apply the features independently. Correlation coefficient scores and information gain are two examples of filter-based feature selection methods. It is worth noting that selection of the appropriate metric for effective application of Filter methods is essential [6].

Wrapper methods apply a set of features as a search problem for feature selection, where various combinations are evaluated and compared to other combinations to select those most suitable. The wrapper methods are computationally expensive compared to filter methods due to cross-validation and the repeated learning steps [28].

### 5.3.4 The discrete wavelet transform method (DWT)

Wavelets are shortwave signals which are identified by localized characteristics in time and frequency. Discrete wavelet transforms (DWT) are capable in signal processing applications such as de-noising, fault diagnosis, etc. DWT method can be implemented using

multi-resolution analysis (MRA) to provide a unique framework to analysis a signal and capture its characteristics. Particularly, DWT can reconstruct a signal based on a scaling function  $\phi(t)$  and a wavelet function  $\psi(t)$ , as shown in Algorithm 6. This reconstruction can be formulated as follows. Figure 5.3.2 illustrates signal reconstruction based on MRA method.

---

**Algorithm 6** DWT Algorithm

---

1) Formulating signal estimation using a scaling function  $\phi(t)$  and a wavelet function  $\psi(t)$ :

$$h(t) = \sum_k a_k \phi_k(t - k) + \sum_k \sum_j d_{j,k} \psi_{j,k}(2^j t - k) \quad (5.3.1)$$

where  $a_k$  and  $d_{j,k}$  represent approximation coefficients and detailed coefficients, respectively. Indices  $k$  and  $j$  denote the translation and dilation factors, respectively.

2) Determination of the approximation coefficients,  $a_k$ , and detailed coefficients,  $d_{j,k}$ , using a filtering procedure [29]:

$$a_k = \int \phi_k(z) h(z) dz = \frac{1}{n} \sum_{t=1}^n \phi_k(z(t)) \quad (5.3.2)$$

$$d_{j,k} = \int \psi_{j,k}(z) h(z) dz = \frac{1}{n} \sum_{t=1}^n \psi_{j,k}(z(t)) \quad (5.3.3)$$

Note that  $h(z)$  denotes a density function, and since  $\int \phi_k(z) h(z) dz$  is the expectation of  $\phi_k(z)$  and  $\int \psi_{j,k}(z) h(z) dz$  is the expectation of  $\psi_{j,k}(z)$ , thus,  $a_k$  and  $d_{j,k}$  are achieved using averaging on their scaling functions and wavelet functions, respectively.

---

### 5.3.5 The remaining useful life (RUL)

The RUL of a component or a system is described as the interval between the current time and the projected end of the useful life which depends on the present state of health and the operational environment. In this chapter, a new Bayesian method is applied on the denoised features to predict the RUL of the system. The proposed RUL prediction method is summarized in Algorithm 7.

In the algorithm 7, there are some points to be taken into consideration as follow:

- $n - m$  is the length of sliding windows.

---

**Algorithm 7** Applying Bayesian method
 

---

- 1) Choosing  $q^{th}$  feature of  $S$  selected features
- 2) Setting a healthy data set:  $x_q^{(1)}, x_q^{(2)}, \dots, x_q^{(m-1)}$
- 3) Setting a training set: the sliding window data with degradation trend is selected:  $x_q^{(m)}, x_q^{(m+1)}, \dots, x_q^{(n)}$
- 4) Setting the failure threshold ( $FC$ ):

- Calculating mean of the healthy data set:

$$\mu_q = \frac{1}{m-1} \sum_{i=1}^{m-1} x_q^{(i)} \quad (5.3.4)$$

- Calculating standard deviation of the healthy data set:

$$\sigma_q = \sqrt{\frac{1}{m-1} \sum_{i=1}^{m-1} (x_q^{(i)} - \mu_q)^2} \quad (5.3.5)$$

- Calculating the threshold:

$$FC_q = \mu_q + \lambda_q \sigma_q \quad (5.3.6)$$

- 5) Identifying an optimal affine function of discrete time  $t$  on the de-noised feature over a sliding window:

$$(y_t)_q = (\hat{c}_1 t + \hat{c}_2 + e_t)_q \quad (5.3.7)$$

- 6) Estimating the probability of failure  $p(F_{t_0+j})$  at time  $t_0 + j$ :

$$p_q(F_{t_0+j}) = p_q(F_{t_0+j} | H_{t_0:t_0+j-1}) p_q(H_{t_0:t_0+j-1}) \quad (5.3.8)$$

$$p_q(F_{t_0+j} | H_{t_0:t_0+j-1}) = Q_q\left(\frac{FC - y_{t_0+j}}{\sigma \sqrt{j+1}}\right) \quad (5.3.9)$$

$$\begin{aligned} p_q(H_{t_0:t_0+j-1}) &= [1 - p(F_{t_0+1} | H_{t_0})]_q \times [1 - p(F_{t_0+2} | H_{t_0:t_0+2})]_q \\ &\cdots \times [1 - p(F_{t_0+j-1} | H_{t_0:t_0+j-2})]_q \end{aligned} \quad (5.3.10)$$

- 7) Calculating the  $RUL$ :

$$RUL_q = (t_{Failure} - t_{Prediction})_q \quad (5.3.11)$$


---

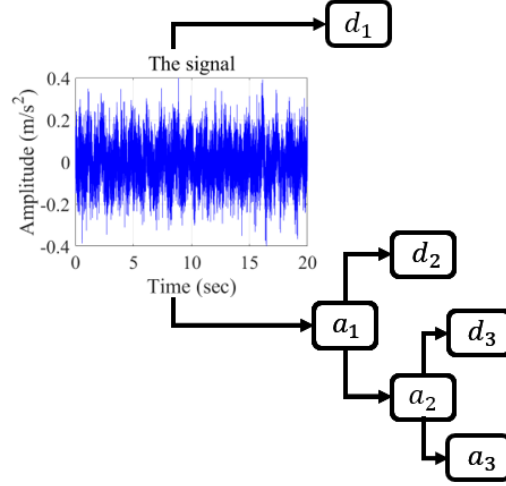


FIGURE 5.3.2: The decomposition of a signal based on MRA method

- $\lambda_k$  in Equation 5.3.6 is the complete failure criteria coefficient.
- In Equation 5.3.7,  $e_t$  denotes a Gaussian white noise error and  $\hat{c}_1$  and  $\hat{c}_2$  are estimated parameters of optimal affine function of time.
- In Equation 5.3.8,  $p(F_{t_0+j})$  is the probability of failure at  $t_0+j$ . Moreover,  $p_q(F_{t_0+j}|H_{t_0:t_0+j-1})$  denotes the probability of being healthy conditional to a failure at  $t_0+j$  and  $p(H_{t_0:t_0+j-1})$  is the probability of staying healthy until  $t_0+j-1$ . The derivation of Equation (5.3.8) can be found in [30].
- The function  $Q$  in Equation 5.3.9 is the standard probability Gaussian distribution function.
- Based on the Equation 5.3.11, RUL is the time difference between the time of a complete failure,  $t_{Failure}$ , defined as the deficiency of the bearing to fulfil its tasks and the time at which predication is made,  $t_{Prediction}$ . Based on Gaussian distribution theory, the failure probability sequences,  $p(F_{t_0+j})$ , of the prediction horizon  $j$  exhibit monotonic growth. Thus, the time of failure,  $t_{Failure}$  is determined at a time  $j$  where the probability of failure is at its maximum.

### 5.3.6 Fusion method

An ordered weighted averaging (OWA) operator, introduced by Yager et al. [31], is a powerful tool to aggregate data from various sources to enhance the accuracy of the RUL prediction. The aggregated RUL is formulated as follows.

$$RUL = \sum_{q=1}^S w_q RUL_q \quad (5.3.12)$$

where  $S$  is the number of selected features,  $RUL_q$  is the remaining useful life obtained by  $q^{th}$  feature and  $w_q$  is its associated weighting factor. The OWA operator task is to optimize the weighting factors for aggregation purposes. For this purpose, several approaches can be applied. In this paper, a gradient descent strategy is engaged to determine weighting factors. In the following, Algorithm 8 is presented for learning the  $q$  weights of the OWA weighting vector from  $L$  observations. It is worth noting that this learning problem is a constrained optimization problem, as the OWA weights must meet the following constraints.

$$\begin{aligned} \sum_{q=1}^S w_q &= 1 \\ w_q &\in [0, 1] \end{aligned} \quad (5.3.13)$$

## 5.4 Simulation studies and experimental results

This section introduces the structure of the proposed fault prognosis system and considers experimental test studies to investigate the performance of the RUL method. In the sections that follow, failure scenarios are illustrated. Afterward, the proposed structure of the fault prognosis is developed. Then, the accuracy of the proposed prognosis method is evaluated with historical field data from wind turbine bearings.

---

**Algorithm 8** Learning weighting factors  $w_q$ 


---

1) Setting a collection of  $L$  observation each comprised of an  $S$ -tuple of arguments:  $v_{i1}, v_{i2}, \dots, v_{iS}$  and an aggregated value:  $b_i$  (for every  $i = 1, \dots, L$ ) to meet the following condition.

$$f(v_{i1}, v_{i2}, \dots, v_{iS}) = b_i \quad (5.3.14)$$

2) Reordering arguments of the  $i^{th}$  observation by  $u_{i1}, u_{i2}, \dots, u_{iS}$  where  $u_{ij}$  is the  $j^{th}$  largest element of the argument collection  $v_{i1}, v_{i2}, \dots, v_{iS}$

3) Simplifying Equation 5.3.14 by taking advantage of the OWA aggregation linearity characteristics with respect to the ordered arguments (for every  $i = 1, \dots, L$ ):

$$u_{i1}w_1 + u_{i2}w_2 + \dots + u_{iS}w_S = b_i \quad (5.3.15)$$

4) Relaxing Equation 5.3.15 by looking for OWA weights that approximate the aggregation operator by minimizing the instantaneous errors,  $e_i$ :

$$e_i = \frac{1}{2}(u_{i1}w_1 + u_{i2}w_2 + \dots + u_{iS}w_S - b_i)^2 \quad (5.3.16)$$

5) Representing the following transformation to circumvent the constraints on the  $w_q$  ( $q \in [1, S]$ ) in Equation 5.3.13.

$$w_q = \frac{\exp \eta_q}{\sum_{j=1}^S \exp \eta_j} \quad (5.3.17)$$

6) Rewriting Equation 5.3.16 with respect to the parameters  $\eta_i$ .

$$e_i = \frac{1}{2} \left( u_{i1} \frac{\exp \eta_1}{\sum_{j=1}^S \exp \eta_j} + u_{i2} \frac{\exp \eta_2}{\sum_{j=1}^S \exp \eta_j} + \dots + u_{iS} \frac{\exp \eta_S}{\sum_{j=1}^S \exp \eta_j} - b_i \right)^2 \quad (5.3.18)$$

7) Updating the parameters  $\eta_q$  by using the following rule inspired by the gradient descent strategy.

$$\eta_q(g+1) = \eta_q(g) - \beta \frac{\partial e_i}{\partial \eta_q} \Big|_{\eta_q = \eta_q(g)} \quad (5.3.19)$$

$\beta$  denotes the learning rate ( $0 \leq \beta \leq 1$ ) and  $\eta_q(g)$  indicates the estimate of  $\eta_q$  after the  $g^{th}$  iteration. Note that the partial derivative  $\frac{\partial e_i}{\partial \eta_q}$  is computed by introducing  $\hat{b}_i$  as the estimate of the aggregated value  $b_i$  for notational simplification as follows.

$$\frac{\partial e_i}{\partial \eta_q} = w_q(u_{iq} - \hat{b}_i)(\hat{b}_i - b_i) \quad (5.3.20)$$


---

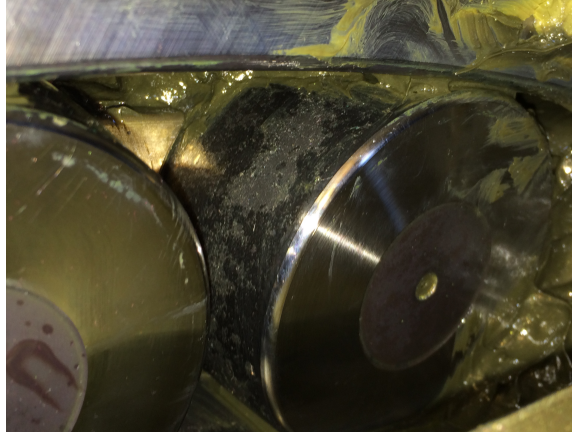


FIGURE 5.4.1: Outer raceway failure

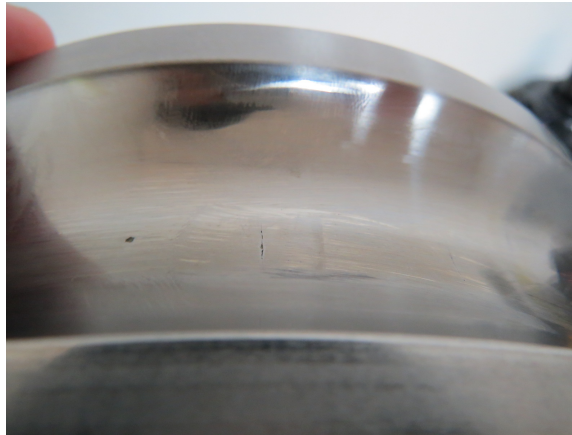


FIGURE 5.4.2: Inner raceway failure

### 5.4.1 Failure Scenarios

This study is based on data from three different commercial wind farm sites. Two farms are based in Southern Ontario and the third is located in Western Prince Edward Island. In total, data from 136 turbines is considered.

Two bearing failures were prominent among this population, i.e., outer raceway failures and inner raceway failures. Figure 5.4.1 shows the outer raceway of a main-shaft bearing on which severe macro-pitting, micro-pitting, and indentations can be observed. Figure 5.4.2 depicts a generator DE bearing with a potential inner race failure.

The failure study was the review of ten-years of raw vibration data that included healthy and faulty states. It is worth noting that twice a month, vibration signals are recorded for 90 sec at a sampling rate of  $640\frac{1}{s}$  for the main-shaft bearing and over 4 sec with a sampling



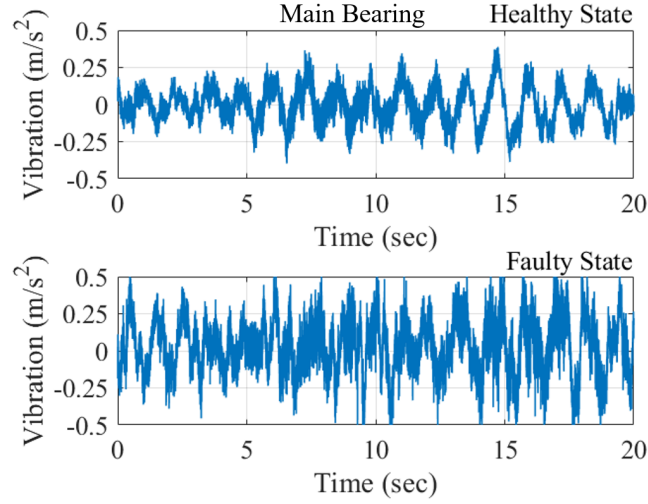


FIGURE 5.4.3: Vibration signal samples of the main-shaft bearing with outer raceway failure recorded in healthy and faulty states

rate of  $15360\frac{1}{s}$  for the generator DE bearing. Figure 5.4.3 compares the amplitudes of the faulty state and the healthy state of the main-shaft bearing. It is evident that the amplitude of faulty state fluctuates between  $-0.5\frac{m}{s^2}$  and  $0.5\frac{m}{s^2}$  which is much more than the healthy state that fluctuates between  $-0.25\frac{m}{s^2}$  and  $0.25\frac{m}{s^2}$ .

Moreover, the amplitudes of the faulty state and the healthy state of the generator DE bearing are compared in Figure 5.4.4. It is seen that the amplitude of faulty state fluctuates between  $-10\frac{m}{s^2}$  and  $10\frac{m}{s^2}$  which is higher than the amplitude of healthy state fluctuating between  $-5\frac{m}{s^2}$  and  $5\frac{m}{s^2}$ .

**Remark 1:** It should be emphasized that due to the unobservability of the failure dynamic in vibration signals, it is necessary to extract next level features from the vibration data to enable identification of the failure dynamic.

### 5.4.2 The proposed feature extraction and selection

For this project, time domain statistical methods are engaged to seek the best features for failure dynamics identification. Many such time domain features can be considered. Caution must be exercised, as considering all of them may not result in better failure modelling. Thus, the filter-based selection method is here used to select the most appropriate features.

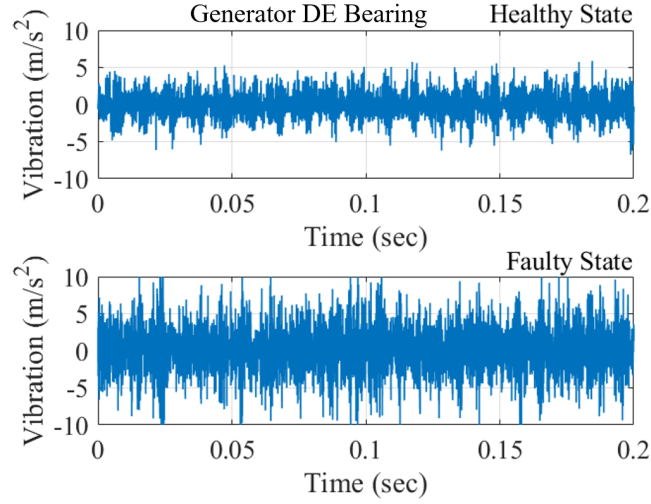


FIGURE 5.4.4: Vibration signal samples of the generator DE bearing with the inner raceway failure recorded in healthy and faulty states

To this end, a two-step filter-based method is proposed. The first step includes selecting the potential features in identifying failure dynamics by comparing the means and variances between a healthy and degraded state. Here, if the number of selected features in the first filtration step is still significant, the second filtration step is executed. In the second step, the most potential features are selected by developing a correlation metric with bearing wear size (recorded monthly by maintenance group after fault detection) and each feature. This implies that the feature magnitude increases in a monotonic manner with bearing damage.

Three features emerged including root mean square (RMS), peak to peak, and variance are identified as the best candidate features for RUL estimation of the outer raceway failure category. The degradation trend that was common to the faulty bearings was observable in these features as shown in Figure 5.4.5. For the inner raceway failure category, root mean square (RMS), peak to peak and band power were identified as the best features to support RUL estimation. The ascending tendency typical of the faulty bearings was detectable in these features as shown in Figure 5.4.6.

Moreover, the complete failure criteria coefficient required in Equation (5.3.6) for each feature are presented in Table 5.4.1. These coefficients are chosen by careful investigation of the historical complete failures and previous studies [17, 9, 32].

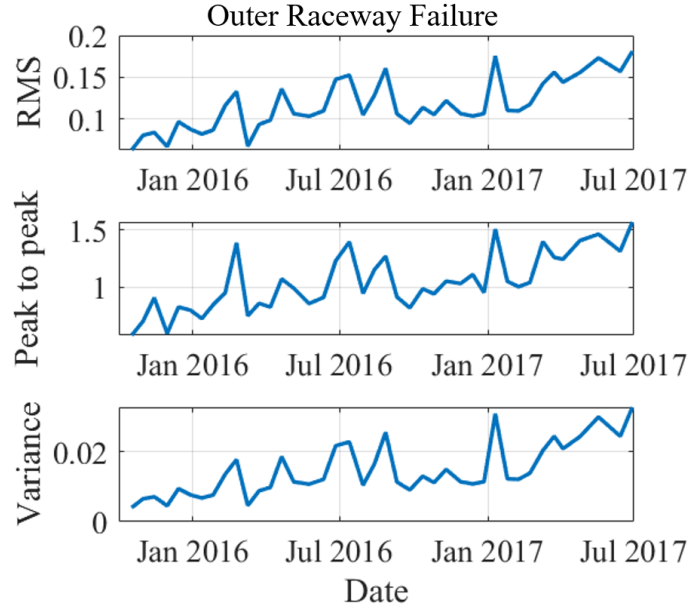


FIGURE 5.4.5: Selected features for outer raceway failure

TABLE 5.4.1: Complete failure criteria coefficient  $\lambda_k$  for each feature

Failure	Outer raceway	Inner raceway
Variance	9	-
Band power	-	18
RMS	6	13.2
Peak to peak	6.9	18.4

**Remark 2:** The complete failure criteria are usually chosen based on the type of bearing and the nature of the failure.

### 5.4.3 The proposed de-noising method

Since extracted features are noisy, to improve prognosis accuracy, features required some de-noising. Here a multi resolution analysis was applied to achieve this. The noisy signals have major high frequency components that appear mostly in the first detail coefficient,  $d_1$  (see Figure 5.3.2). Thus, to eliminate the noise, the noisy features are reconstructed into detail signal and approximation signal using Equation (5.3.1). Then, just the approximation signal,  $a_1$ , (see Figure 5.3.2) is used going forward.

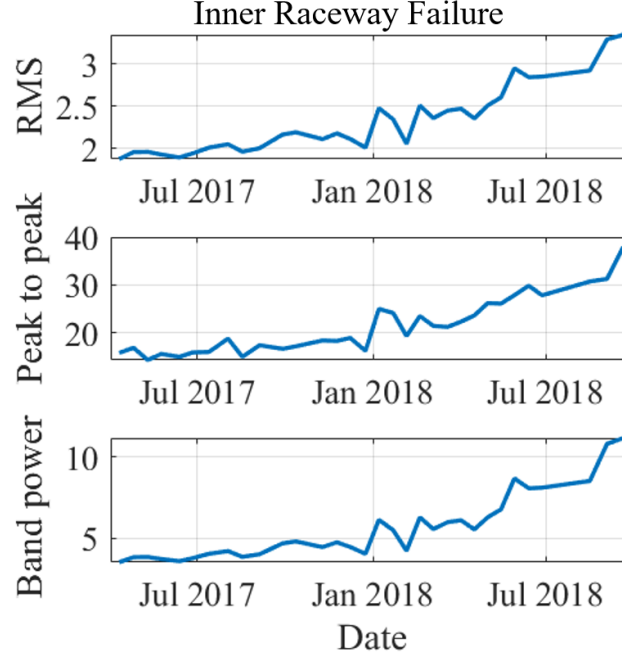


FIGURE 5.4.6: Selected features for inner raceway failure

#### 5.4.4 The proposed RUL

RUL estimates were facilitated by way of an adaptive Bayesian algorithm applied to fit an optimal affine function over a sliding window of three months of de-noised feature signals. For this purpose, an optimal affine model of failure parameter is identified by using Equation (5.3.7). Then, for the estimation of likelihood function, the failure criterion, determined through Equations (5.3.4–5.3.6), were substituted into likelihood Equation (5.3.9). Next, the probability of failure was calculated by substituting Equation (5.3.9) and Equation (5.3.10) in Equation (5.3.8). Finally, the prediction horizon that maximizes the probability of failure determines the RUL prediction.

#### 5.4.5 The proposed Fusion

After calculating the RULs obtained from various features, they are combined by the OWA operator into a unique framework to enhance the accuracy of the prediction. For this purpose, Algorithm 8 is utilized to optimize the weighting factors of the OWA operator. The learning algorithm is started with initial values  $\eta_q(0) = 0$ ,  $q \in [1, 3]$  (the number of selected

TABLE 5.4.2: The estimated values of the  $\eta_q$ 

Failure	Outer raceway	Inner raceway
VAR	0.882	-
BP	-	-0.265
RMS	0.356	0.73
P2P	-1.62	-0.065

TABLE 5.4.3: Fusion weights estimated by the OWA operator for each feature

Failure	Outer raceway	Inner raceway
Variance	0.598	-
Band power	-	0.203
RMS	0.353	0.549
Peak to peak	0.049	0.248

features), with initial values of the OWA weights  $w_q = 0.33$ . A learning rate of  $\beta = 0.35$  is used. The estimated values of the  $\eta_q$  after 187 iterations for outer raceway failure and 202 iterations for inner raceway failure are shown in Table 5.4.2. As a result, Table 5.4.3 presents the weighting factors for various features in two failure categories. Then, Equation (5.3.12) is applied to predict the fused RUL.

Furthermore, to evaluate the accuracy of the RUL, a relative accuracy (RA) measure is considered [30]. The RA index takes a value in a range of  $[0, 1]$ . The larger value of the RA indicates a higher accuracy of the system.

### 5.4.6 Test results

In this subsection, two bearing failures are examined using experimental data to assess the performance of the proposed RUL method. In order to evaluate the proposed RUL method, the RULs obtained by the proposed fusion method (OWA) are compared to the Choquet integral fusion technique [33] and individual features [34, 6].

#### Outer raceway failure

The data from the main-shaft bearing of a wind turbine, T31, installed in 2008 is used to evaluate our proposed approach. This bearing experienced outer raceway failure on June 29<sup>th</sup> 2017. Figure 5.4.7 displays the RULs obtained by various features, Choquet and OWA.

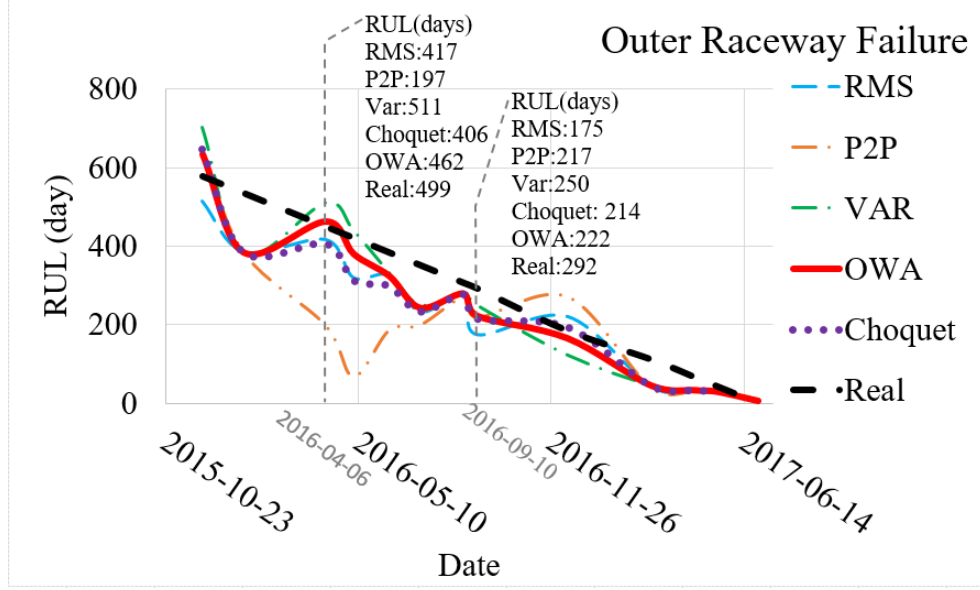


FIGURE 5.4.7: Comparison of the RUL estimated by each feature and OWA for outer raceway failure

The PDFs of the RULs at the chosen sampling points for combined features (Choquet and OWA) are determined in Figure 5.4.8 for outer raceway failure.

Figures 5.4.7 shows that the anticipated RUL using Choquet fusion method on April 6<sup>th</sup> 2016 was 406 days. This represents a relative accuracy of 90.4%. Predictions of 417 days (relative accuracy of 92.9%), 197 days (relative accuracy of 43.9%) and 511 days (relative accuracy of 86.2%) are also shown based on RMS, P2P and the VAR features, respectively. The integrated RUL that uses the OWA operator yielded an estimate of 462 days; an improved relative accuracy of 97%, better than the Bayesian algorithm achieved from individual features and Choquet.

For another case, the RUL on September 10<sup>th</sup> 2016 was 214 days based on the use of Choquet fusion. This provided a relative accuracy of 73.3%. RULs of 175, 217 and 250 were achieved through utilization of the RMS, P2P and VAR features respectively. Again here, the integrated RUL driven by the OWA operator provided a better estimate of 222 days with a relative accuracy of 76% compared to Choquet.

From Figure 5.4.8, the following point can be observed. The predicted PDFs of RULs at the chosen sampling points by OWA are highest compared to Choquet, and can cover the real RUL well. This means that our approach possesses the highest RUL prediction

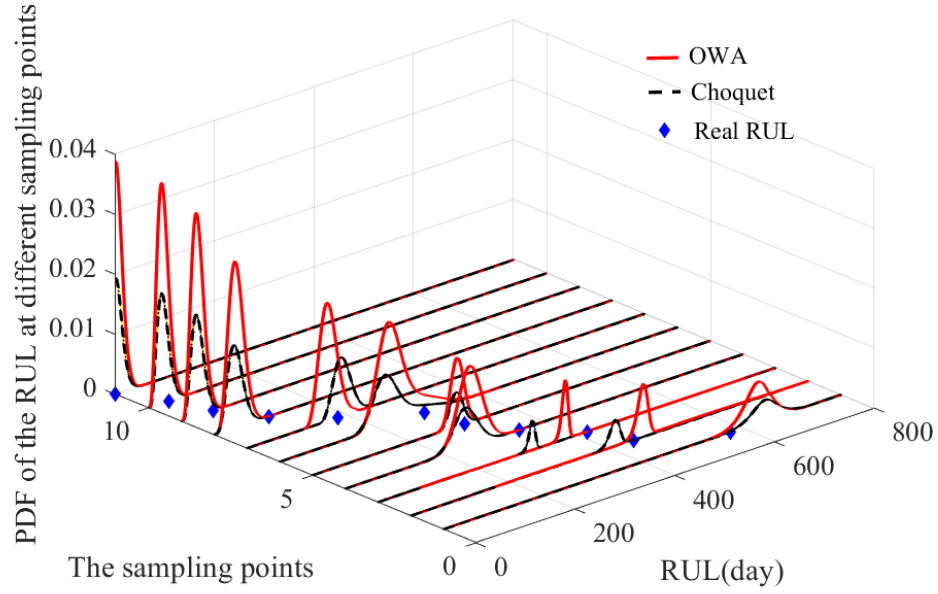


FIGURE 5.4.8: Predicted PDFs of the RULs of outer raceway failure at the chosen sampling points for OWA

accuracy with the smallest prediction uncertainty at the chosen sampling points.

### Inner raceway failure

The generator DE bearing of wind turbine,  $T61$ , was installed in 2011 in Southwestern Ontario. This bearing experienced inner raceway failure on September 20<sup>th</sup> 2018. Figure 5.4.9 reveals the RULs obtained by various features, Choquet and OWA. The PDFs of the RULs at the chosen sampling points for the combined features (Choquet and OWA) are shown in Figure 5.4.10 for inner raceway failure.

It is noted from Figures 5.4.9 that the anticipated RUL on November 9<sup>th</sup> 2017 was 324 days. This represents a relative accuracy of 85.7% based on the Choquet application. Using RMS, P2P and BP features, estimates of 247, 327 days and 351 days respectively, were possible. The integrated RUL prediction based on the OWA operator yielded the best estimate of 289 days (98.6% accurate).

In a second case of March 20<sup>th</sup> 2018, Choquet approach produced a 164 day estimate (92.7% accurate). 142 (92.8% accurate), 112 (73.2% accurate) and 190 (75.8% accurate) day predictions were made by the RMS, P2P and VAR, respectively. Furthermore, the OWA

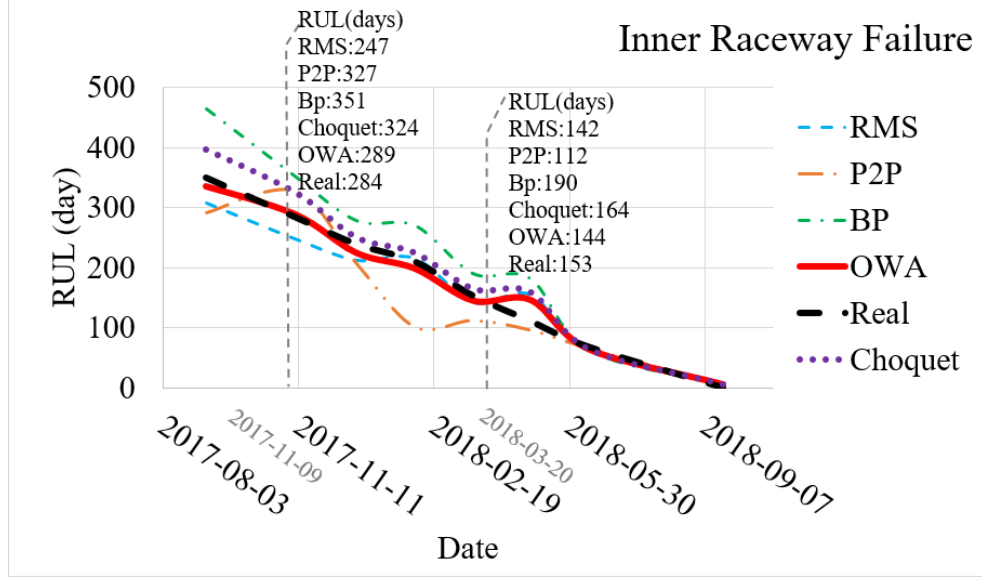


FIGURE 5.4.9: Comparison of the RUL estimated by each feature and OWA for inner raceway failure

estimate was 94.3% accurate at 144 days. The OWA technique again produced the most accurate prediction compared to the Bayesian algorithm obtained from individual features and Choquet fusion method.

Again here from Figure 5.4.10, it can be observed that our approach results in the highest RUL prediction accuracy with the smallest prediction uncertainty at the chosen sampling points compared to Choquet due to the highest predicted PDFs of RULs at the chosen sampling points by OWA.

## 5.5 Conclusion

This chapter proposed a novel real-time RUL prediction method for major bearings critical to wind turbine operation. Two prominent failure types, outer raceway and inner raceway degradations, were investigated. The described method employed comprehensive feature extraction, feature selection, and signal de-noising to detect dynamic failure characteristics. Then, the RUL of the bearings was predicted by an adaptive Bayesian algorithm based on features extracted from raw vibration signals. Finally, a new fusion method built on an ordered weighted averaging (OWA) operator was applied to combine the RUL obtained



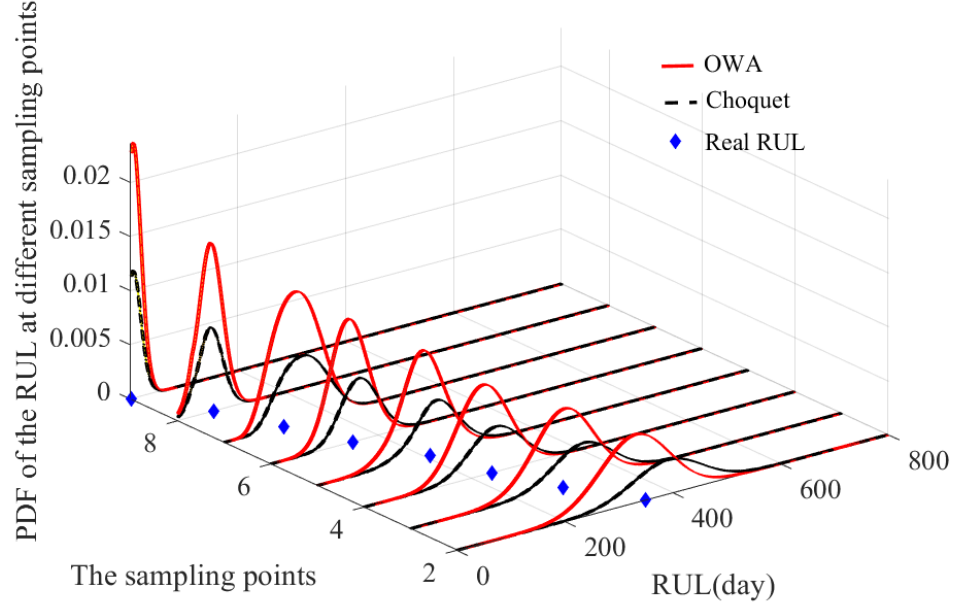


FIGURE 5.4.10: Predicted PDFs of the RULs of inner raceway failure at the chosen sampling points for OWA

from different features to improve prediction accuracy. Two experimental case studies demonstrated, for the data considered here, that the proposed real-time fusion RUL method could notably improve prediction over Bayesian algorithm obtained from single-feature driven methods and the Choquet integral fusion approach.

The principal advantage of the proposed method includes the ability to accurately capture the dynamics of the failures through strategic feature extraction and selection. This was bolstered through the employment of DWT de-noising techniques and the application of a real-time Bayesian algorithm suitable for modelling the uncertainty inherent in the failure prediction of bearings. Finally, the engagement of an OWA operator that combined RULs obtained from various single features revealed a better way to provide relatively accurate RUL predictions.

## 5.6 List of Abbreviations

AE	Acoustic Emission
ANFIS	Adaptive Neuro-fuzzy inference systems
CMS	Condition Monitoring Systems
DE	Drive End
DWT	Discrete Wavelet Transforms
EKF	Extended Kalman filter
FFT	Fast Fourier Transform
HHT	Hilbert Huang transform
HSS	High-Speed Shaft
ICP	Integrated Circuit-Piezoelectric
IMS	Intermediate-Speed Shaft
LSS	Low-Speed Shaft
MRA	Multi-Resolution Analysis
NDE	Non-Drive End
OA	Oil Analysis
OWA	Ordered Weighted Averaging
PF	Particle filter
SM	Strain Measurement
RMS	Root Mean Square
RUL	Remaining Useful Life
SIOS	Structural information of the spectrum
SVR	Support vector regression
TCM	Turbine Condition Monitoring
TSP	Time to Start Prediction
VA	Vibration analysis

## REFERENCES

- [1] B. Nivedh, “Major failures in the wind turbine components and the importance of periodic inspections,” *Wind Insid*, 2014.
- [2] F. Cheng, L. Qu, W. Qiao, and L. Hao, “Enhanced particle filtering for bearing remaining useful life prediction of wind turbine drivetrain gearboxes,” *IEEE Transactions on Industrial Electronics*, 2018.
- [3] L. R. Rodrigues, “Remaining useful life prediction for multiple-component systems based on a system-level performance indicator,” *IEEE/ASME Transactions on Mechatronics*, vol. 23, no. 1, pp. 141–150, 2018.
- [4] A. P. Ompusunggu, J.-M. Papy, and S. Vandenplas, “Kalman-filtering-based prognostics for automatic transmission clutches,” *IEEE/ASME Transactions on Mechatronics*, vol. 21, no. 1, pp. 419–430, 2016.
- [5] F. P. G. Márquez, A. M. Tobias, J. M. P. Pérez, and M. Papaelias, “Condition monitoring of wind turbines: Techniques and methods,” *Renewable Energy*, vol. 46, pp. 169–178, 2012.
- [6] D. Siegel, C. Ly, and J. Lee, “Methodology and framework for predicting helicopter rolling element bearing failure,” *IEEE Trans. Reliability*, vol. 61, no. 4, pp. 846–857, 2012.
- [7] W. Ahmad, S. A. Khan, and J.-M. Kim, “A hybrid prognostics technique for rolling element bearings using adaptive predictive models,” *IEEE Transactions on Industrial Electronics*, vol. 65, no. 2, pp. 1577–1584, 2018.
- [8] Z. Chen, Y. Yang, Z. Hu, and Q. Zeng, “Fault prognosis of complex mechanical systems based on multi-sensor mixtured hidden semi-markov models,” *Proceedings of the Institution of Mechanical Engineers, Part C: Journal of Mechanical Engineering Science*, vol. 227, no. 8, pp. 1853–1863, 2013.

- [9] R. K. Singleton, E. G. Strangas, and S. Aviyente, “Extended kalman filtering for remaining-useful-life estimation of bearings,” *IEEE Transactions on Industrial Electronics*, vol. 62, no. 3, pp. 1781–1790, 2015.
- [10] M. Qiu, W. Li, F. Jiang, and Z. Zhu, “Remaining useful life estimation for rolling bearing with sios-based indicator and particle filtering,” *IEEE Access*, vol. 6, pp. 24 521–24 532, 2018.
- [11] W. Caesarendra, A. Widodo, P. H. Thom, B.-S. Yang, and J. D. Setiawan, “Combined probability approach and indirect data-driven method for bearing degradation prognostics,” *IEEE Transactions on Reliability*, vol. 60, no. 1, pp. 14–20, 2011.
- [12] C. Chen, B. Zhang, and G. Vachtsevanos, “Prediction of machine health condition using neuro-fuzzy and bayesian algorithms,” *IEEE Transactions on instrumentation and Measurement*, vol. 61, no. 2, pp. 297–306, 2011.
- [13] F. Cheng, L. Qu, and W. Qiao, “Fault prognosis and remaining useful life prediction of wind turbine gearboxes using current signal analysis,” *IEEE Transactions on Sustainable Energy*, vol. 9, no. 1, pp. 157–167, 2018.
- [14] A. Soualhi, H. Razik, G. Clerc, and D. D. Doan, “Prognosis of bearing failures using hidden markov models and the adaptive neuro-fuzzy inference system,” *IEEE Transactions on Industrial Electronics*, vol. 61, no. 6, pp. 2864–2874, 2014.
- [15] M. Xia, T. Li, T. Shu, J. Wan, Z. Wang *et al.*, “A two-stage approach for the remaining useful life prediction of bearings using deep neural networks,” *IEEE Transactions on Industrial Informatics*, 2018.
- [16] Z.-Q. Wang, C.-H. Hu, and H.-D. Fan, “Real-time remaining useful life prediction for a nonlinear degrading system in service: Application to bearing data,” *IEEE/ASME Transactions on Mechatronics*, vol. 23, no. 1, pp. 211–222, 2018.
- [17] A. Soualhi, K. Medjaher, and N. Zerhouni, “Bearing health monitoring based on hilbert–huang transform, support vector machine, and regression,” *IEEE Transactions on Instrumentation and Measurement*, vol. 64, no. 1, pp. 52–62, 2015.

- [18] M. Elforjani and S. Shanbr, “Prognosis of bearing acoustic emission signals using supervised machine learning,” *IEEE Transactions on Industrial Electronics*, vol. 65, no. 7, pp. 5864–5871, 2018.
- [19] D. Wang and K.-L. Tsui, “Statistical modeling of bearing degradation signals,” *IEEE Transactions on Reliability*, vol. 66, no. 4, pp. 1331–1344, 2017.
- [20] M. Blodt, P. Granjon, B. Raison, and G. Rostaing, “Models for bearing damage detection in induction motors using stator current monitoring,” *IEEE transactions on industrial electronics*, vol. 55, no. 4, pp. 1813–1822, 2008.
- [21] M. Kordestani, M. Rezamand, R. Carriveau, D. S. Ting, and M. Saif, “Failure diagnosis of wind turbine bearing using feature extraction and a neuro-fuzzy inference system (anfis),” in *International Work-Conference on Artificial Neural Networks*. Springer, 2019, pp. 545–556.
- [22] T. Liu, K. Zhu, and L. Zeng, “Diagnosis and prognosis of degradation process via hidden semi-markov model,” *IEEE/ASME Transactions on Mechatronics*, vol. 23, no. 3, pp. 1456–1466, 2018.
- [23] M. Kordestani, M. Saif, , M. E. Orchard, R. Rezavi-Far, and K. Khorasani, “Failure prognosis and applications—a survey of recent literature,” *IEEE transactions on reliability*, pp. 1–22, 2019.
- [24] Y. Feng, Y. Qiu, C. J. Crabtree, H. Long, and P. J. Tavner, “Monitoring wind turbine gearboxes,” *Wind Energy*, vol. 16, no. 5, pp. 728–740, 2013.
- [25] K. Zipp. (2012) Bearings 101. [Online]. Available: <https://www.windpowerengineering.com/mechanical/nacelle/bearings-101/>
- [26] J. R. Stack, T. G. Habetler, and R. G. Harley, “Fault classification and fault signature production for rolling element bearings in electric machines,” *IEEE Transactions on Industry Applications*, vol. 40, no. 3, pp. 735–739, 2004.

- [27] W. Caesarendra and T. Tjahjowidodo, “A review of feature extraction methods in vibration-based condition monitoring and its application for degradation trend estimation of low-speed slew bearing,” *Machines*, vol. 5, no. 4, p. 21, 2017.
- [28] S. Das, “Filters, wrappers and a boosting-based hybrid for feature selection,” in *Icml*, vol. 1, 2001, pp. 74–81.
- [29] S. G. Mallat, “A theory for multiresolution signal decomposition: the wavelet representation,” *IEEE transactions on pattern analysis and machine intelligence*, vol. 11, no. 7, pp. 674–693, 1989.
- [30] M. Kordestani, A. Zanj, M. E. Orchard, and M. Saif, “A modular fault diagnosis and prognosis method for hydro-control valve system based on redundancy in multisensor data information,” *IEEE Transactions on Reliability*, no. 99, pp. 1–12, 2018.
- [31] R. R. Yager, J. Kacprzyk, and G. Beliakov, *Recent developments in the ordered weighted averaging operators: theory and practice*. Springer, 2011, vol. 265.
- [32] X. Jin, Y. Sun, Z. Que, Y. Wang, and T. W. Chow, “Anomaly detection and fault prognosis for bearings,” *IEEE Transactions on Instrumentation and Measurement*, vol. 65, no. 9, pp. 2046–2054, 2016.
- [33] S. Jullien, L. Valet, G. Mauris, P. Bolon, and S. Teyssier, “An attribute fusion system based on the choquet integral to evaluate the quality of composite parts,” *IEEE transactions on Instrumentation and Measurement*, vol. 57, no. 4, pp. 755–762, 2008.
- [34] W. Teng, X. Zhang, Y. Liu, A. Kusiak, and Z. Ma, “Prognosis of the remaining useful life of bearings in a wind turbine gearbox,” *Energies*, vol. 10, no. 1, p. 32, 2016.

---

## CHAPTER 6

# *RUL Estimation of Wind Turbine Bearings Under Varying Operating Conditions*

---

### 6.1 Introduction

Wind turbine bearings are critical elements to facilitate constrained relative rotation between two components. Due to high loading, corrosive, high-temperature, and high-speed environments in which bearings usually operate, faults can emerge on the bearing components after a period of service time. Bearing faults such as corrosion, spalling, and pitting on the raceways will intensify friction, causing overheating and may lead to complete failure of the bearing. Major bearing failure in wind turbines can create significant downtime from time-consuming reactive maintenance practices [1]. Therefore, the process of health state evaluation, fault detection and failure prognosis, i.e., estimation of Remaining Useful Life (RUL) of bearings can lessen the production downtime and maintenance cost [2]. Proper Condition-Monitoring Systems (CMS) are an essential component of this pursuit. Vibration Analysis (VA) has been confirmed to be very useful CMS in assessing the inception of bearing faults since bearing defects typically cause a machine to vibrate abnormally [3]. Therefore, study on bearing failure prognosis using VA receives much attention in the wind turbine maintenance field recently.

A prognosis approach is presented by Ahmad et al. [4] using regression-based techniques to learn the degradation trend and project the RUL of bearings. This RUL approach

employs a gradient-based method to define a Time to Start Prediction (TSP) using linear regression analysis, which produces a relatively more accurate RUL prediction. Wang et al. [5] develop a two-stage strategy prognosis including, first, evaluation of degradation by determining the deviation of extracted features from a known healthy state and, then, predicting the RUL of the bearing using an enhanced Kalman filter and an Expectation–Maximization (EM) algorithm. The results confirm that their proposed RUL approach reach higher estimation accuracy and narrower PDFs in comparison with Gebraeel’s model [6] and Si’s model [7]. Qiu et al. [8] present a new prognostic method by implementing Particle Filtering (PF) to determine bearings RUL. The process applies the Structural Information of the Spectrum (SIOS) algorithm to build a new health indicator for bearing deterioration monitoring. Then, the RUL is predicted using the PF method with the help of the SIOS-based indicator. Chen et al. [9] present a generic PF-based framework with application in bearing spalling fault diagnosis and failure prognosis. The results suggest that the system is capable of meeting performance requirements. Li et al. [10] propose an intelligent RUL prediction method based on deep learning. Multi-scale feature extraction is executed employing convolutional neural networks. Experiments on an available rolling bearing dataset show a high accuracy of the RUL prediction.

Hybrid methods combine various prognosis methods to enhance RUL accuracy [11]. In Soualhi et al. [12], a hybrid prognosis approach that combines the Hilbert Huang Transform (HHT) to extract feature indexes from raw vibration signals, Support Vector Machine (SVM) to detect the degradation states, and the Support Vector Regression (SVR) for the estimation of the RUL of ball bearings is proposed. The experimental results confirm that the use of the HHT, the SVM, and the SVR is a suitable strategy to enhance the detection, diagnostic, and prognostic of bearing degradation. A hybrid prognosis approach using SVM method, Artificial Neural Network (ANN) model, and Gaussian process regression is introduced by Elforjani and Shanbr [13] to estimate the RUL of slow speed bearings. It is concluded that neural networks model with a back propagation learning algorithm outperforms the other models in predicting the RUL for slow speed bearings. A hybrid prognosis method based on signal processing and deep learning method is developed in Zhu et al. [14] for bearings. For this aim, a Time-Frequency Representation (TFR) of the failure is



identified by Wavelet Transform (WT) with vibration signal. The WT method detects non-stationary properties of bearing degradation signals. After this, a bilinear interpolation is implemented on the TFR data to decrease the dimension. Finally, a Multi-Scale Convolutional Neural Network (MSCNN) is utilized to predict the bearing RUL. The test result with historical data shows a high accuracy of the prognosis method.

In VA-based prognosis methods, degradation dynamics are identified using time domain and frequency domain features via vibration signals for all operating conditions. However, in practice, environmental data such as wind speed and temperature ambient influence failure dynamics as well. The primary motivation of this research work is to consider the effect of environmental conditions in real-time VA-based failure prognosis. Assumptions about the system description and data collection are as follows:

- Integrated Circuit-Piezoelectric (ICP) accelerometers sensors are used to record the vibration signals leveraged for failure prognosis.
- The SCADA data is collected and processed by a device known as the “M-system” that is located in the nacelle of the turbine. Then, the SCADA data is forwarded to the Turbine Condition Monitoring (TCM) site server located at wind farm substations and can be real-time available through the TCM site server.

In this research work, a hybrid failure prognosis method is proposed to predict the bearing RUL. Our proposed prognosis approach is implemented in two off-line and online phases. In the off-line phase, SCADA data is utilized to detect failure severity through a combination of a Kernel Fuzzy C-Means (KFCM) and a Hidden Markov Model (HMM). The KFCM clusters various operating states using environmental conditions from SCADA data. Then, the Viterbi-based HMM is employed to determine the switching time between the defined operating states and the Viterbi Algorithm is employed to tune and validate the HMM. Meanwhile, vibration signals are used to identify failure dynamics for each class of the operating state through the signal processing method using de-noising, feature extraction, and feature selection. Afterward, in the online phase, damage progression models are determined on features selected from vibration signals, conditional to the defined operating states, using SCADA data. Then, several realizations of HMM are generated for

anticipating future state in which wind turbine operates. A real-time Bayesian algorithm is implemented to predict the bearing RUL of each generated realization. Finally, RUL estimates of realizations are averaged to predict an accurate RUL for faulty bearings.

The main contributions of this study are as follows:

- The damage progression is characterized using the different operating states to mimic a real condition in which wind turbines operate. This proposed prognosis framework potentially improves the accuracy of RUL prediction.
- Another notable contribution is the engagement of the KFCM, the HMM methods and the Viterbi Algorithm. It optimizes the clustering accuracy using fuzzy C means. Furthermore, the HMM allows the switching between operating states based on probability transient matrix that correctly utilizes the severe environmental conditions. Here, the Viterbi Algorithm is employed to tune and validate the HMM.
- Additional novelty is revealed in the implementation of integrated adaptive Bayesian algorithm and generated realizations of the HMM in the online phase. Generated realizations of the HMM allows precise prediction of the future state in which wind turbines operate. Moreover, the Bayesian algorithm is proper to characterize uncertainty inherited in the prediction horizon. This enhances the RUL accuracy.

This chapter is organized as follows: Section 6.2 demonstrates the description of wind turbine bearings and the type of failures. A brief theory of the proposed fault prognosis method is provided in Section 6.3. Design implementations and experimental results are presented in 6.4. Finally, a summary of key findings is provided in Section 6.5.

## 6.2 Wind Turbine Bearings

Bearings are mechanical parts that facilitate the desired motion between moving parts by reducing friction. Bearings which transfer loads using rolling elements are known as a rolling bearing. Primary components of rolling bearings include rolling elements, inner ring, outer ring, and cage are shown in Figure 6.2.1. The seals are used only in some

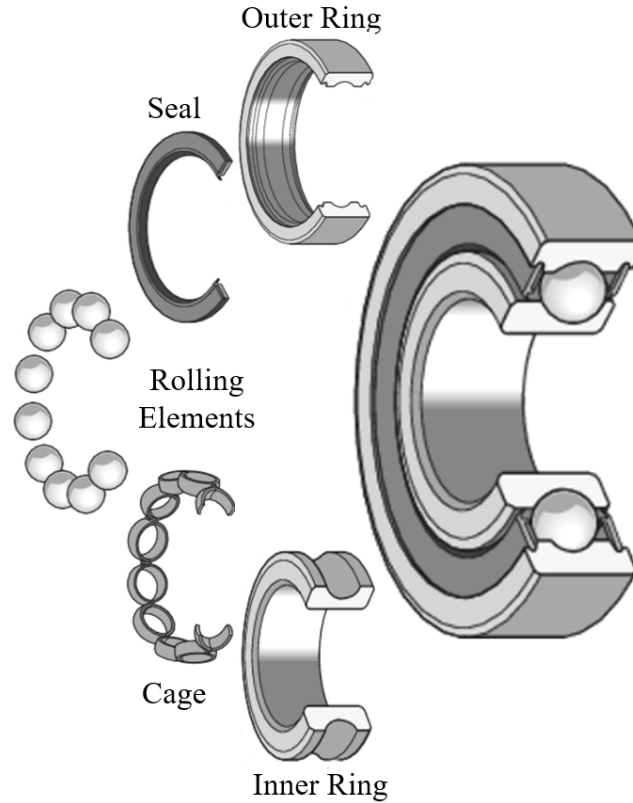


FIGURE 6.2.1: Rolling bearings components

particular applications. The inner ring is located on the shaft of the machine. The outer ring is fixed to the housing of the device. The rolling elements, either balls or rollers, rotate against the inner and outer ring raceways. These rolling elements transfer the load acting on the bearing via small surface contacts separated by a thin lubricating film. The cage keeps the rolling elements apart to avoid metal-to-metal contact between them during operation.

Bearings applications in a wind turbine comprise of yaw, pitch, generator, main-shaft, and gearbox bearings, which are mounted in the nacelle. The gearbox bearings include an Intermediate-Speed Shaft (IMS), High-Speed Shaft (HSS), Low-Speed Shaft (LSS), and planetary bearings. The generator bearings provide insulation against electric currents, decreasing the risk of premature bearing failures due to erosion from electrical currents. The main-shaft bearings support the shaft that holds the hub and rotor [15].

The vibration data used in this study is provided by accelerometers that monitor the planet, main-shaft bearing, IMS, HSS, generator Drive End (DE) and Non-Drive End

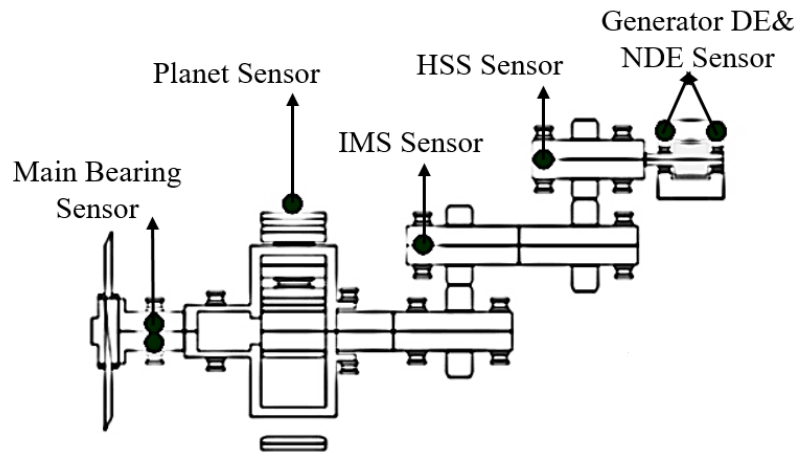


FIGURE 6.2.2: Bearing Sensors Configuration

(NDE) are shown in Figure 6.2.2.

### 6.2.1 The bearing failures

Bearing failures can be classified into two categories of distributed and localized defects. The distributed type describes degradation over large areas of the surface that have become rough, irregular, or deformed. A typical example is the overall surface roughness caused by contamination or lack of lubricant. This type of failure is difficult to predict and to characterize by distinct frequencies. On the other hand, a single-point defect is localized and can be characterized by distinct frequencies, which typically appear in the machine vibration. A representative example of a localized defect is a pit or spall. Depending on which component the bearing has affected, the single point defects can be categorized into inner raceway and outer raceway defects [16, 17].

## 6.3 A preliminary theory of the proposed fault prognosis method

This section introduces the preliminary theory of the proposed failure prognosis. Figure 6.3.1 shows the block diagram of the proposed failure prognosis method.

The procedure of the block diagram is explained as follows. In the off-line phase,

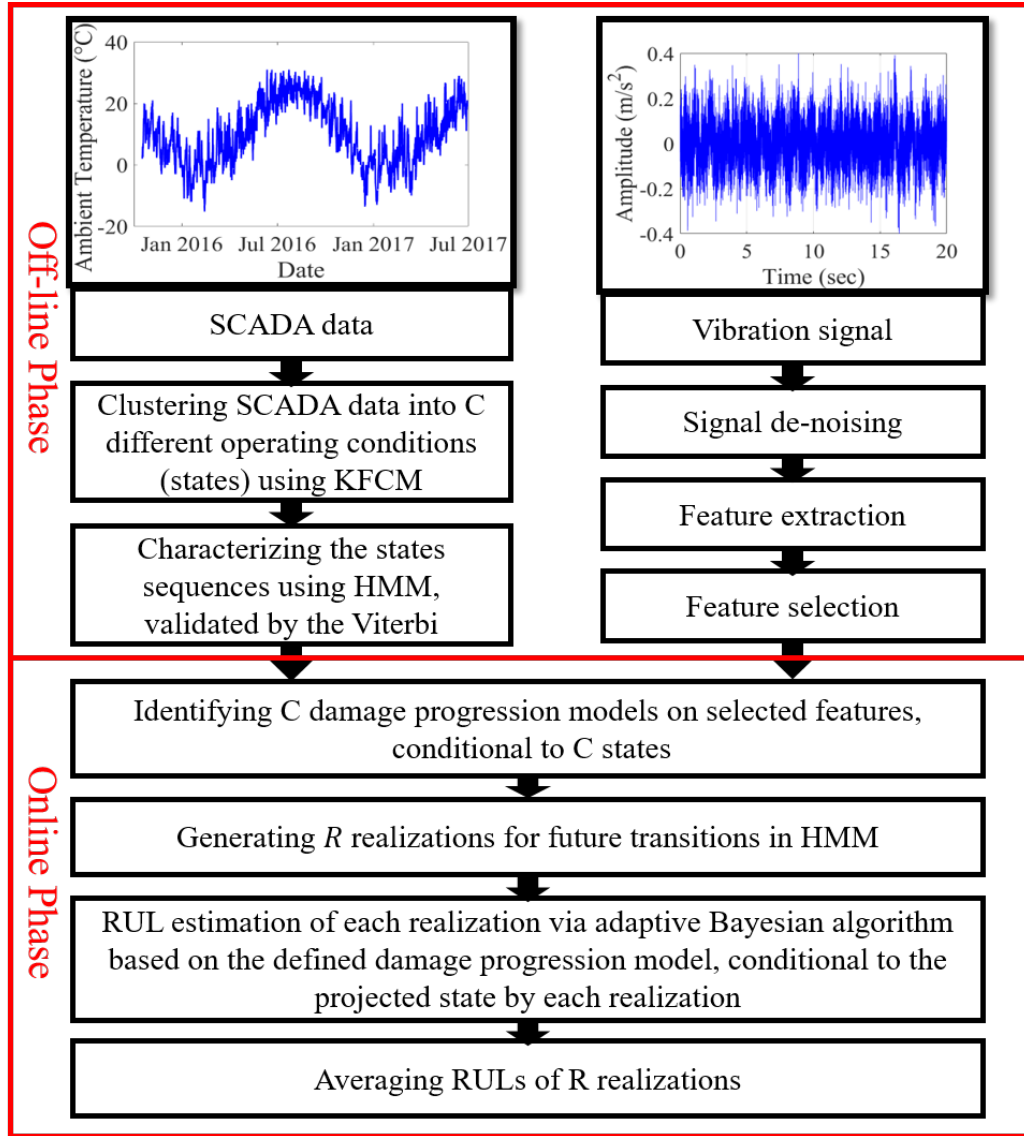


FIGURE 6.3.1: The block diagram of the proposed failure prognosis method.

SCADA data is partitioned into  $C$  operating condition states employing KFCM. Then, the most likely sequences between states are determined using an HMM. Here, the Viterbi Algorithm is employed to tune and validate the HMM. Meanwhile, vibration signals are de-noised through a Discrete Wavelet Transform (DWT) method. Next, feature extraction and feature selection are performed on the de-noised vibration signals to capture the dynamic of failure. In the online phase,  $C$  damage progression models are identified on the selected features conditional to  $C$  operation states obtained from SCADA data. Then,  $R$  realizations for future transitions in HMM are generated to determine the most likely state in which wind turbine will operate in the future. For each realization, RUL is predicted via an adaptive Bayesian algorithm on  $C$  defined damage progression models conditional to the projected state. Finally, RUL estimates of  $R$  realizations are averaged to obtain an accurate RUL.

In the following, brief underlying theories of the proposed techniques are presented.

### 6.3.1 KFCM-based clustering

Clustering aims at partitioning a set of multivariate data points into meaningful clusters, where all members within the same group share similar properties, while data points in different clusters are highly dissimilar to each other. KFCM, presented in Algorithm 9, is a robust clustering technique for nonlinear separation of clusters. The KFCM accomplishes this goal by mapping the data to a higher dimensional feature space by employing a nonlinear mapping function  $\Phi$ , which can be calculated with a kernel function  $K$  [18, 19].

The following points concerning Algorithm 9 are worth highlighting.

- The E–M algorithm recursively continue until a convergence condition is satisfied.
- In the E-step, the weight  $w_{ic}$  is determined by applying Lagrange multipliers to transform the constrained objective  $\sum_{c=1}^C w_{ic} = 1$  as an unconstrained optimization model and forcing the derivatives to zero with respect to  $w_{ic}$ .
- In the M-step, the distance  $\Phi_{d_{ic}^2}$  is calculated by using a kernel function  $K$  [20]. Note that Algorithm 10 is employed to solve for the kernel function  $K$  [18].

**Algorithm 9** Kernel Fuzzy C-Means based clustering

- 1) Let  $X = [x_1, x_2, \dots, x_N]$  ( $x_i \in \mathbb{R}$ ) be a set of  $N$  unlabeled data points.
- 2) Partitioning the data set  $X$  into  $C$  clusters by minimizing the distance objective (the distance  $\Phi_{d_{ic}^2}$  between  $x_i$  and the centroid  $v_c$  weighted by  $w_{ic}$ ) with a nonlinear mapping function  $\Phi$  in feature space which can be determined using a kernel function  $K$ :

$$\min \sum_{c=1}^C \sum_{i=1}^N w_{ic}^p \Phi_{d_{ic}^2} = \min \sum_{c=1}^C \sum_{i=1}^N w_{ic}^p \|\Phi(x_i) - \Phi(v_c)\|^2 \quad (6.3.1)$$

Where  $p$  is the exponent.

- 3) The weight  $w_{ic}$  and the distance  $\Phi_{d_{ic}^2}$  is updated by the expectation–maximization (E–M) algorithm:

- E-step:

$$w_{ic} = \frac{1}{\sum_{j=1}^C \left( \frac{\Phi_{d_{ic}^2}}{\Phi_{d_{ij}^2}} \right)^{\frac{1}{p-1}}}, i = 1, 2, \dots, N, c = 1, 2, \dots, C \quad (6.3.2)$$

- M-step:

$$\Phi_{d_{ic}^2} = K_{ii} - 2 \times \frac{\sum_{j=1}^N w_{jc}^p K_{ij}}{\sum_{j=1}^N w_{jc}^p} + \frac{\sum_{m=1}^N \sum_{n=1}^N w_{mc}^p w_{nc}^p K_{mn}}{\sum_{m=1}^N \sum_{n=1}^N w_{mc}^p w_{nc}^p} \quad (6.3.3)$$

### 6.3.2 Hidden Markov Models and the Viterbi Algorithm

An HMM depicts stochastic sequences of unobservable states as HMM in a probabilistic form via observable sensor signals. An HMM is a sequence of states, the probability of each is dependent only on the state instantly preceding it [21]. Let  $q_t \in [s_1, s_2, \dots, s_n]$  as the value of hidden state at time  $t$  where  $n$  is the number of hidden states and  $o_t \in [v_1, v_2, \dots, v_m]$  as the observed state that the measuring value of sensor where  $m$  expresses the possible number of the observed value corresponding each state, then an HMM is specified by the following components:

- An initial probability distribution over states,  $\pi = (\pi_1, \pi_2, \dots, \pi_n)$
- A transition probability matrix,  $A = (a_{ij})$ : indicates the probability that the state is  $s_j$  at time  $t - 1$ , conditional to, the state is  $s_i$  at time  $t$ , as defined as:

$$a_{ij} = P(q_t = s_i | q_{t-1} = s_j), 1 \leq i, j \leq n \quad (6.3.8)$$

**Algorithm 10** Kernel function determination

1) Given the data collection  $X = [x_1, x_2, \dots, x_N]$  ( $x_i \in \mathbb{R}$ ).

2) Estimating the data center  $v$  :

$$v = \frac{1}{N} \sum_{i=1}^N x_i \quad (6.3.4)$$

3) Calculating the mean distance  $\bar{d}$  :

$$\bar{d} = \frac{1}{N} \sum_{i=1}^N d_i \quad (6.3.5)$$

Note that  $d_i$  is the distance between data point  $x_i$  and the data center  $v$ .

4) Calculating of the bandwidth  $h$  based on the distance variance of all data points in the collection:

$$h = \frac{1}{N-1} \sum_{i=1}^N (d_i - \bar{d})^2 \quad (6.3.6)$$

5) Determination of kernel function in the form of radial basis function (RBF):

$$K_{ij} = K(x_i, x_j) = \exp\left(-\frac{\|x_i - x_j\|^2}{h}\right) \quad (6.3.7)$$

- A confusion matrix,  $B = (b_{jk})$ : : indicates the probability that the hidden state is  $s_j$  while  $v_k$  as the observed state, as described as:

$$b_{jk} = P(o_t = v_k | q_t = s_j), 1 \leq j \leq n, 1 \leq k \leq m \quad (6.3.9)$$

Here the challenge is to find the most likely sequence of hidden states  $Q = [q_1, q_2, \dots, q_t]$  based on the system parameter  $\lambda = (\pi, A, B)$  and observation sequence  $O = [o_1, o_2, \dots, o_t]$ . The task of determining the most probable sequence of hidden states based on the sequence of observations is known as decoding or inference. The Viterbi is a robust decoding algorithm for HMMs which computes the most probable sequence (as well as its probability) as indicated in Algorithm 11 [22].

### 6.3.3 Signal de-noising based on DWT method

DWT method is suitable for signal processing applications such as de-noising, fault diagnosis, etc. DWT method can be implemented using multi-resolution analysis (MRA) to



**Algorithm 11** Viterbi algorithm

1) Initialization:

$$\delta_1(i) = \pi_i b_{io_1} \psi_1(i) = 0, 1 \leq i \leq n \quad (6.3.10)$$

2) Recursion:

$$\begin{aligned} \delta_{t+1}(j) &= \max_{1 \leq i \leq n} [\delta_t(i) a_{ij}] b_{jo_{t+1}} \\ \psi_{t+1}(j) &= \arg \max_{1 \leq i \leq n} [\delta_t(i) a_{ij}] b_{jo_{t+1}}, 1 \leq t \leq T, 1 \leq j \leq n \end{aligned} \quad (6.3.11)$$

3) Computing States Sequences (with retrospect):

$$P(Q, O|\lambda) = \max_{1 \leq i \leq n} \delta_T(i), Q_{t-1} = \psi_t(Q_t), T \geq t \geq 1 \quad (6.3.12)$$

provide a unique framework for analyzing a signal and capture its characteristics. Particularly, DWT can reconstruct a signal based on a scaling function  $\phi(t)$  and a wavelet function  $\psi(t)$ . This reconstruction can be formulated as follows.

$$f(t) = \sum_k a_k \phi(t - k) + \sum_k \sum_j d_{j,k} \psi(2^j t - k) \quad (6.3.13)$$

where  $a_k$  and  $d_{j,k}$  represent approximation coefficients and detailed coefficients, respectively. Indexes  $k$  and  $j$  denote the translation and dilation factors, respectively. It is worth noting that the approximation and detailed coefficients are determined using filtering procedure introduced by Mallat [23]. Figure 6.3.2 illustrates signal reconstruction based on MRA method.

Note that detailed coefficient ( $d_1$ ) contain the noise of faulty signals. Therefore, this coefficient must be discarded to improve the quality of the signals.

**Remark 1:** It should be emphasized that while vibration data can directly help with fault diagnosis, it does not directly support failure prognosis due to the unobservability of the failure dynamic. Rather, it is essential to extract next level features from the vibration data to enable identification of the failure dynamic.

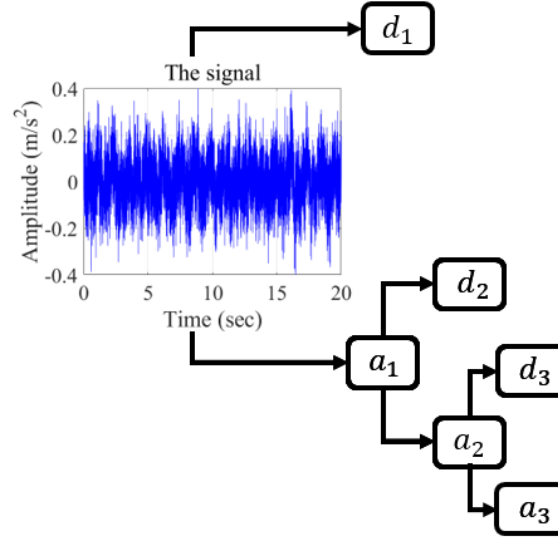


FIGURE 6.3.2: The decomposition of a signal based on MRA method

### 6.3.4 Feature extraction

For monitoring dynamic components, specifically, rolling element bearings, the recorded input signals for CMS typically includes vibration signals. For identifying the failure dynamics, vibration signals are analyzed with signal processing techniques which result in several feature categories. Time domain statistical methods are engaged to seek the best features for failure dynamics identification due to their robustness in bearing failure prognosis. They utilize time domain characteristics of signals to extract features. The most relevant time domain features are shown in Table 6.3.1 [24]:

### 6.3.5 Feature selection

Applying all potential features obtained in the feature extraction step for failure prognosis may increase the computational complexity of the system or even lead to reduced accuracy. In these cases, a subset of the appropriate features must be chosen.

There are several feature selection procedures in the literature. The Filter-based and Wrapper techniques are two popular examples. Filter-based feature selections apply a statistical metric to sort features, and the highest ranked features are chosen. Correlation coefficient scores and information gain are two examples of filter-based feature selection

TABLE 6.3.1: Time domain features for signal  $x$ 

Features	Formula
Mean	$A_1 = \frac{1}{N} \sum_{i=1}^N x_i$
Standard Deviation	$A_2 = \sqrt{\frac{1}{N-1} \sum_{i=1}^N (x_i - A_1)^2}$
Root Mean Square	$A_3 = \sqrt{\frac{1}{N} \sum_{i=1}^N x_i^2}$
Variance	$A_4 = \frac{\frac{1}{N} \sum_{i=1}^N (x_i - A_1)^3}{[\frac{1}{N} \sum_{i=1}^N (x_i - A_1)^2]^{\frac{3}{2}}}$
Peak to peak	$A_5 = \max(x) - \min(x)$
Waveform factor	$A_6 = \frac{A_3}{\frac{1}{N-1} \sum_{i=1}^N  x_i }$
Peak factor	$A_7 = \frac{x_{peak}}{A_3}$
Impulse factor	$A_8 = \frac{x_{peak}}{\frac{1}{N-1} \sum_{i=1}^N  x_i }$
Margin factor	$A_9 = \frac{x_{peak}}{(\frac{1}{N} \sum_{i=1}^N  x_i )^2}$
Kurtosis factor	$A_{10} = \frac{\sum_{i=1}^N x_i^4}{N \times A_3}$
Skewness	$A_{11} = E[(\frac{x-A_1}{A_2})^3]$
Kurtosis	$A_{12} = E[(\frac{x-A_1}{A_2})^4]$

methods. It is worth noting that the selection of the proper metric for efficient application of Filter methods is inevitable [25]. These methods often apply the features independently. However, Wrapper methods use a set of features as a search problem for feature selection, where various combinations are assessed and compared to select the most suitable. The wrapper methods are computationally expensive compared to filter methods due to cross-validation and the repeated learning steps [26].

### 6.3.6 Bayesian RUL Prediction Algorithm

Bayesian inference is a robust set of tools for the establishment of the mathematical formulation of the observed events and the factors in the models affecting the observed data. Bayesian method can be employed on the observed data conditional to each operating condition (state) to predict the RUL of the dynamic system as described in Algorithm 12.

The following are key points concerning Algorithm 12.

- The time of a complete failure,  $t_{Failure}$  signifies as the deficiency of the bearing to

**Algorithm 12** Bayesian based RUL estimation

- 1) Choosing  $q^{th}$  feature of  $p$  selected features
- 2) Setting a healthy data set:  $x_q^{(1)}, x_q^{(2)}, \dots, x_q^{(y-1)}$
- 3) Setting a training set: the sliding window data with degradation trend is selected:  $x_q^{(y)}, x_q^{(y+1)}, \dots, x_q^{(z)}$
- 4) Setting the failure threshold ( $FC$ ):

- Calculating mean of the healthy data set:

$$\mu_q = \frac{1}{y-1} \sum_{i=1}^{y-1} x_q^{(i)} \quad (6.3.14)$$

- Calculating standard deviation of the healthy data set:

$$\sigma_q = \sqrt{\frac{1}{y-1} \sum_{i=1}^{y-1} (x_q^{(i)} - \mu_q)^2} \quad (6.3.15)$$

- Calculating the threshold:

$$FC_q = \mu_q + \lambda_q \sigma_q \quad (6.3.16)$$

- 5) Identifying an optimal affine function of discrete time  $t$  on the de-noised feature over a sliding window:

$$(y_t)_q = (\hat{c}_1 t + \hat{c}_2 + e_t)_q \quad (6.3.17)$$

- 6) Estimating the probability of failure  $p(F_{t_0+j})$  at time  $t_0 + j$ :

$$p_q(F_{t_0+j}) = p_q(F_{t_0+j} | H_{t_0:t_0+j-1}) p_q(H_{t_0:t_0+j-1}) \quad (6.3.18)$$

$$p_q(F_{t_0+j} | H_{t_0:t_0+j-1}) = Q_q\left(\frac{FC - y_{t_0+j}}{\sigma \sqrt{j+1}}\right) \quad (6.3.19)$$

$$\begin{aligned} p_q(H_{t_0:t_0+j-1}) = & \\ & [1 - p(F_{t_0+1} | H_{t_0})]_q \times [1 - p(F_{t_0+2} | H_{t_0:t_0+2})]_q \\ & \dots \times [1 - p(F_{t_0+j-1} | H_{t_0:t_0+j-2})]_q \end{aligned} \quad (6.3.20)$$

- 7) Calculating the  $RUL$ :

$$RUL_q = (t_{Failure} - t_{Prediction})_q \quad (6.3.21)$$

fulfil its tasks and  $t_{Prediction}$  is the predicted time. Based on the Gaussian distribution,  $t_{Failure}$  is described as the time at which the probability of failure is at its peak. The  $p(F_{t_0+j})$  is the probability of failure at  $t_0 + j$  and  $p(H_{t_0:t_0+j-1})$  is the probability of staying healthy until  $t_0 + j - 1$ . The derivation of Equation (6.3.18) can be found in Appendix A [27]. The function  $Q$  is the standard probability Gaussian distribution function.

- $e_t$  denotes a Gaussian white noise error and  $\hat{c}_1$  and  $\hat{c}_2$  are estimated parameters of optimal affine function of time.
- $y - z$  is the length of sliding windows.
- $\lambda_k$  is the complete failure criteria coefficient.

## 6.4 Simulation studies and experimental results

This section introduces the structure of the proposed fault prognosis system and considers experimental test studies to investigate the performance of the RUL method. In the sections that follow, failure scenarios are illustrated. Afterward, the proposed structure of the fault prognosis is developed. Then, the accuracy of the proposed prognosis method is evaluated with historical field data.

### 6.4.1 Failure Scenarios

This study is based on data from 136 turbines of three different commercial wind farm sites. Two farms are located in Southern Ontario and the third is based in Western Prince Edward Island.

Two types of bearing failures were crucial among this population, i.e., outer raceway failures and inner raceway failures. Figure 6.4.1 indicates the outer raceway of a main-shaft bearing on which severe macro-pitting, micro-pitting, and indentations can be observed. Figure 6.4.2 depicts a generator DE bearing with a potential inner race failure.

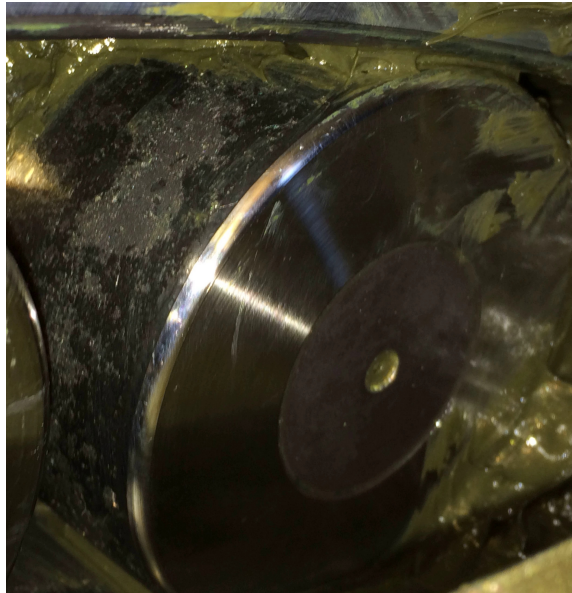


FIGURE 6.4.1: Outer raceway failure



FIGURE 6.4.2: Inner raceway failure

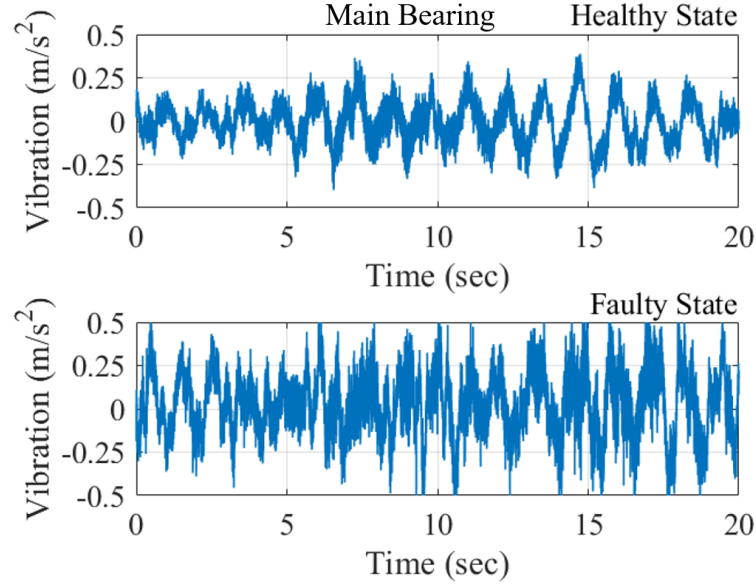


FIGURE 6.4.3: Vibration signal samples of the main-shaft bearing with outer raceway failure recorded in healthy and faulty states

The failure study was the investigation of 10-minute SCADA data for categorizing different operating states and raw vibration data for identifying damage progression model, conditional to each state. Twice a month, vibration signals are recorded for 90 sec at a sampling rate of  $640\frac{1}{s}$  for the main-shaft bearing and over 4 sec with a sampling rate of  $15360\frac{1}{s}$  for the generator DE bearing. The amplitudes of the faulty phase and the healthy phase of the main-shaft bearing are compared in Figure 6.4.3. It is seen that the amplitude of faulty phase fluctuates between  $-0.5\frac{m}{s^2}$  and  $0.5\frac{m}{s^2}$  which is higher than the healthy phase that fluctuates between  $-0.25\frac{m}{s^2}$  and  $0.25\frac{m}{s^2}$ .

Moreover, Figure 6.4.4 compares the amplitudes of the faulty phase and the healthy phase of the generator DE bearing. It is evident that the amplitude of faulty phase fluctuates between  $-10\frac{m}{s^2}$  and  $10\frac{m}{s^2}$  which is much more than the amplitude of healthy phase fluctuating between  $-5\frac{m}{s^2}$  and  $5\frac{m}{s^2}$ .

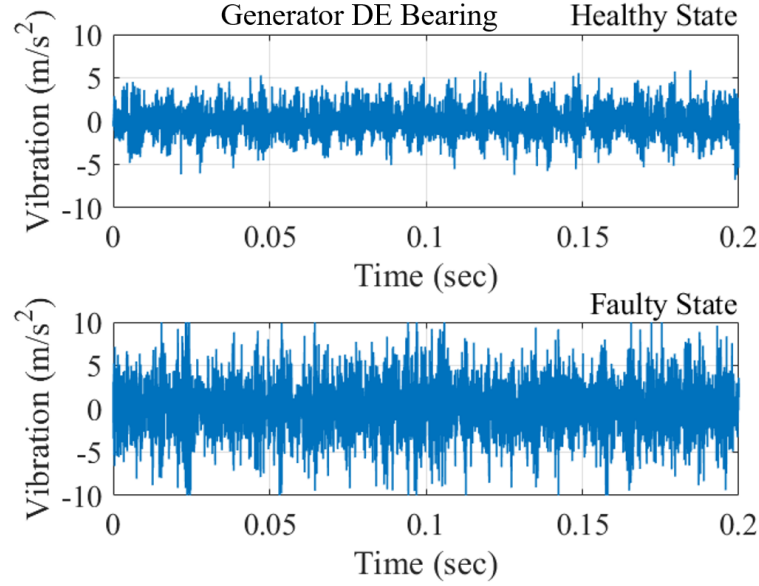


FIGURE 6.4.4: Vibration signal samples of the generator DE bearing with the inner raceway failure recorded in healthy and faulty states

#### 6.4.2 Off-line phase design implementation

In off-line phase, 10-minute SCADA data including ambient temperature, wind speed, active power generated, main-shaft rotational speed, main bearing temperature, generator rotational speed, and generator DE bearing temperature is used to categorize different operating states. An KFCM is employed to achieve this. As a result, two states, so-called normal and aggressive states, are partitioned by utilizing Equation 6.3.1. Following the operating condition is clustered into two states, the wind turbine operating profile is to be characterized. In this regard, an HMM is trained, and the most likely states sequence is determined by using the transition probability matrix, Equation 6.3.8. Here, the Viterbi Algorithm is employed to tune and validate the HMM by applying Equation 6.3.12.

Meanwhile, raw vibration data is considered for identifying damage progression model. Since vibration signals are noisy, to enhance prognosis accuracy, signals are required some de-noising. Here a multi-resolution approach is employed to achieve this. The noisy signals have major high-frequency components that appear principally in the first detail coefficient,  $d_1$  (see Figure 6.3.2). Thus, to remove the noise, the noisy signals are reconstructed into detail signal and approximation signal using Equation (6.3.13). The approximation signal,  $a_1$ ,



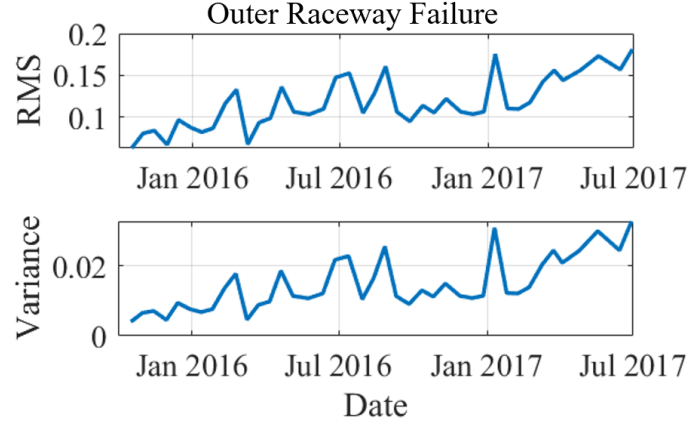


FIGURE 6.4.5: Selected features for the bearing #1 RUL estimation prediction

TABLE 6.4.1: Complete failure criteria coefficient  $\lambda_k$  for each feature

Failure	Outer raceway	Inner raceway
Variance	9	-
Band power	-	18
RMS	6	13.2
Peak to peak	6.9	18.4

(see Figure 6.3.2) is used going forward. Next, twelve time domain features, introduced in Table 6.3.1, are extracted. Afterward, two features, root mean square (RMS) and variance (VAR) are identified as the best candidate features for RUL estimation of the outer raceway failure category using filter-based methods that compare means and variances. The degradation trend that is common to the faulty bearings is observable in these features as shown in Figure 6.4.5. For the inner raceway failure category, root mean square (RMS) and peak to peak (P2P) are identified as the best features to support RUL estimation employing filter-based methods that compare means and variances. The ascending tendency typical of the faulty bearings is detectable in these features as shown in Figure 6.4.6.

The complete failure criteria coefficient required in Equation (6.3.3) for each feature are presented in Table 6.4.1. These coefficients are chosen by careful investigation of the historical complete failures and previous studies [12, 28, 29].

**Remark 2:** The complete failure criteria are usually chosen based on the type of bearing and the nature of the failure.

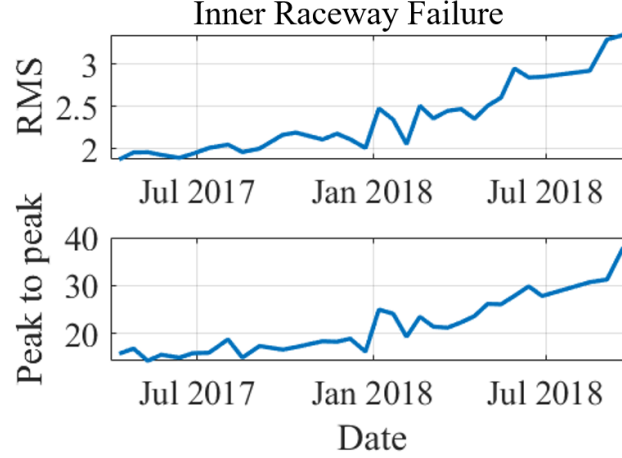


FIGURE 6.4.6: Selected features for the bearing #2 RUL estimation prediction

### 6.4.3 Online phase design implementation

In on-line phase, damage progression models are identified on each selected feature by using Equation (6.3.17), conditional to each operating state obtained from SCADA data, to characterize the evolution in time of the fault feature. As a result, two degradation models are developed precisely associated to normal and aggressive states. For long-term prediction horizons,  $R$  realizations of the HMM, i.e.  $R$  paths for future transitions in the HMM are developed based on the transition probability matrix presented in Equation 6.3.8. Then, the damage progression model associated to the predicted future wind turbine operating state for each realization is used to predict the RUL. RUL estimates are facilitated by way of an adaptive Bayesian algorithm in the following steps. First, for the estimation of likelihood function, the failure criterion, determined through Equations (6.3.14–6.3.16), are substituted into likelihood Equation (6.3.19). Next, the probability of failure is calculated by substituting Equation (6.3.19) and Equation (6.3.20) in Equation (6.3.18). Finally, the prediction horizon that maximizes the probability of failure determines the time to failure and the RUL is estimated using Equation (6.3.21). As a result,  $R$  RULs are predicted through  $R$  realizations which are averaged to achieve an accurate RUL of the faulty bearings.

Furthermore, to evaluate the accuracy of the RUL, a relative accuracy (RA) measure is considered [27]. The RA index takes a value in a range of  $[0, 1]$ . The larger value of the RA indicates a higher accuracy of the system.

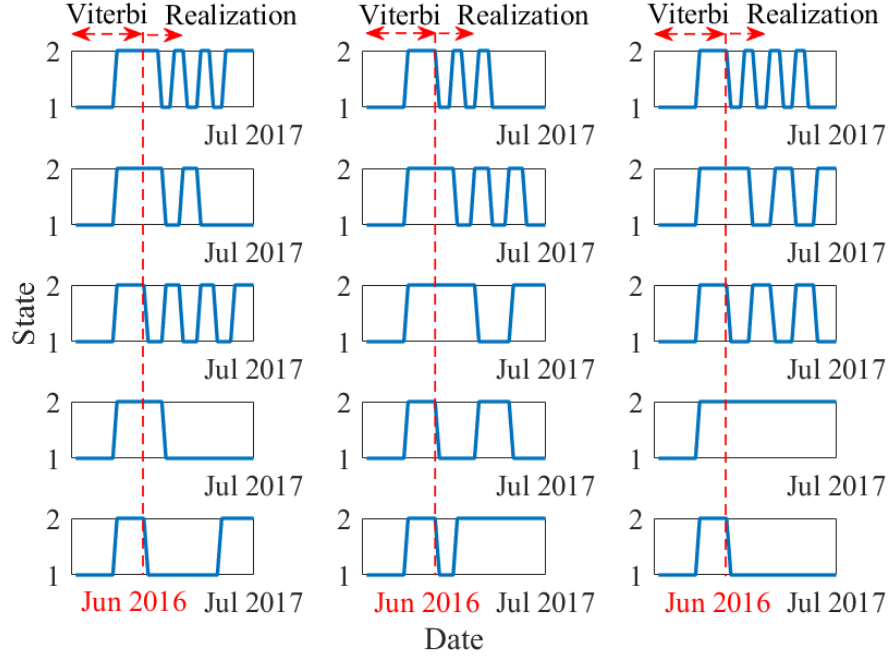


FIGURE 6.4.7: Varying states sequences for outer raceway failure

#### 6.4.4 Test results

In this subsection, two real life bearing failures are utilized to assess the performance of the proposed RUL method.

##### Outer raceway failure

The data from the main-shaft bearing of a wind turbine, *T31*, installed in 2008 is used to evaluate our proposed approach. This bearing experienced outer raceway failure on June 29<sup>th</sup> 2017. Figure 6.4.7 displays the varying operating states sequences achieved by using the HMM algorithm in short-term prediction and by generating realizations in long-term prediction.

Figure 6.4.8 displays the RULs obtained by averaging 15 selected realizations of varying operating conditions (VOC) compared to constant operation condition (COC), i.e. without categorizing different states, and real RUL based on the use of RMS and VAR features. Note that there is no significant change in RUL obtained by averaging more realizations than 15 realizations as indicated in Table 6.4.2 based on RUL estimates of RMS on July 13<sup>th</sup> 2016.

TABLE 6.4.2: Comparison of the RULs estimated by different approach for outer raceway failure

Approach	RA
COC	66.4%
11-realization average	84.6%
13-realization average	88.7%
15-realization average	90.2%
17-realization average	90.8%

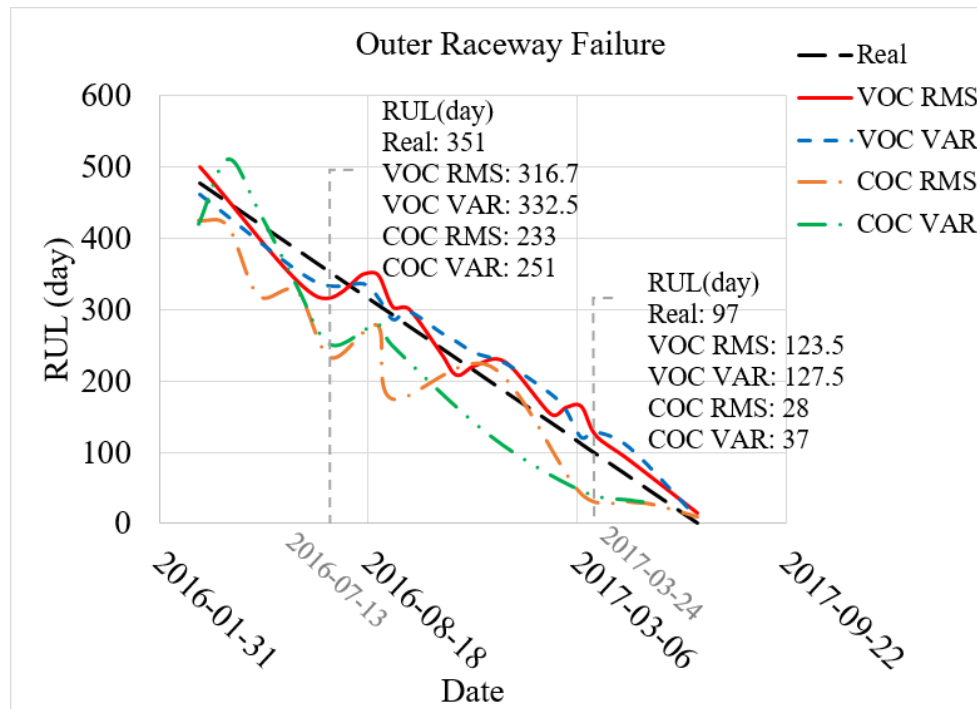


FIGURE 6.4.8: Comparison of the RULs estimated by averaging 15 selected realizations of VOC and COC

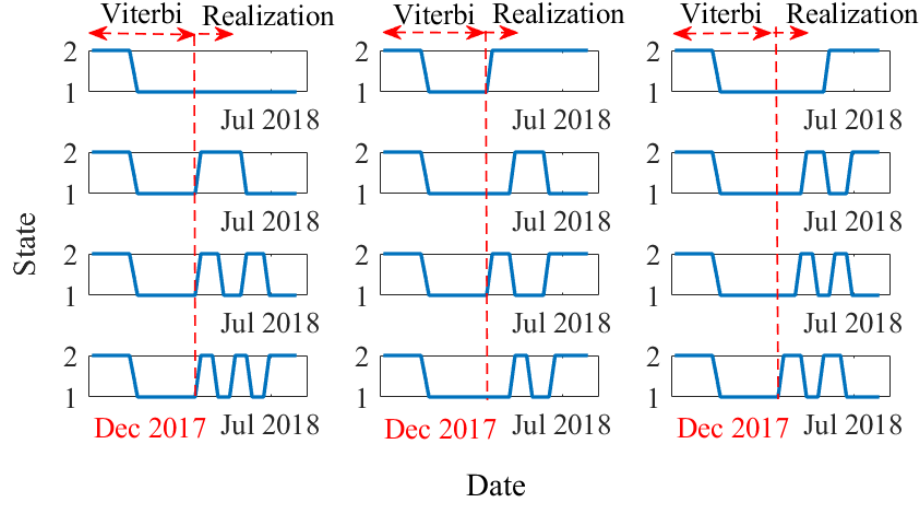


FIGURE 6.4.9: Varying states sequences for inner raceway failure

Figure 6.4.8 shows that the anticipated RUL of the proposed approach on July 13<sup>th</sup> 2016 was 316.7 days based on the degradation trend of the RMS. This represents an improved relative accuracy of 90.2% compared to constant operating condition with RA of 66.4%. Using Variance, estimates of 251 days in COC, was possible. However, considering varying operating conditions, RUL prediction yielded the best estimate of 332.5 days (94.7% accurate).

In a second case of March 24<sup>th</sup> 2017, predictions of 28 days (relative accuracy of 28.8%) and 37 days (relative accuracy of 38%) are also shown based on RMS, and the variance features, respectively. Furthermore, the proposed method estimates were 72.7% at 123.5 days and 68.6% at 127.5 days based on the degradation trend of the RMS, and the variance features, respectively. The proposed technique again produced the most accurate predictions.

### Inner raceway failure

The generator DE bearing of wind turbine, *T61*, was installed in 2011 in Southwestern Ontario. This bearing experienced inner raceway failure on September 20<sup>th</sup> 2018. Figure 6.4.9 displays the varying states sequences achieved by using the HMM algorithm in short-term prediction and by generating realizations in long-term prediction.

Figure 6.4.10 displays the RULs obtained by averaging 12 selected realizations of varying operating conditions (VOC) compared to constant operation condition (COC), and real

TABLE 6.4.3: Comparison of the RULs estimated by different approach for inner raceway failure

Approach	RA
COC	87%
8-realization average	85.4%
10-realization average	87.9%
12-realization average	90.8%
14-realization average	91.3%

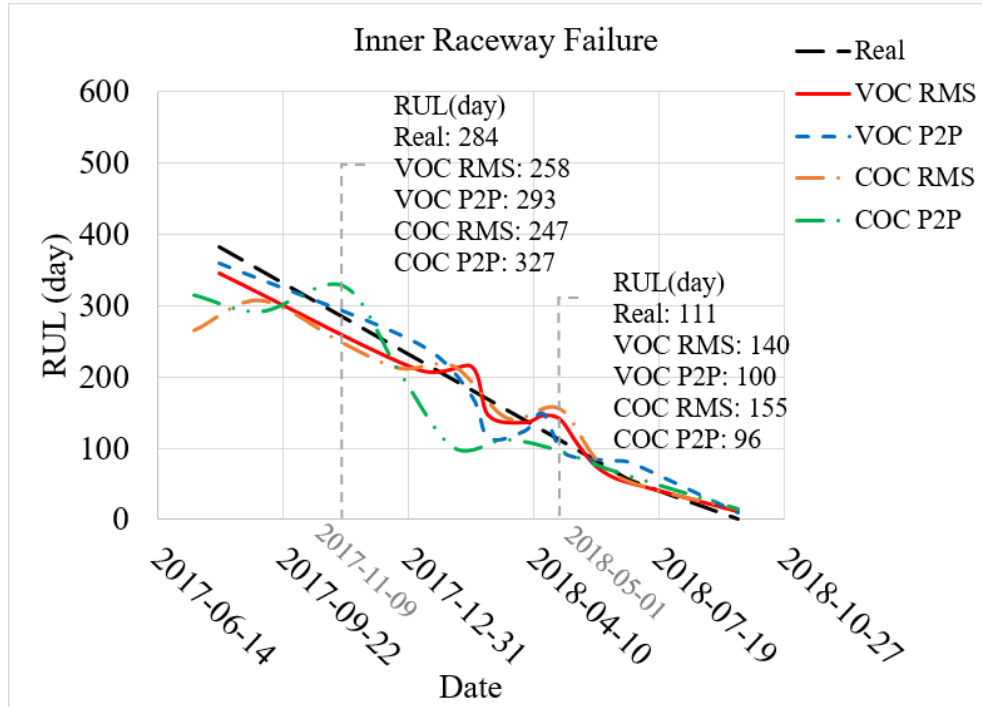


FIGURE 6.4.10: Comparison of the RULs estimated by averaging 12 selected realizations of VOC and COC

RUL based on the use of RMS and VAR features. Note that there is no significant change in RUL obtained by averaging more realizations than 12, as indicated in Table 6.4.3 based on RUL estimates of RMS on November 9<sup>th</sup> 2017.

It is noted from Figure 6.4.10 that the anticipated RUL of the proposed approach on November 9<sup>th</sup> 2017 was 258 days based on the RMS feature application. This represents the better relative accuracy of 90.8% compared to constant operating condition with RA of 87%. Peak to peak feature approach produced a 327 days (85% accurate). Besides, VOC RUL prediction based on the degradation trend of the peak to peak yielded the best estimate

of 293 days (96.8% accurate).

In a second case of May 1<sup>st</sup> 2018, 155 (60% accurate) and 96 (86.5% accurate) day predictions were made by the degradation trend of RMS and peak to peak in constant operating condition respectively. Improved Relative accuracies of 73.8% and 90% were achieved through utilization of the RMS and peak to peak features in varying operating conditions respectively.

## 6.5 Conclusion

This chapter proposed a novel real-time RUL prediction method for major bearings critical to wind turbine operation. Two prominent failure types, outer raceway and inner raceway degradations, were investigated. The described method first employed KFCM to categorize different operating conditions (states), and, then, applied comprehensive signal de-noising, feature extraction from de-noised vibration signals, and feature selection to detect dynamic failure characteristics and identifying damage progression models, conditional to each operating state. An HMM was then used to characterize the most likely states sequence for short-term prediction, and R realizations of HMM were generated for long-term prediction horizons. Here, the Viterbi Algorithm is employed to tune and validate the HMM by applying. The damage progression model associated to the predicted future wind turbine operating state for each realization was used to predict the RUL. Finally, RULs estimates of generated realizations were averaged to improve prediction accuracy. Two experimental case studies demonstrated, for the data considered here, that the proposed real-time fusion RUL method could notably improve prediction over considering constant operating condition.

## 6.6 List of Abbreviations

ANFIS	Adaptive Neuro-fuzzy inference systems
ANN	Artificial Neural Network
CMS	Condition Monitoring Systems
COC	Constant Operating Condition
DE	Drive End
DWT	Discrete Wavelet Transforms
EKF	Extended Kalman filter
FFT	Fast Fourier Transform
HMM	Hidden Markov Model
HSS	High-Speed Shaft
ICP	Integrated Circuit-Piezoelectric
IMS	Intermediate-Speed Shaft
LSS	Low-Speed Shaft
KFCM	Kernel Fuzzy C-Means
MC	Markov Chain
MRA	Multi-Resolution Analysis
NDE	Non-Drive End
OWA	Ordered Weighted Averaging
PF	Particle filter
P2P	Peak to peak
RA	Relative Accuracy
SM	Strain Measurement
RMS	Root Mean Square
RUL	Remaining Useful Life
SVM	Support Vector Machine
SVR	Support vector regression
TCM	Turbine Condition Monitoring
VA	Vibration analysis
VAR	Variance
VOC	Varying Operating Condition



## REFERENCES

- [1] F. Cheng, L. Qu, W. Qiao, and L. Hao, “Enhanced particle filtering for bearing remaining useful life prediction of wind turbine drivetrain gearboxes,” *IEEE Transactions on Industrial Electronics*, 2018.
- [2] A. P. Ompusunggu, J.-M. Papy, and S. Vandenplas, “Kalman-filtering-based prognostics for automatic transmission clutches,” *IEEE/ASME Transactions on Mechatronics*, vol. 21, no. 1, pp. 419–430, 2016.
- [3] F. P. G. Márquez, A. M. Tobias, J. M. P. Pérez, and M. Papaelias, “Condition monitoring of wind turbines: Techniques and methods,” *Renewable Energy*, vol. 46, pp. 169–178, 2012.
- [4] W. Ahmad, S. A. Khan, and J.-M. Kim, “A hybrid prognostics technique for rolling element bearings using adaptive predictive models,” *IEEE Transactions on Industrial Electronics*, vol. 65, no. 2, pp. 1577–1584, 2018.
- [5] Y. Wang, Y. Peng, Y. Zi, X. Jin, and K.-L. Tsui, “A two-stage data-driven-based prognostic approach for bearing degradation problem,” *IEEE Transactions on Industrial Informatics*, vol. 12, no. 3, pp. 924–932, 2016.
- [6] N. Z. Gebraeel, M. A. Lawley, R. Li, and J. K. Ryan, “Residual-life distributions from component degradation signals: A bayesian approach,” *IIE Transactions*, vol. 37, no. 6, pp. 543–557, 2005.
- [7] X.-S. Si, W. Wang, C.-H. Hu, M.-Y. Chen, and D.-H. Zhou, “A wiener-process-based degradation model with a recursive filter algorithm for remaining useful life estimation,” *Mechanical Systems and Signal Processing*, vol. 35, no. 1-2, pp. 219–237, 2013.
- [8] M. Qiu, W. Li, F. Jiang, and Z. Zhu, “Remaining useful life estimation for rolling bearing with sios-based indicator and particle filtering,” *IEEE Access*, vol. 6, pp. 24 521–24 532, 2018.

- [9] C. Chen, D. Brown, C. Sconyers, G. Vachtsevanos, B. Zhang, and M. E. Orchard, "A. net framework for an integrated fault diagnosis and failure prognosis architecture," in *2010 IEEE AUTOTESTCON*. IEEE, 2010, pp. 1–6.
- [10] X. Li, W. Zhang, and Q. Ding, "Deep learning-based remaining useful life estimation of bearings using multi-scale feature extraction," *Reliability Engineering & System Safety*, vol. 182, pp. 208–218, 2019.
- [11] L. Liao and F. Köttig, "Review of hybrid prognostics approaches for remaining useful life prediction of engineered systems, and an application to battery life prediction," *IEEE Transactions on Reliability*, vol. 63, no. 1, pp. 191–207, 2014.
- [12] A. Soualhi, K. Medjaher, and N. Zerhouni, "Bearing health monitoring based on hilbert–huang transform, support vector machine, and regression," *IEEE Transactions on Instrumentation and Measurement*, vol. 64, no. 1, pp. 52–62, 2015.
- [13] M. Elforjani and S. Shanbr, "Prognosis of bearing acoustic emission signals using supervised machine learning," *IEEE Transactions on Industrial Electronics*, vol. 65, no. 7, pp. 5864–5871, 2018.
- [14] J. Zhu, N. Chen, and W. Peng, "Estimation of bearing remaining useful life based on multiscale convolutional neural network," *IEEE Transactions on Industrial Electronics*, vol. 66, no. 4, pp. 3208–3216, 2019.
- [15] K. Zipp. (2012) Bearings 101. [Online]. Available: <https://www.windpowerengineering.com/mechanical/nacelle/bearings-101/>
- [16] M. Blodt, P. Granjon, B. Raison, and G. Rostaing, "Models for bearing damage detection in induction motors using stator current monitoring," *IEEE transactions on industrial electronics*, vol. 55, no. 4, pp. 1813–1822, 2008.
- [17] J. R. Stack, T. G. Habetler, and R. G. Harley, "Fault classification and fault signature production for rolling element bearings in electric machines," *IEEE Transactions on Industry Applications*, vol. 40, no. 3, pp. 735–739, 2004.

- [18] D.-M. Tsai and C.-C. Lin, “Fuzzy c-means based clustering for linearly and nonlinearly separable data,” *Pattern recognition*, vol. 44, no. 8, pp. 1750–1760, 2011.
- [19] B. Schölkopf, A. Smola, and K.-R. Müller, “Nonlinear component analysis as a kernel eigenvalue problem,” *Neural computation*, vol. 10, no. 5, pp. 1299–1319, 1998.
- [20] M. Girolami, “Mercer kernel-based clustering in feature space,” *IEEE Transactions on Neural Networks*, vol. 13, no. 3, pp. 780–784, 2002.
- [21] D. A. Pola, H. F. Navarrete, M. E. Orchard, R. S. Rabié, M. A. Cerda, B. E. Olivares, J. F. Silva, P. A. Espinoza, and A. Pérez, “Particle-filtering-based discharge time prognosis for lithium-ion batteries with a statistical characterization of use profiles,” *IEEE Transactions on Reliability*, vol. 64, no. 2, pp. 710–720, 2015.
- [22] A. Viterbi, “Error bounds for convolutional codes and an asymptotically optimum decoding algorithm,” *IEEE transactions on Information Theory*, vol. 13, no. 2, pp. 260–269, 1967.
- [23] S. G. Mallat, “A theory for multiresolution signal decomposition: the wavelet representation,” *IEEE transactions on pattern analysis and machine intelligence*, vol. 11, no. 7, pp. 674–693, 1989.
- [24] W. Caesarendra and T. Tjahjowidodo, “A review of feature extraction methods in vibration-based condition monitoring and its application for degradation trend estimation of low-speed slew bearing,” *Machines*, vol. 5, no. 4, p. 21, 2017.
- [25] D. Siegel, C. Ly, and J. Lee, “Methodology and framework for predicting helicopter rolling element bearing failure,” *IEEE Trans. Reliability*, vol. 61, no. 4, pp. 846–857, 2012.
- [26] S. Das, “Filters, wrappers and a boosting-based hybrid for feature selection,” in *Icml*, vol. 1, 2001, pp. 74–81.
- [27] M. Kordestani, A. Zanj, M. E. Orchard, and M. Saif, “A modular fault diagnosis and prognosis method for hydro-control valve system based on redundancy in multisensor data information,” *IEEE Transactions on Reliability*, no. 99, pp. 1–12, 2018.

- [28] R. K. Singleton, E. G. Strangas, and S. Aviyente, “Extended kalman filtering for remaining-useful-life estimation of bearings,” *IEEE Transactions on Industrial Electronics*, vol. 62, no. 3, pp. 1781–1790, 2015.
- [29] X. Jin, Y. Sun, Z. Que, Y. Wang, and T. W. Chow, “Anomaly detection and fault prognosis for bearings,” *IEEE Transactions on Instrumentation and Measurement*, vol. 65, no. 9, pp. 2046–2054, 2016.

---

# CHAPTER 7

## *Conclusion*

---

In this dissertation, the task of failure detection and failure prognosis for critical wind turbine components was investigated from multiple aspects. In this regard, five novel approaches were examined on wind turbine generators, blades, and bearings. The concluding remarks of each developed methodology would be briefly outlined in the following sections.

Chapter 2 focuses on non-parametric and parametric life data analyses to predict the reliability of the wind turbine generators based on truncated/limited data records. Besides, a Naive prediction interval procedure is proposed to provide an approximate range for the RUL of each generator. It is shown how reliable a subset of wind turbine generators is and how electrical loads may influence turbine generator reliability. These outcomes may be leveraged further by the research community for companion applications like prognostic maintenance and investment decision support systems.

In Chapter 3, a new condition monitoring approach for extracting fault signatures in wind turbine blades by utilizing the data from a real-time Supervisory Control and Data Acquisition (SCADA) system. A hybrid fault detection system based on a combination of Generalized Regression Neural Network Ensemble for Single Imputation (GRNN-ESI) algorithm, Principal Component Analysis (PCA) and wavelet-based Probability Density Function (PDF) approach is proposed in this Chapter. It is illustrated the effectiveness and high accuracy of the proposed monitoring approach to detect incipient blade faults.

Chapter 4 focuses thoroughly on a recent literature review on modeling developments for prediction of the RUL of faulty wind turbine bearings. The pros and cons of each prognosis method are also highlighted. Furthermore, shortcomings of the existing methods

are highlighted, and a number of challenges that merit further study are summarized. Note that most of these challenges are addressed in the next two chapters.

In Chapter 5, a novel hybrid real-time RUL prediction method for major bearings critical to wind turbine operation is developed. The proposed method employs comprehensive feature extraction, feature selection, and signal de-noising to detect dynamic failure characteristics. RUL of the faulty bearings is forecast via adaptive Bayesian algorithm using the extracted features. Next, a robust fusion method based on an ordered weighted averaging (OWA) operator is applied to the RUL obtained from the features to improve accuracy. The efficiency of the method is evaluated using data from historical failures across three different Canadian wind farms.

Chapter 6 introduces a hybrid prognosis method using real-time Supervisory Control and Data Acquisition (SCADA) and vibration signal to predict Remaining Useful Life (RUL) for wind turbine bearings. The SCADA data is utilized to determine the role of environmental conditions such as wind speed and ambient temperature in the severity of failure dynamics using a Kernel Fuzzy C-Means (KFCM) and a Hidden Markov Model (HMM) that is validated using the Viterbi Algorithm. For this purpose, the KFCM method is used to categorize different operating states in which wind turbines operate. The HMM is then used during the prediction stage to characterize epistemically uncertainty associated with future operating conditions and the most likely switching between different operating states. Here, clustered data is used to identify a collection of empirical health degradation models which are conditional on the operating conditions for the plant. Afterward, for each state, failure dynamics are identified from the vibration signal using a combination of signal denoising, feature extraction, and feature selection. Finally, RUL of the faulty bearings is forecasted via adaptive Bayesian Algorithm using the failure dynamics on the selected features, conditional to each operating state. The efficacy of the method is validated using experimental data from three different Canadian wind farms.

## 7.1 Contributions

The most important contributions of this dissertation are summarized as follows:

- The first contribution of this dissertation is in the application of ALTA lifetime analysis method for reliability estimation of wind turbine generators to help illustrate a possible relationship between varying loads and generator reliability.
- An additional contribution is to provide early fault detection due to applying the wavelet-based PDF method that can accurately estimate the probability density functions of principal components (PCs) and consequently detect incipient wind turbine blade faults.
- Another contribution is revealed in the application of the adaptive Bayesian algorithm. An affine function of time is identified in the performance degradation data obtained from the characteristic features. The proposed Bayesian algorithm is suitable for modeling the uncertainty inherent in the prediction horizon of the bearings and is suitable for online implementation.
- A notable contribution is in the engagement of a fusion method that utilizes an OWA operator which combines the RULs obtained from various features, to produce a more accurate RUL prediction.
- Finally, the damage progression is characterized using the different operating states to mimic a real condition in which wind turbines operate. This proposed prognosis framework potentially improves the accuracy of RUL prediction. The main concept is to recognize that the damage progression is a function of the stress applied to each component.

## 7.2 Future Work

Health monitoring of critical wind turbine components is becoming an increasingly significant field of research in the years to come and possess the potential to contribute a proper framework for condition-based maintenance. In the following, some challenges that merit for future research efforts in this field are highlighted.

- Identifying the type of blade fault.

Employing Classification approaches to distinguish different wind turbine blade failure modes, such as crack and erosion in the blade

- Considering components interactions for the prognosis task.

Component interactions should be investigated in the damage progression (for instance, the interaction between bearings and gears in a gearbox). More signal processing methods could also be applied to the machine degradation process to distinguish components fault signals from each other.

- Application of particle filter

The particle filter is a potential technique to capture the nonlinear dynamics and enhance the accuracy of failure prognosis. Caution must be exercised, as it may increase the computation complexity which may be a negative aspect for the real-time implementation of the method.

- Investigating coincident failures

Developing methods to isolate coincident failures in a system and predict the RUL of the system

- Considering online health monitoring with the task of the prognosis

It is beneficial to implement an online health assessment to evaluate the accuracy of the prognosis due to uncertainties associated with the prediction horizon of the failure.



# **APPENDICES**

---

## APPENDIX A

### *Bayesian RUL Prediction Algorithm*

---

A recursive RUL scheme based on an adaptive Bayesian algorithm is used in this dissertation to project the remaining lifetime of several faulty wind turbine bearings. The proposed RUL method is illustrated in Figure 8.0.1. It is noted from Figure 8.0.1 that an optimal affine function of time can be identified on the extracted feature over a sliding window as follows [1, 2]:

$$y_t = \hat{m}t + \hat{n} + e_t \quad (\text{A.0.1})$$

where  $e_t \sim N(0, \sigma^2)$  is a Gaussian white noise error with zero mean and variance  $\sigma^2$  and  $m$  and  $n$  are parameters of optimal affine linear function. Then,  $y_{t_0} \sim N(\hat{m}t_0 + \hat{n}, \sigma^2)$ , and any  $j$  step ahead prediction distribute in a Gaussian random variable:

$$\hat{y}_{t_0+j} \sim N(\hat{y}_0 + mj, (j+1)\sigma^2) \quad (\text{A.0.2})$$

A non-stationary Bernoulli process can be applied to model failure. A probability space can be defined by considering healthy state and complete failure state at time  $t_k$  with  $H_{t_k}$  and  $F_{t_k}$  notations as follows:

$$\Omega_{failure} = \{H_{t_0}, H_{t_0+1}, \dots, H_{t_0+j-1}, F_{t_0+j}\} \quad (\text{A.0.3})$$

$\Omega_{failure}$  denotes the probability space including all possible Bernoulli sequences where the component remains healthy until time  $t_0 + j$  in which a complete failure occurs in the component. The probability of failure,  $p(F_{t_0+j})$ , at  $t = t_0 + j$  can be obtained by conditional probability as follows:

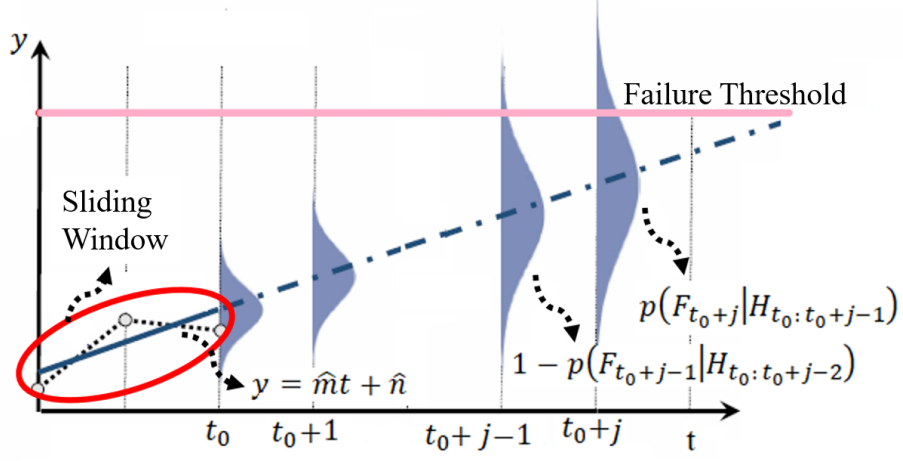


FIGURE A.0.1: The adaptive Bayesian RUL method

$$p(F_{t_0+j}) = \frac{p(F_{t_0+j}, H_{t_0:t_0+j-1})}{p(H_{t_0:t_0+j-1}|F_{t_0+j})} \quad (\text{A.0.4})$$

$p(F_{t_0+j}, H_{t_0:t_0+j-1})$  is the probability of failure at  $t = t_0 + j$  and simultaneously being healthy until  $t = t_0 + j - 1$ .  $p(H_{t_0:t_0+j-1}|F_{t_0+j})$  denotes the probability of being healthy conditional to a failure at  $t = t_0 + j$ .  $p(H_{t_0:t_0+j-1}|F_{t_0+j})$  is equivalent to one because here failure in the physical system occurs just once, and Eq. (8.0.4) can be rewritten employing the joint probability definition as follows:

$$p(F_{t_0+j}) = p(F_{t_0+j}|H_{t_0:t_0+j-1})p(H_{t_0:t_0+j-1}) \quad (\text{A.0.5})$$

where  $p(H_{t_0:t_0+j-1})$  denotes the probability of staying healthy until  $t = t_0 + j - 1$ . Probability  $p(F_{t_0+j}|H_{t_0:t_0+j-1})$  is known as likelihood function, and can be estimated as follows:

$$\begin{aligned} p(F_{t_0+j}|H_{t_0:t_0+j-1}) &= p(y_{t_0+j} > FC) \\ &= Q\left(\frac{FC - y_{t_0+j}}{\sigma\sqrt{j+1}}\right) \end{aligned} \quad (\text{A.0.6})$$

The function  $Q$  is the tail of the standard probability Gaussian distribution. In this study, the adaptive Bayesian algorithm is employed to fit an affine function of  $y_{(t_0+j)}$  to the denoised feature data of the bearings over a sliding window, noted from Figure 8.0.1. The complete failure criterion (FC), threshold, can be obtained as follows:

$$FC = \mu + \lambda\sigma \quad (\text{A.0.7})$$

Where  $\lambda$  is the failure threshold coefficient. Variables  $\mu$  and  $\sigma$  are mean and standard deviation of the healthy data set, respectively, and can be estimated as follow:

$$\mu = \frac{1}{m} \sum_{i=1}^m x^{(i)} \quad (\text{A.0.8})$$

$$\sigma = \sqrt{\frac{1}{m} \sum_{i=1}^m (x^{(i)} - \mu)^2} \quad (\text{A.0.9})$$

After calculating the likelihood function; function  $p(H_{t_0:t_0+j-1})$  can then be determined by using properties of the probability as follows:

$$\begin{aligned} p(H_{t_0:t_0+j-1}) &= [1 - p(F_{t_0+1}|H_{t_0})] \times [1 - p(F_{t_0+2}|H_{t_0:t_0+2})] \\ &\cdots \times [1 - p(F_{t_0+j-1}|H_{t_0:t_0+j-2})] \end{aligned} \quad (\text{A.0.10})$$

Based on Gaussian distribution theory, the failure probability sequences,  $p(F_{t_0+j})$  of the prediction horizon  $j$  exhibit monotonic growth. The predicted time of the failure or the RUL of the system is determined at a time  $j$  where the probability of failure is at its peak [1, 2].

## REFERENCES

- [1] D. E. Acuña and M. E. Orchard, “Particle-filtering-based failure prognosis via sigma-points: Application to lithium-ion battery state-of-charge monitoring,” *Mechanical Systems and Signal Processing*, vol. 85, pp. 827–848, 2017.
- [2] M. Kordestani, A. Zanj, M. E. Orchard, and M. Saif, “A modular fault diagnosis and prognosis method for hydro-control valve system based on redundancy in multisensor data information,” *IEEE Transactions on Reliability*, no. 99, pp. 1–12, 2018.

# VITA AUCTORIS

NAME: Milad Rezamand

PLACE OF BIRTH: Kerman, Iran.

EDUCATION: Bachelor of Science in Mechanical Engineering, Shahid Bahonar University of Kerman, Kerman, Iran, 2008.

Master of Science in Aerospace Engineering, K.N.T University of Technology, Tehran, Iran, 2012.

Doctor of Philosophy in Mechanical Engineering, University of Windsor, Windsor, Ontario, Canada, 2019.